4

RESULTS AND DISCUSSION

Medicinal plants have contributed a rich health to human beings. Plant extracts and their bioactive compounds present in them which are responsible for anticancer activity have to be screened for their valuable information. A huge reservoir of bioactive compounds exists in many species of plants of Earth, only a small percentage of which have been examined and continued to be an important source of anticancer agents. Worldwide effects are ongoing to identify new anticancer compounds from plants. With the current decline in the number of new molecular entities from the pharmaceutical industry, novel anticancer agents are being sought from traditional medicines.Traditionally, drugs used for cancer chemotherapy are organic compounds, either synthetic or natural products and include alkylating agents, antibiotics, alkaloids, enzymes and hormones (Ashok *et al*., 2009).

The common free radicals are oxygen-reactive species (ROS), which are formed during natural metabolism and are in dynamic balance between their biosynthesis and their removal by antioxidant systems in human bodies. When the mechanism of antioxidant protection becomes unbalanced by factors such as ageing and deterioration of physiological functions, resulting in oxidative stress and thus can lead to cell injury and various relevant diseases such as cardiovascular diseases, cancer and accelerated ageing (Huang *et al*., 2009).

Cancer is an abnormal type of tissue growth in which the cells exhibit an uncontrolled division, relatively in an autonomous fashion, leading to a progressive increase in the number of dividing cells. Dalton's Ascites Lymphoma is transplantable, malignant tumor which appeared originally as lymphocytes in a mouse. It grows in both solid and ascitic form (Kanchana and Balakrishna 2011). Transplantable Dalton's lymphoma ascites tumor cells into Swiss albino mice are

an important experimental approach to study the antioxidative and antitumorigenic effect of medicinal plants (Isha *et al*., 2011; Sundaresan and Subbiah, 2012).

Cancer is one of the ailments which cannot be completely subdued by chemotherapy. The chemotherapeutic agents though effective against various types of tumor are not totally free from side effects (Lakshmi *et al*., 2010). Many Indian plants like black pepper, asafoetida, pippali and garlic are quoted to be useful in different types of cancer. Antioxidants play an important role in inhibiting and scavenging free radicals, thus providing protection to human against degenerative diseases like cancer (Otsuki *et al*., 2010).

The thumb challenge in nanotechnology is for the development of efficient and green chemistry involved experimental protocols for the synthesis of nanomaterials for a required size, shape and despersivity (Massich *et al*., 2010). In the current drive of developing green clean technologies for the nanomaterials synthesis, these aspects assume considerable importance. Using different plant extracts and reducible bio-excretory in the synthesis of novel metalNPs is an attractive possibility (Smuleac *et al*., 2011). Nanobiotechnology is a blend of nanotechnology and biotechnology comprises of nanoparticle synthesis using plants have found to be advantageous being non-carcinogenic, non-pathogenic and biocompatible during both synthesis and application. The efficacy of medicinal plants when used in the synthesis of functionalized NPs with a biological-shell and metal-core can synergycally act for the prevention of different diseases like cancer. For the required shape, size and dispersivity, the controlled synthesis of NPs can be done using extracellular plant extract by biosynthetic methods in a much easier way and can be utilized for many pharmaceutical and medical applications. Surface modification allows for better and more accurate targeting of cancer cells compared to conventional methods and there is a great potential that NPs would meet the pressing need for better cancer therapy (Ramachandran and Shanmughavel 2010). Among the various inorganic metalNPs, silver (Ag) NPs have received substantial attention for various reasons. Silver is an effective antimicrobial agent, exhibits low toxicity and has diverse *in vitro* and *in vivo*

applications. The inorganic NPs are found to be effective in scavenging oxygen based free radicals (Gavhane *et al*., 2012).

In the present research, "**Antioxidant and Antitumorigenic efficacy of methanolic extracts of *Gloriosa superba* and Silver Nanoparticles of methanolic extracts of *Gloriosa superba* to DLA tumor cells**" the *in vitro* and *in vivo* studies were carried out in three phases. The phases I and II constituted the *in vitro* studies and the phase III involved the *in vivo* studies.

In the first phase, MGsSTL and AgMGsSTL were characterized by phytochemical screening, HPTLC, UV-Visible Spectroscopy, FT-IR, SEM with EDX, TEM, DLS, Zeta-Potential, and XRD analysis.

In the second phase, *in vitro* antioxidative role of the methanolic extract of *Gloriosa superba* seeds, tubers and leaves (MGsSTL) and silver NPs of methanolic extract of *Gloriosa superba* seeds, tubers and leaves (AgMGsSTL) was assessed by their scavenging of DPPH, hydroxyl, superoxide radicals, hydrogen peroxide and nitric oxide against the standard antioxidant Vitamin C. The identification of the minimum concentration of the MGsSTL and AgMGsSTL for the fifty percent cytotoxic effect (ED_{50}) to DLA tumor cells by MTT assay and trypan blue exclusion methods. Apoptotic effect of AgMGsSTL to DLA cells by flow cytometry was also carried out.

In the third phase, the selected ED_{50} of MGsSTL and AgMGsSTL were evaluated for their antioxidative role against the standard antioxidant silymarin and the antitumorigenic effect in DLA tumor induced Swiss albino mice.

The results of the study are furnished and discussed under the following headings:

Phase I

4.1 Characterization of MGsSTL and AgMGsSTL

4.1.1 Phytochemical constituents of MGsSTL

4.1.1.1 Preliminary screening

4.1.1.2 High Performance Thin Layer liquid Chromatography (HPTLC)

4.1.2 Characterization of MGsSTL and AgMGsSTL

4.1.2.1 UV-VisibleSpectroscopy

4.1.2.2 Fourier Transform Infrared spectroscopy (FT-IR)

4.1.2.3 Scanning electron microscope (SEM) and Energy Dispersive Spectroscopy (EDX)

4.1.2.4 Transmission electron microscope (TEM)

4.1.2.5 Dynamic light Scattering (DLS)

4.1.2.6 Zeta-Potential

4.1.2.7 X-RAY Diffraction (XRD) analysis

Phase II

4.2 *In vitro* antioxidant and antitumorigenic potential of MGsSTL and AgMGsSTL

4.2.1 Antioxidant potential of MGsSTL and AgMGsSTL

4.2.1.1 Scavenging of DPPH radical (DPPH)

4.2.1.2 Scavenging of Hydroxyl radical ($OH^{\cdot}$)

4.2.1.3 Scavenging of Superoxide radical ($^{\cdot}O_2^-$)

4.2.1.4 Scavenging of Hydrogen peroxide (H_2O_2)

4.2.1.5 Scavenging of Nitric Oxide (NO)

4.2.2 Antitumorigenic potential of MGsSTL and AgMGsSTL to DLA tumor cells

4.2.2.1 MTT cell proliferation assay

4.2.2.2 Trypan blue exclusion assay

4.2.2.3 Apoptotic effect of AgMGsSTL to DLA tumor cells by flow cytometry.

Phase III

4.3 *In vivo* antioxidative and antitumorigenic effect of MGsSTL and AgMGsSTL in DLA tumor induced mice

4.3.1 Effect on the activities of enzymic antioxidants

4.3.1.1 Catalase (CAT)

4.3.1.2 Superoxide dismutase (SOD)

4.3.1.3 Glutathione S- transferase (GST)

4.3.1.4 Glutathione peroxidase (GPx)

4.3.1.5 Glutathione reductase (GR)

4.3.2 Effect on the levels of non enzymic antioxidants

4.3.2.1 Vitamin A

4.3.2.2 Vitamin E

4.3.2.3 Vitamin C

4.3.2.4 Reduced Glutathione (GSH)

4.3.3 Effect on the rate of lipid peroxidation (LPO)

4.3.4 Effect on the mortality rate of DLA tumor induced mice

4.3.5 Effect on the Histological appearance of hepatocytes of normal and DLA induced Swiss albino mice

Phase I

4.1 Characterization of MGsSTL and AgMGsSTL

In this Phase, characterization of MGsSTL and AgMGsSTL was done by Phytochemical screening, HPTLC, UV-Visible Spectroscopy, FT-IR, SEM with EDX, TEM, DLS, Zeta-Potential, and XRD analysis.

4.1.1 Phytochemical constituents of MGsSTL

To determine the bioactive constituents of MGsSTL, the preliminary phytochemical screening was carried out.

4.1.1.1 Preliminary screening

Phytochemical examination of plants which have a suitable history of use in folklore for the treatment of cancer had induced the isolation of principles with antitumor activity. Plant extracts and their bioactive compounds present in them are responsible for anticancer activity have to be screened for their valuable information. Plant derived natural products such as flavanoids, terpenes, and

alkaloids have received considerable attention in recent years, due to their diverse pharmacological properties including cytotoxic and cancer chemopreventive effects. Plants have a long history of use in the treatment of cancer (Prema *et al*., 2011). A variety of plant secondary metabolites have been reported to act as antioxidants and among them alkaloid and phenolic compounds form a major group (Rafat *et al*., 2010). Major classes of phytochemicals present in plants are polyphenols, terpenoids and essential oils, alkaloids and polypeptides (Siddiqui *et al*., 2009). Tannins may be monomeric or polymeric and can be divided into condensed and hydrolysable tannins. Most important extractable components are waxes, phenolic aldehydes and coumarins, the group of phenolic compounds also included the chemical families of flavonoids and tannins (Fernandes *et al*., 2009).

Preliminary phytochemical screening was carried out in this phase which revealed the presence of major secondary metabolites. The phytochemical analysis of MGsS showed the presence of Carbohydrates, Alkaloids, Glycosides, Flavonoids, Tannins, Steroids, Terpenoids and Phenolics (Table 2). Phytochemical analysis of the MGsT showed the presence of Carbohydrates, Alkaloids and Flavonoids (Table 2). Phytochemical analysis of the MGsL showed the presence of Carbohydrates, Alkaloids, Flavonoids and Steroids (Table 2).

Table 2

Phytochemical constituents of MGsSTL

Phytochemicals	MGsS	MGsT	MGsL
Carbohydrates	+	+	+
Alkaloids	+++	+++	+
Glycosides	+	-	-
Flavonoids	+	+	+
Tannins	+	-	-
Steroids	+	-	+
Saponins	-	-	-
Terpenoids	+	-	-
Phenolics	+	-	-

Presence (+), Absence (-)

Baskar *et al*., (2012) also reported the presence of Glycosides, alkaloids, saponins, flavonoids, phenolilc compounds and terpenoids in ethanol extract of *Erythrina variegate* and showed significant antitumor and cytotoxics effects against DLA and human cancer cell lines. Methanol extract of *Cleome viscosa* showed the presence of triterpenes and flavonoids which may act as anticancer and antioxidant against EAC bearing Swiss albino mice (Gopal *et al*., 2012). Flavonoids, Phenolic compounds, Tannins, Glycosides, Saponins and Carbohydrates in ethanolic extract of *Achyranthes bidentata* possess anticancer activity against DAL and EAC (Kota *et al*., 2012). Cytotoxicity and anticancer activity of ethanolic extract of *Aerva sanguinolenta* is probably due to the presence of flavonoids (Lalee, *et al*., 2012). Merina *et al*., (2012) also reported the potential anticancer molecules such as Vincristine, Vinblastin, Taxol, Camptothecin and Podophyllotoxin in *Blumea balsamifera, Boerhaavia diffusa, Citrus maxima, Emblica officinalis* Gaertn, *Calotropis procera and Moringa oleifera*. Flavonoids and related phytoconstituents present in methanolic extract of roots of *Barlaria buxifolia* showed the cytotoxic activity to DLA cell lines (Shivakumar *et al*., 2012). Cytotoxicity and anticancer activity of methanolic extract of *Alangium salvifolium* against DLA cells are probably due to the presence of flavonoids and deoxytubulosine (Venkateshwarlu *et al*., 2012).

Phytochemical screening revealed the presence of Carbohydrates, Alkaloids, Glycosides, Flavonoids, Steroids, Terpenoids and Phenolics in the MGsSTL, which could be responsible for their antioxidant and antitumorigenic activity. Alkaloids have been found to possess antioxidant and antitumorigenic effect (Woongchon *et al*., 1991) which provide some additional insight into the *in vitro* and *in vivo* cytotoxic activity of the MGsSTL.

4.1.1.2 High Performance Thinlayer Liquid Chromatography (HPTLC)

The HPTLC analysis was carried out to confirm the presence of alkaloids and their derivatives in MGsSTL using colchicines as standard. Chromatographic fingerprint is a holistic, valid and rapid method. HPTLC is a valuable quality

assessment tool for the evaluation of botanical materials. It allows the analysis of a broad number of compounds both efficiently and cost effectively. HPTLC studies have shown that it is more versatile than ordinary TLC methods, as the spots were well resolved (Jirge *et al*., 2011).

This technique can be used to rectify many qualitative and quantitative analytical problems in a wide range of fields including medicines, pharmaceutical, chemistry, biochemistry and toxicology (Ramya *et al*., 2010). In addition, HPTLC was recommended for identification of phytochemical constituents of the medicinal plants and finds solution for the taxonomical problems. This can be used in the pharmaceutical industry as a pharmacogonstical tool to identify the medicinally important plant. In addition it can be adopted as a chemo-taxonomical tool in the plant systematic. Further, the separation and characterization of the bioactive principles from the plants have to be evaluated and reported (Patil *et al*., 2010).

In the present study HPTLC analysis was carried out to confirm the presence of alkaloids and their derivatives in MGsSTL using colchicines as standard using ethyl acetate-methanol-water (10: 1.35 : 1) as the mobile phase. Tables 3, 4, 5 and Figures 31, 32, 33, 34 show the alkaloid profile of MGsSTL against colchicine standard. Colchicine Rf value was found to be 0.48. Out of 14 peaks 9^{th} alkaloid peak was found to be colchicines in MGsS as its Rf value corresponds to the Rf value of the standard colchicines. Yellow, Orange yellow, Brownish yellow coloured zone at Daylight mode were present in the track chromatogram, After derivatization, the chromatogram confirmed the presence of Alkaloid/Nitrogen containing compound (Heterocyclic compound) against the standard colchicines.

The alkaloid profile, UV- visible chromatogram pattern, densitogram displays at 254 nm showed the presence of colchicines (peak 9), two colchicines derivatives (peaks 7 and 13) and 11 unknown alkaloids in MGsS: two colchicines derivatives (peaks 9 and 10) and 13 unknown alkaloids in MGsT and 10 unknown alkaloids in MGsL.

The superimposed HPTLC fingerprints (Figure 35) also revealed the presence of alkaloids in MGsSTL. HPTLC fingerprinting is proved to be a linear, precise, accurate method for herbal formulation and can be used further in quality control of non- established herbals.

Table 3

HPTLC - Peak table for alkaloid profile of MGsS

Track	Peak	Rf	Height	Area	Assigned substance
MGsS	1	0.01	76.1	741.2	Unknown
MGsS	2	0.06	162.0	4811.3	Unknown
MGsS	3	0.14	85.7	1732.1	Unknown
MGsS	4	0.19	18.3	356.8	Unknown
MGsS	5	0.23	23.5	448.0	Unknown
MGsS	6	0.30	21.9	448.2	Unknown
MGSS	7	0.34	33.5	1051.9	Alkaloid 1
MGsS	8	0.40	27.5	617.1	Unknown
MGsS	9	0.48	709.9	40637.5	Alkaloid 2
MGsS	10	0.67	19.1	472.7	Unknown
MGsS	11	0.73	23.2	488.5	Unknown
MGsS	12	0.77	167.2	4261.1	Unknown
MGsS	13	0.83	119.8	3083.7	Alkaloid 3
MGsS	14	0.91	400.2	27557.3	Unknown
COL	1	0.48	585.8	18066.1	Colchicine standard

Table 4

HPTLC - Peak table for alkaloid profile of MGsT

Track	Peak	Rf	Height	Area	Assigned substance
MGsT	1	0.01	90.4	1037.9	Unknown
MGsT	2	0.07	64.8	1387.2	Unknown
MGsT	3	0.13	28.4	416.8	Unknown
MGsT	4	0.15	30.5	494.6	Unknown
MGsT	5	0.18	32.5	630.2	Unknown
MGsT	6	0.26	100.0	4185.7	Unknown
MGsT	7	0.34	123.7	4096.2	Unknown
MGsT	8	0.37	121.0	4159.4	Unknown
MGsT	9	0.46	542.6	17752.0	Alkaloid 1
MGsT	10	0.50	368.8	8696.5	Alkaloid 2
MGsT	11	0.61	149.0	7763.9	Unknown
MGsT	12	0.66	24.0	498.8	Unknown
MGsT	13	0.77	61.7	2120.7	Unknown
MGsT	14	0.82	273.5	8546.8	Unknown
MGsT	15	0.91	421.4	33871.9	Unknown
COL	1	0.48	585.8	18066.1	Colchicine standard

Table 5

HPTLC - Peak table for alkaloid profile of MGsL

Track	Peak	Rf	Height	Area	Assigned substance
MGsL	1	0.03	16.1	213.6	Unknown
MGsL	2	0.08	13.0	205.5	Unknown
MGsL	3	0.21	27.1	559.8	Unknown
MGsL	4	0.23	25.6	618.5	Unknown
MGsL	5	0.35	13.5	291.4	Unknown
MGsL	6	0.47	44.0	999.8	Unknown
MGsL	7	0.51	23.4	514.2	Unknown
MGsL	8	0.60	16.9	555.7	Unknown
MGsL	9	0.66	12.3	92.1	Unknown
MGsL	10	0.90	472.1	36653.7	Unknown
COL	1	0.48	585.8	18066.1	Colchicine standard

Plate IV

HPTLC Chromatogram pattern of MGsSTL

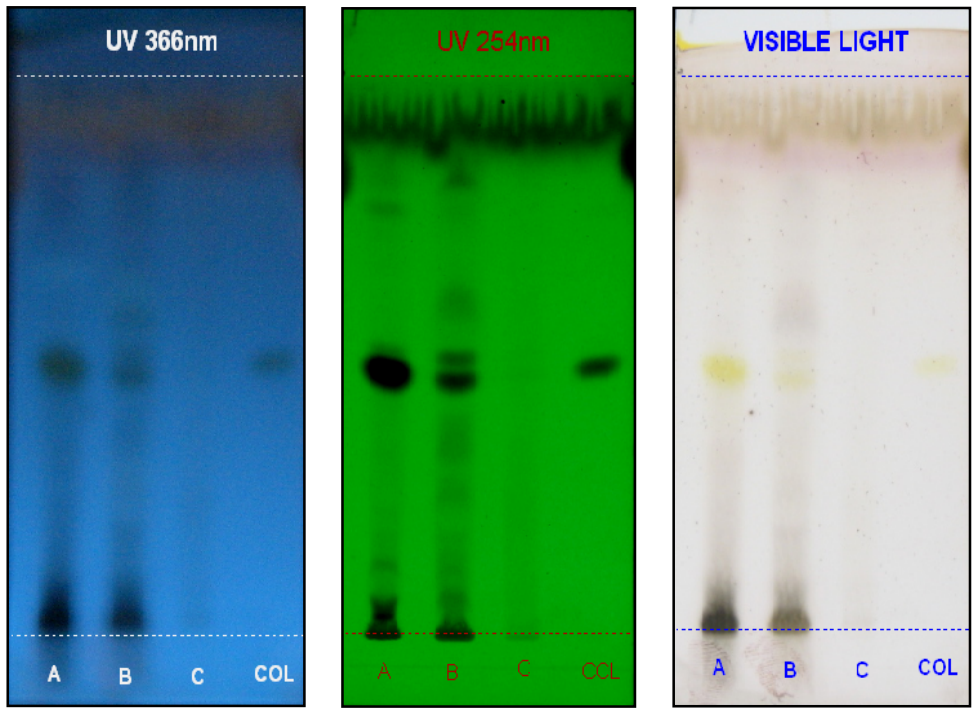

Figure 31

Track A –MGsS Baseline display and Peak densitogram display

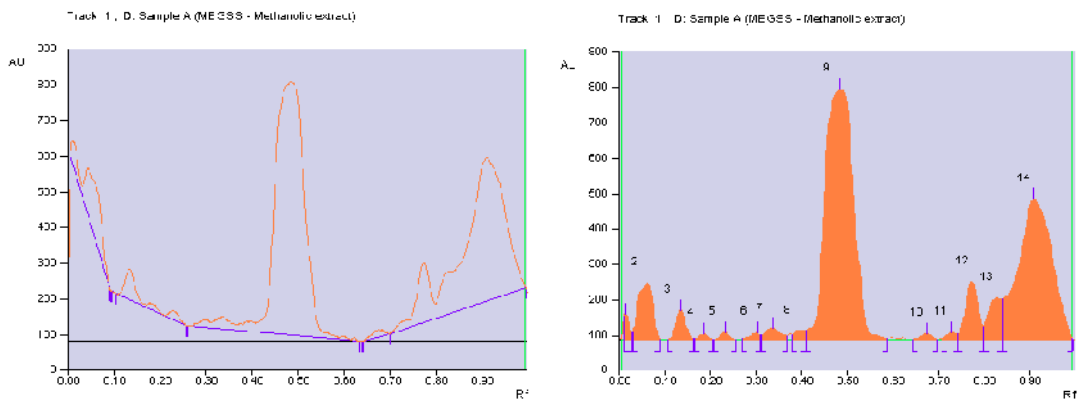

Figure 32

Track B –MGsT Baseline display and Peak densitogram display

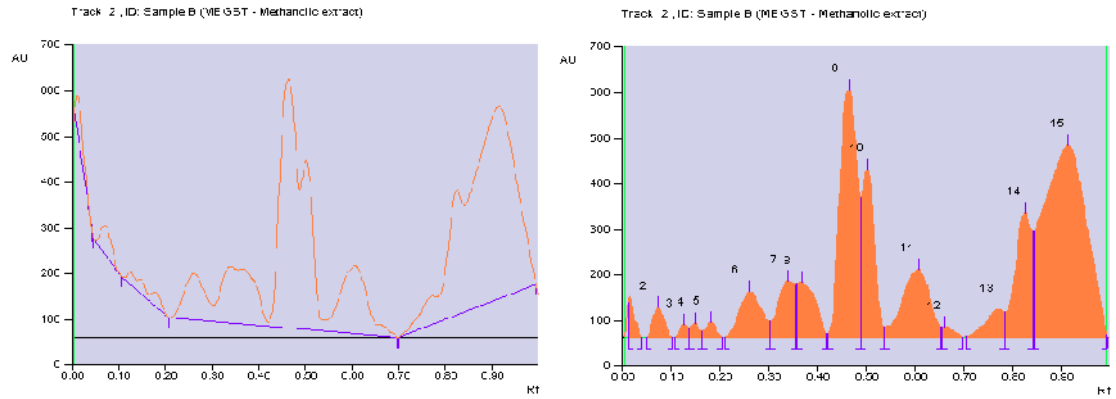

Figure 33

Track C –MGsL Baseline display and Peak densitogram display

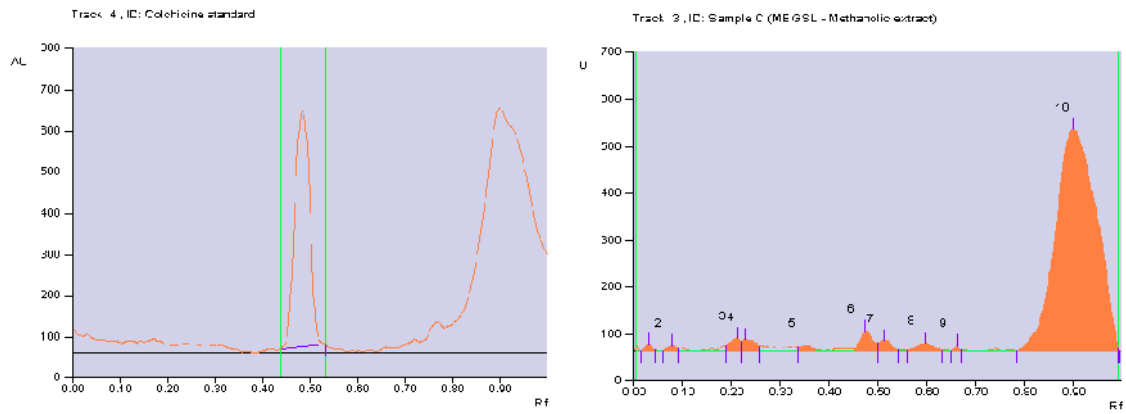

Figure 34

Track D – Colchicine standard Baseline display and Peak densitogram display

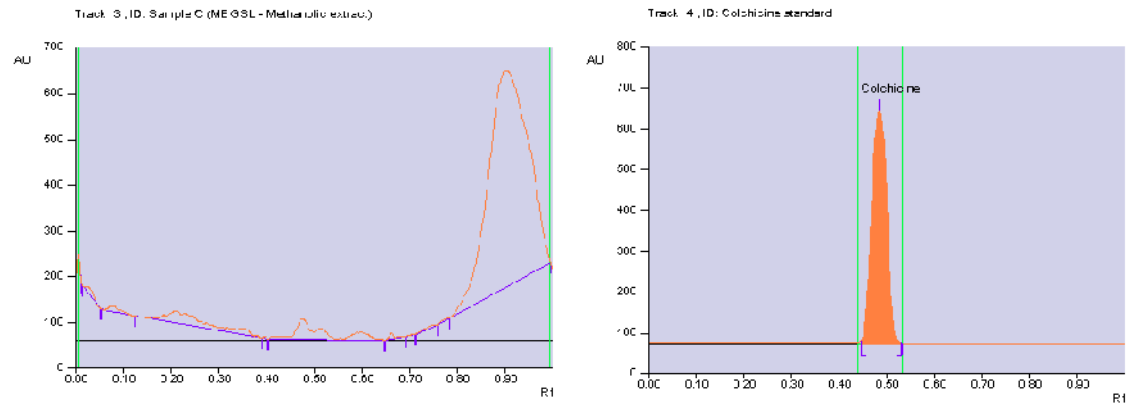

Figure 35

3D display of HPTLC chromatogram of MGsSTL and colchicine

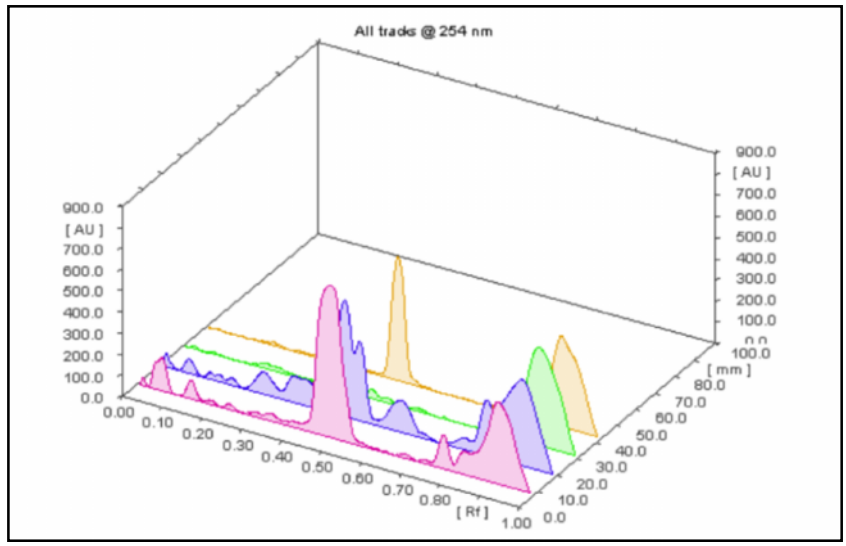

Similarly presence of macrocyclic alkaloids- budmunchiamines in methanolic extract of *Albizia amara* was reported by Rajkumar and Sinha (2010). Methanol mixture of *Clerodendrum viscosum* vent roots showed bands for flavonoid (Prasanth *et al*., 2012) in HPTLC analysis. *Spermacoce hispida* using HPTLC showed the presence of alkaloids, flavonoids, phenolics, steroids, tannins and terpenoids (Rathi *et al*., 2011). HPTLC analysis of N-hexane extract of the whole plant of *Emilia sonchifolia* confirmed the presence of terpenoids (Sophia *et al*., 2011). Yamunadevi *et al*., (2011) showed the presence of 30 different types of steroids in the methanolic extract of stem, leaves, root, flower and seeds of *Aerva lanata*. Methanolic extract of *Albizia lebbeck* leaves demonstrated the presence of 4 different types of alkaloids (Bobby *et al*., 2012). Lakshmi *et al*., (2012) showed the presence of quercetin and rutin in the Acacia Catechu ethanolic leaf extract. The presence of alkaloids and phenolic compounds (Quercetin) of *Barleria cristata* Linn. leaves; Ferulic acid in *Lycopodium clavatum* in HPTLC fingerprint were reported by (Narmadha and Devaki 2012; Srivastava *et al*., 2012).

Cancer is the leading cause of death in developing countries like India. As there is an enormous increase in the population day by day, the alternative therapy in the market is getting its glimpse. The cheap herbal drug is an ideal choice to the rural and poor people to treat effectively the cancers of various type may highly be recommended. Based on that the siddha medicines are coming up in combination with metals and other essential supplements to improve the immune status of the cancer patients in India. The above study revealed the role of *Gloriosa superba* plant and their phytochemicals may be effectively used for cancer treatment.

Results of the phase I and II revealed the antioxidant and antitumorigenic potential of MGsSTL and AgMGsSTL against DLA tumor cells. The presence of colchicine, colchicine derivatives, unknown alkaloids and other related phytoconstituents may be responsible for their activity. Further studies are warranted, for the isolation of the constituents responsible for the activity and also to explore the exact mechanism of action.

4.1.2 Characterization of MGsSTL and AgMGsSTL

Plants or their extracts can be efficiently used in the synthesis of gold and AgNPs as a greener route. Control over the shape and size of NPs seems to be very easy with the use of plants. Such NPs produced using plants have been used in various applications for human benefit. Elucidation of the mechanism of plant-mediated synthesis of NPs is a very promising area of research (Kumar and Yadav, 2009).

4.1.2.1 UV–Visible spectroscopy

The synthesized silver NPs (AgNPs) were analyzed periodically using UV-Visible (UV-Vis) spectrophotometer .The absorbance of the NPs was measured in the range 400-800nm.

Longitudinal plasmon vibrations corresponding to AgNPs were convincing with UV spectral peak and with no absorption peak in control i.e. without reductant. In metalNPs, the conduction band and valence band lies very close to each other in which electrons move freely. These free electrons give rise to a surface plasma

resonance absorption band, occurring due to collective oscillation of electrons in resonance with light wave (Srivastava *et al*., 2011).

The UV-Visibleabsorption spectra of the MGsSTL and AgMGsSTL were shown in figures 36, 37 and 38. Absorption spectra of AgMGsS formed in the reaction media has absorbance maxima at 360 and 440 nm and thus remarkable broadening of peak indicated that the particles are polydispersed. The absorption peak of the AgMGsT and AgMGsL was found at 350 nm. This clearly indicated the interaction between AgNPs and biomolecules present in the MGsSTL.

AgNPs synthesized by biomass of *Lactobaciluus acidophilus* 01 strain revealed the typical silver plasmon absorption maxima at 430nm (Namasivayam *et al*., 2011). AgNPs using *Andrographis paniculata* showed a strong plasmon resonance which was centered approximately at 410 nm (Panneerselvam *et al*., 2011). AgNPs using *Anthoceros* (Bryophyta- Anthocerotae) showed a peak at 425nm (Kulkarni *et al*., 2012). Paul *et al*., (2012) also reported a similar absorption maximum at 445nm by the silver complex during the reaction with the *Musa sapientum* L. leaves and indicated the formation of AgNPs. Colloidal solutions of AgNPs synthesized from *Svensonia hyderobadensis* have absorbance peaks at 300 nm (Rao and Savithramma 2012).

Figure 36

UV-Visible spectra of MGsS and AgMGsS

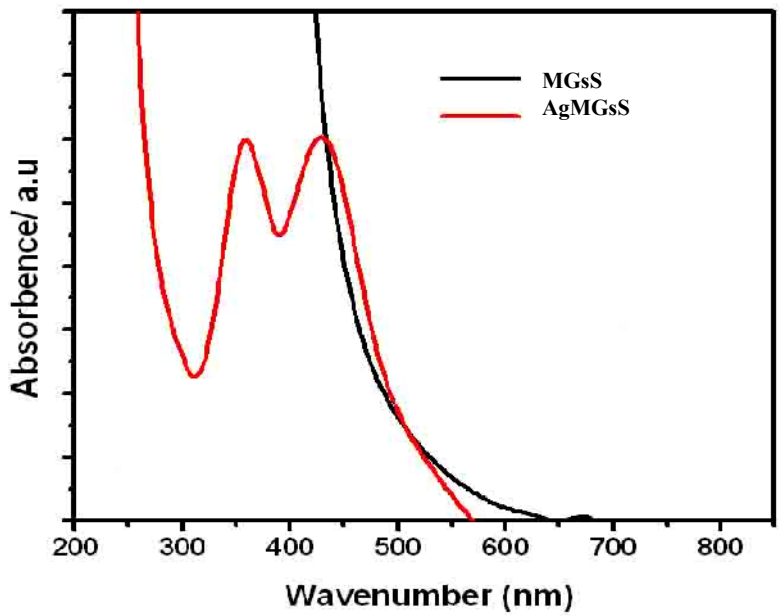

Figure 37

UV-Visible spectra of MGsT and AgMGsT

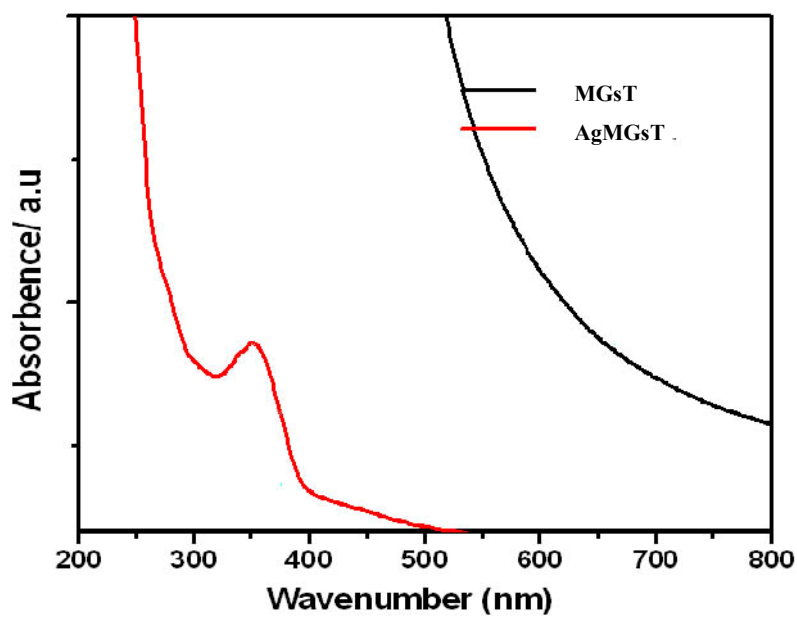

Figure 38

UV-Visible spectra of MGsL and AgMGsL

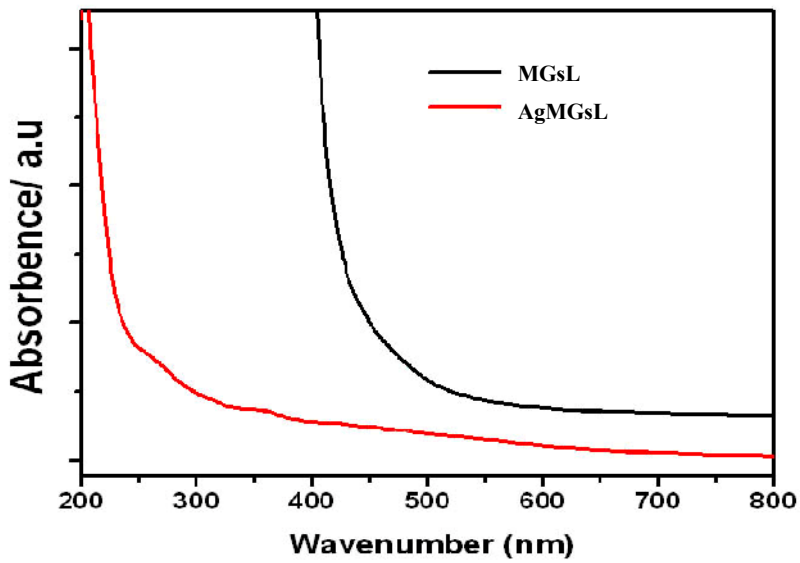

AgNPs of *Senna siamea* leaf extract at surface plasmon resonance band at about 470 nm (Reddy and Gandhi 2012). Colloidal solutions of AgNPs synthesized from *Boswellia* ovaliofoliolata*, Shorea tumbuggaia, Svensonia* hyderobadensis, *Thespesia populnea and V. rosea* have absorbance peaks at 400 nm, 350 nm and 360 nm 340 nm and 335 nm respectively (Savithramma *et al*., 2012). AgNPs synthesized using *Urospora* sp. showed intense band at 430 nm (Suriya *et al*., 2012).

The optimized nano silver thus obtained was quantified and characterized using UV-Visiblespectroscopy. The results emphasized the potent application of MGsSTL in the synthesis of nano silver with economic viability and ease in scaling up for mass production.

4.1.2.2 Fourier Transform Infrared (FT-IR) spectroscopy

It has been reported (Li *et al*., 2007) in literature that plant constituents involved in the reduction and capping of nanoparticle can be identified by FTIR technique. Infrared (IR) radiation refers broadly to that part of the electromagnetic

spectrum between the visible and microwave regions. Of greatest practical use to the organic chemist is the limited portion between 4000 and 400 cm-1 (Udhayakala *et al*., 2011).

An infrared spectrum (IR) represents a fingerprint of a sample with absorption peaks which correspond to the frequencies of vibrations between the bonds of the atoms making up the material. Because each different material is a unique combination of atoms, no two compounds produce the exact same IR. Therefore, IR results is a positive identification (qualitative analysis) of every different kind of material. In addition, the size of the peaks in the spectrum is a direct indication of the amount of material present. With modern software algorithms, IR is an excellent tool for quantitative analysis. Because all of the frequencies are measured simultaneously, most measurements by FT-IR are made in a matter of seconds rather than several minutes (Ali *et al*., 2011 and Vahabi *et al*., 2011).

Measurement was carried out in FTIR to identify the functional group of the compounds present in the MGsSTL and AgMGsSTL. The synthesized silver nanoparticle was confirmed by changes that occurred in the FTIR spectrum after synthesis.

The spectrums of MGsS and synthesized AgMGsS are represented in Figure 39. The peaks 3788- 3414 cm-1 reveal C-H,O-H,N-H stretching vibrations of alcohols and phenols; 3005.10 cm-1 reveal C-H stretching vibrations of aromatic rings; 2924 - 2854 cm-1 reveal C-H stretching vibrations of alkanes, 2299.15 cm^{-1} reveal C=N stretching vibrations of nitriles; 2210.42 cm-1 reveal C=C stretching vibrations of alkynes; 1975.11-1901.81 cm-1 reveal fingerprint region C-H of phenyl ring substitution overtones. 1743.65-1739.79 cm-1 reveal C=O stretching vibrations of aldehydes, ketones, carboxylic acids, esters; 1624.06 cm-1 reveal N-H bending vibrations of primary amine; 1527.62- 1523.76 cm-1 reveal NO_2 asymmetrical stretching vibrations of nitro compounds;1454.33- 1369.46 cm-1 reveal C-H scissoring and bending vibrations of alkanes; 1327.03 cm-1 reveal NO_2 symmetric stretching vibrations of nitro compounds; 1253.73 cm-1 reveal C-O

stretch of alcohols, ethers, carboxylic acids, esters; 1219.01-875.68 cm-1 reveal C-N stretch of amines; 806.25 cm^{-1} reveal out of plan C-H bending vibrations of phenyl ring substitution bands. The FTIR values showed reduction and capping of silver ion which may be due to the presence of alkaloids (colchicine and its derivatives). Particularly the peak at 3788.19, 3734.19, 2854, 1743.65, 1527.62, 1381.03, 1056.99 cm^{-1} of MGsS changed to 3730.33, 3618.46, 2924.09, 2858.51, 1739.79, 1523.76, 1369.46, 1022.27 cm-1 after synthesis confirming the reduction of silver ion to silverNPs (AgMGsS).

These absorbance bands are known to be associated with the stretching vibrations for –C C–C O, –C C– [(in-ring) aromatic], –C–C– [(in-ring) aromatic], C–O (esters, ethers) and C–O (polyols).

The FTIR spectrums of MGsT and synthesized AgMGsT are represented in Figure 40. The peaks 3599.17- 3414cm-1 revealed C-H,O-H,N-H stretching vibrations of hydrogen bonded alcohols and phenols; 2924.09cm-1 reveal C-H stretching vibrations of alkanes; 2854.65 cm-1 reveal O-H stretching vibrations of carboxylic acids; 2233.57- 2160.27 cm-1 reveal C-N conjugated nitriles and any isocyanides; 1755.22-1681.93 cm-1 reveal C=O stretching vibrations of aldehydes, ketones, carboxylic acids, esters; 1647.21-1608.63 cm-1 reveal bending (scissoring) vibrations in N-H of primary amine; 1512.19 cm-1 reveal asymmetrical stretch in NO_2 of nitro compounds; 1450.47-1377.17 cm-1 reveal scissoring and bending in C-H of alkanes; 1315.45 cm-1 reveal stretch in C-N of amines;1246.02 cm-1 reveal stretch in C-O of alcohols, ethers, carboxylic acids, esters; 1157.29-1041.56 cm-1 reveal stretch in C-N of amines; 1018.41 cm-1 reveal C-O stretch of alcohols, ethers, carboxylic acids, esters and 933.55-709.80 cm-1 reveal out of plan C-H bending vibrations of alkenes. The FTIR values showed reduction and capping of silver ion which may be due to the presence of alkaloids. Particularly the peak at 1647.21, 1381.03, 860.25, 763.81 cm-1 of MGsT changed to 1639.49, 1377.17, 879.54, 783.10 cm-1 after synthesis confirming the reduction of silver ion to silverNPs (AgMGsT).

The FTIR spectrums of MGsL and synthesized AgMGsL are represented (Figure 41). The peaks 3595.31 - 3414 cm-1 reveal C-H,O-H,N-H stretching vibrations of hydrogen bonded alcohols and phenols; 2924.09cm-1 reveal C-H stretching vibrations of alkanes; 2854.65 cm-1 reveal O-H stretching vibrations of carboxylic acids; 1786.08 cm-1 reveal fingerprint region in C-H of phenyl ring substitution overtones; 1724.36-1685.79 cm-1 reveal stretch in C=O of aldehydes, ketones, carboxylic acids, esters; 1627.92 cm-1 reveal N-H bending (scissoring) vibrations in primary amine; 1516.05 cm-1 reveal N-H bending vibrations of amide II band; 1442.75-1381.03 cm-1 reveal scissoring and bending in C-H of alkanes; 1330.88 cm-1 reveal stretching in C-N of amide III band; 1257.59 cm-1 reveal stretch in C-O of alcohols, ethers, carboxylic acids, esters; 1157.29-1033.85 cm-1 reveal C-N stretch of amines; 1014.56 cm-1 reveal C-O stretch of alcohols, ethers, carboxylic acids, esters and 898.83- 744.52 cm-1 reveal out of plan C-H bending vibrations of alkenes.

Figure 39

FT-IR spectra of MGsS and AgMGsS

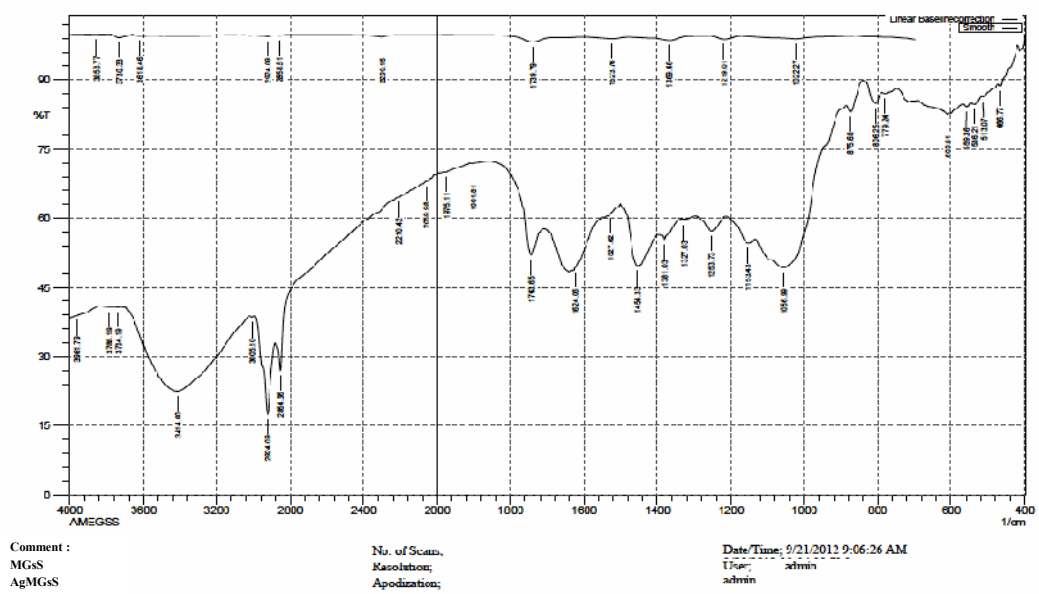

The FTIR values showed reduction and capping of silver ion which may be due to the presence of alkaloids. Particularly the peak at 1442.75, 1381.03, 1033.85 cm-1 of MGsL changed to 1415.75, 1330.88, 1014.56 cm-1 after synthesis confirming the reduction of silver ion to silverNPs (AgMGsL).

The FTIR spectrum of MGsS showed 28 peaks; MGsT showed 21 peaks and MGsL showed 20 peaks. Compared to the standard colchicine FTIR spectrum, MGsS and AgMGsS showed significant peaks at 2924 (both) corresponding to -CH_2- group, peak at 1527 (MGsS) reduced to 1523 (AgMGsS) corresponding to –NH_2– groups; and for the MGsT significant peak found at 1647 reduced to 1639 (AgMGsT) attributed to –CO– groups and for MGsL and AgMGsL no such significant peaks of colchicine and colchicine derivatives were found but other phytoconstituents may be responsible for capping. Hence, it may be assumed that these -CH_2- groups, –CO– groups and –NH_2– groups of colchicine and colchicine derivatives and also other phytoconstituents of MGsS, MGsT and MGsL are responsible for capping and efficient stabilization, reduction of silver ions and formation of the NPs.

Figure 40

FT-IR spectra of MGsT and AgMGsT

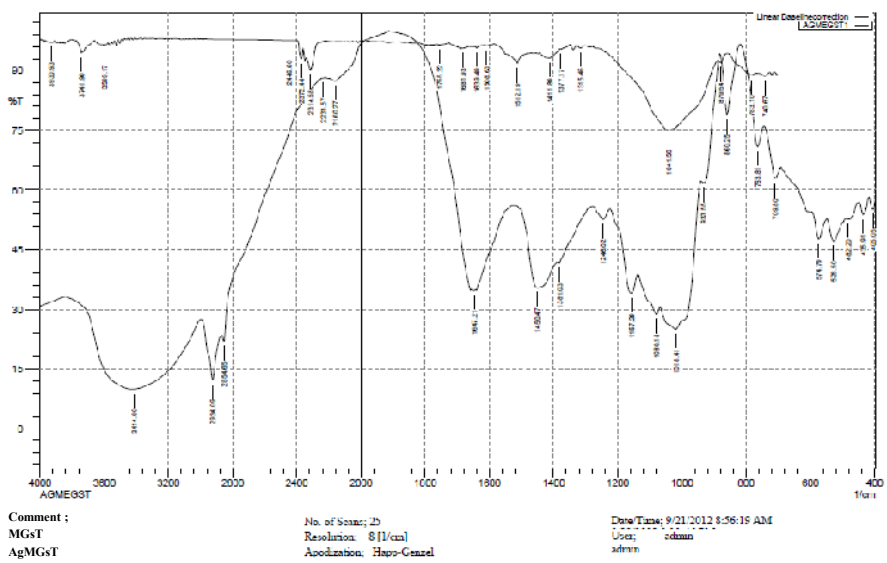

Our findings were also supported by several research. Jain *et al*., (2009) who stated that the 1226 cm-1 band arises most probably from the C–O group of polyols such as hydroxyl flavones and catechins present in the papaya fruit extract which are responsible for the reduction of Ag ions. Mallikarjuna *et al*., (2011) who showed that the FTIR analysis of silver NPs of *Ocimum sanctum* confirmed the carbonyl group from the amino acid residues and proteins has the stronger ability to bind metal indicating that the proteins could possibly from the metalNPs (i.e., capping of silver NPs) to prevent agglomeration and thereby stabilize the medium. Carboxyl (-C=O), hydroxyl (-OH) and amine (N-H) groups of mulberry leaves extract are mainly involved in reduction of Ag+ to Ag^{o} NPs (Awwad and Salem 2012). Hydroxyl, alkanes, C=C of benzene, aromatic amines and aliphatic amines functional groups of *Bryophyllum pinnatum* leaf extract strongly supported the capping behaviour of bioreduced AgNPs synthesized which in turn imparted the high stability of the synthesized AgNPs (Baishya *et al*., 2012).

Figure 41

FT-IR spectra of MGsL and AgMGsL

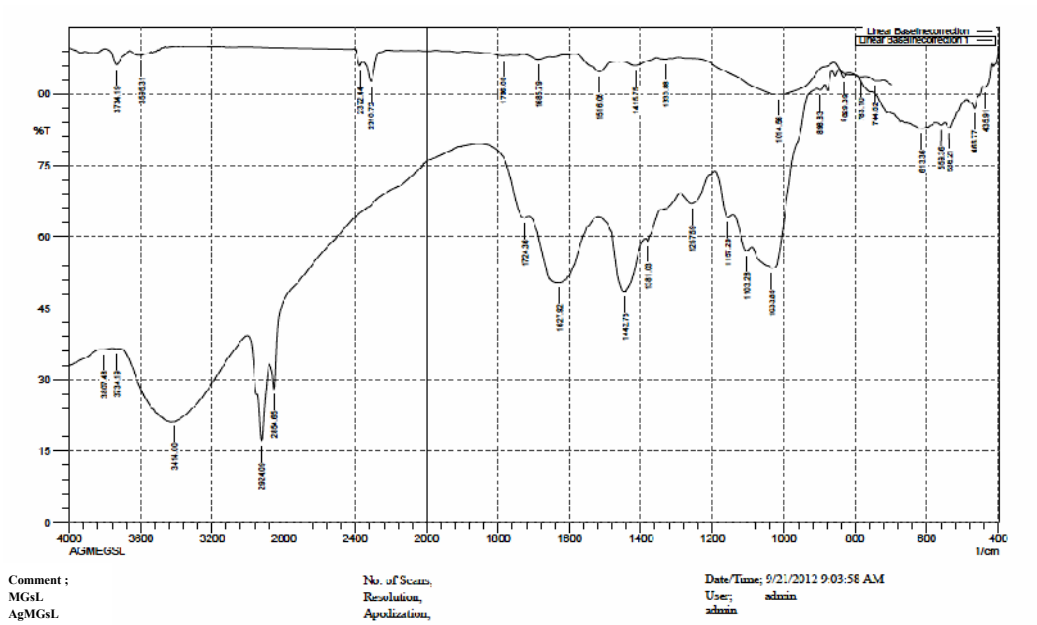

Anthraquinones, carbohydrates, glycosides, cardiac glycosides, amino acid, phytosterols, fixed oils and fats, phenolic compounds, tannins, flavonoids, steroids and saponins of leaf extract of *Cassia tora L. as reducing as well as capping agent of* AgNPs (Sathya and Ambikapathy *et al*., 2012). Stabilization is achieved by the phenolic as well as aromatic compounds present in the extract of Ocimum sanctum (Ramteke *et al*., 2013). Capping and stabilization AgNPs is also achieved by alkenes, alcohols, amines, carboxylic acids and amines group of *Nerium oleander* (Roni *et al*., 2013).

Peak at 1728 cm−1 and disappearance of the peak at 2122 cm−1 confirmed that the reduction of the silver ions is coupled to the oxidation of the hydroxyl and carbonyl groups, indicative of more extensively oxidized nature of the Anogeissus latifolia (Kora *et al*., 2012). Peak at 3399 cm^{-1}, 2145 cm^{-1} 1648 cm^{-1} and 727cm^{-1} correspond to N-H, C=C group, C=O functional group and C-Cl functional group present in *Azadiracta indica* are involved in the formation of AgNPs (Natarajan *et al*., 2012). Particularly the peak at 1635 cm-1 of extract changed to 1637 cm-1 after synthesis confirming the reduction of silver ion to AgNPs by the alkaloids present in the *Datura metel* flower (Nethradevi *et al*., 2012). FTIR spectroscopy of *Cassia auriculata* leaf extract indicated that the compounds attached with silver NPs could be polyphenols with aromatic ring and bound amide (Parveen *et al*., 2012). Carboxyl (–C=O), hydroxyl (–OH) and amine (–NH) groups of *Callicarpa maingayi* stem bark extracts are mainly involved in fabrication of AgNPs (Shameli *et al*., 2012). *Spirulina* have been recorded the peak in the region of frequency ranges from 1750-1735 cm-1 representing C=O stretching vibration (ester and amino acid) and from 1435-1405 cm-1 peak are present in the CH_2 bending vibration (Venkatesan *et al*., 2012).

The FTIR analysis confirmed that the bioreduction of silver ions to AgNPs was due to the reduction by capping material of MGsSTL. The present study, thus showed a simple green route for rapid and economical synthesis of silver NPs.

4.1.2.3 Scanning Electron Microscope (SEM) and Energy Dispersive Spectroscopy (EDX)

The size of the AgNPs was determined by the Scanning Electron Microscopy (SEM) and elemental composition of the AgNPs was further confirmed by the Energy Dispersive X-ray (EDX) analysis.

The SEM uses a focused beam of high-energy electrons to generate a variety of signals at the surface of solid specimens. The signals that derive from electron sample interactions reveal the information about the sample including external morphology (texture), chemical composition, crystalline structure and orientation of materials making up the sample. In most applications, datas are collected over a selected area of the surface of the sample, and a two-dimensional image is generated that displays spatial variations in these properties. For this purpose, thin films of the samples were prepared on carbon coated copper grids by just dropping a very small amount of the sample on the grid, extra solution was removed using a blotting paper and the films on the SEM grid were allowed to dry under a mercury lamp for 5 min (Rao and Savithramma 2011 and Priya *et al*., 2011). Energy Dispersive Analysis of X-ray (EDAX) gives qualitative as well as quantitative status of elements that may be involved in the formation of AgNPs (Vimala *et al*., 2011).

The SEM images of AgNPs are shown in Figures 42 to 45 which ranged from 35 - 42 nm for AgMGsS and 44 - 90 nm for AgMGsT. It gave a clear image of highly dense AgNPs. The SEM image showed the silver nanostructures of AgMGsS and AgMGsT.

The UV-Visible spectral analysis is reconfirmed using other advanced spectroscopic techniques like XRD and Energy Dispersive X-ray (EDAX) analysis. Figures 42, 43, 44 and 45 show the EDX plot of SEM image of AgMGsS and AgMGsT. The EDAX reading proved the presence of silver present in the EDAX pictures of AgMGsS and AgMGsT. This is probably due to the presence of substrate over which the nanoparticle was held during SEM microscopy. Metallic silver nanocrystals generally show typical optical absorption peak approximately at

3 keV due to surface plasmon resonance. This analysis revealed that the nano-structures were formed solely of silver.

Figure 42

SEM micrograph of AgMGsS

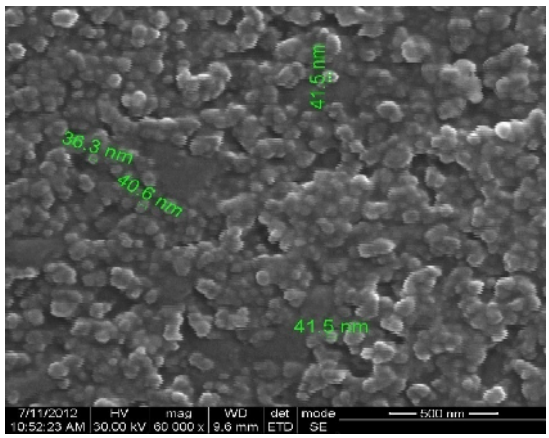

Figure 43

EDAX spectrum of AgMGsS

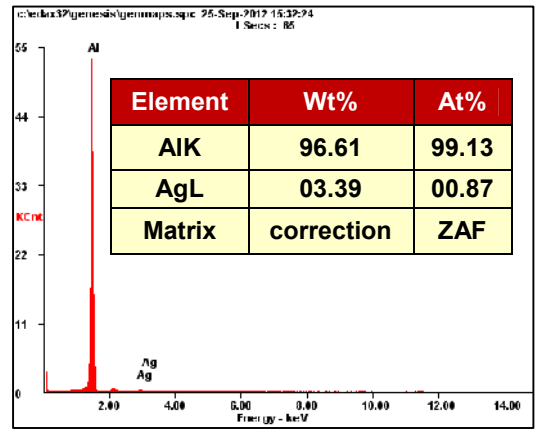

Element	Wt%	At%
AlK	96.61	99.13
AgL	03.39	00.87
Matrix	correction	ZAF

Similar findings of the SEM and EDX characterization revealed that the AgNPs synthesised from *Glycyrrhiza glabra root extract* having nearly spherical shape particles of size 20–30 nm (Dinesh *et al*., 2012). AgNPs using *Chromolaena odorata* leaf extract showed relatively hexagonal shape AgNPs formed with diameter range 40-60 nm and EDX spectrometer confirmed the presence of elemental silver signals of the AgNPs (Geetha *et al*., 2012).

Figure 44

SEM micrograph of AgMGsT

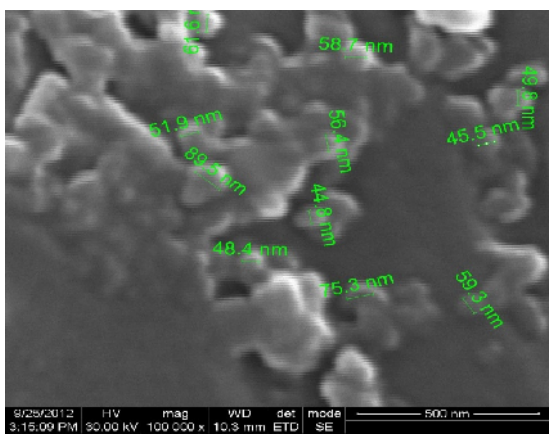

Figure 45

EDAX spectrum of AgMGsT

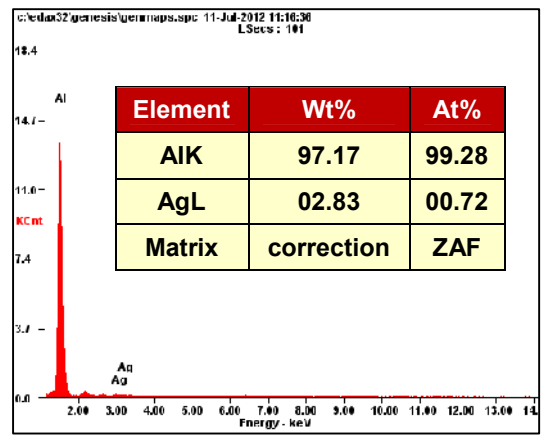

Element	Wt%	At%
AlK	97.17	99.28
AgL	02.83	00.72
Matrix	correction	ZAF

SEM micrograph of AgNPs using mushroom extracts showed spherical aggregated form and its size range was found to be 80-100 nm (Mirunalini *et al*., 2012). NPs of *Ulva fasciata* crude ethyl acetate extract having spherical shape and poly-dispersed with size ranging from 28 to 41 nm (Rajesh *et al*., 2012). AgNPs of *Azadirachta indica*- neem leaf extract revealed the particles size of 40nm-130nm (Renugadevi and Aswini 2012). AgNPs of Ashwagandha ranges from 5nm - 40nm (Nagati *et al*., 2012). AgNPs from *Cardiospermum helicacabum* leaf extracts have skew spheroid in shape and in the range of 5-50nm (Vishnudas *et al*., 2012).

The SEM and EDX images showed the high density AgMGsST further confirmed the development of silver nanostructures.

4.1.2.4 Transmission Electron Microscope (TEM)

The collected silver NPs were characterized by XRD and TEM for formation of crystalline structure, mean size and morphology (Das *et al*., 2011). TEM is commonly used for imaging and analytical characterization of the NPs to assess the shape, size, and morphology. The outstanding resolution achieved by TEM is an excellent fit for these extremely challenging studies (Zargar *et al*., 2011).

The TEM (Figures 46 and 47) analysis expose predominantly spherical shaped AgNPs. The high resolution TEM images of AgMGsS indicated good crystallinity of the NPs compared to AgMGsT. The morphology of AgMGsS was found to be more clearly seen than that of AgMGsT and the particles are being predominantly spherical, polydispersed and ranged in size from 20-69 nm and capped by plant constituents that prevented their aggregation.

Inherent capping offers additional advantage of the stability in the green chemical synthesis. Some NPs appear to have assembled into very open, quasi-linear super structures rather than a dense closely packed assembly and some are dense closely packed. The TEM images also revealed that NPs are not in physical contact but are separated by uniform interparticle distance. The reason for these large-sized particles is due to the aggregation of two or more NPs together which in turn result due to the presence of excess amounts of reducing moieties and the

interactions between stabilizing molecules bound to the surface of particles and secondary reduction process on the surface of the preformed nuclei. It was noticeable that the edges of the particles were lighter than the centers, suggesting that some bioorganic compounds such as alkaloids (colchicines and its derivatives) in MGsS and MGsT, capped the silver NPs contributing to reduction of Ag+ ions to Ag^0.

Figure 46

TEM micrograph of AgMGsS

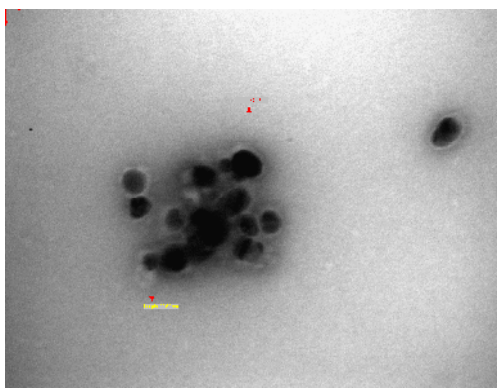

Figure 47

TEM micrograph of AgMGsT

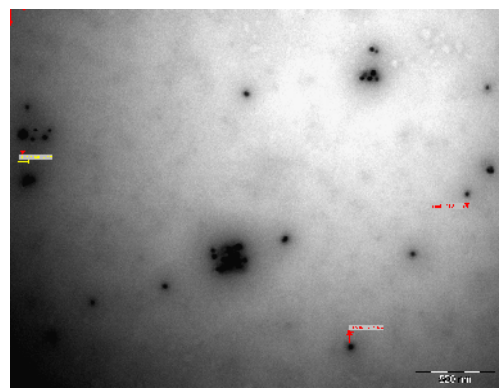

The above result was supported by the uniform spherical NPs of nanosilver (Nanocid®) in the size range of 7–20 nm (Moaddab *et al*., 2011). *Cleome Viscosa* showed spherical AgNPs with the average size range from 7 nm to 50 nm which could be correlated with the morphology of the spherical NPs (SudhaLakshmi *et al*., 2011). Silver and gold NPs using Pomegranate peel extract showed that the average particle size of AgNPs were 5 ±1.5 nm whereas the AuNPs were found to be 10 ±1.5 nm (Ahmad *et al*., 2012). AgNPs from the extract of seed of *Punica granatum* suggested that the size of particles is 5- 20nm (Chauhan and Upadhyay 2012). AgNPs synthesized by the Seaweed *Ulva lactuca* revealed that AgNPs were spherical in shape and measured 20-56nm in size (Devi and Bhimba 2012). This corroborates with the previous observation of the leaf extract of *Morinda pubescens* synthesised AgNPs ranged from 20-40nm and equally spherical shaped orthorhombic crystals (Mary and Inbathamizh 2012). AgNPs of *Panicum virgatum* with the size range between 20 and 40 nm (Mason *et al*., 2012).

Thus, the TEM analysis showed the presence of uniform, spherical, polydispersed AgMGsS and AgMGsT with the size 20-69 nm and were capped by their bioorganic compounds such as colchicine and colchicine derivatives and other phytoconstituents.

4.1.2.5 Dynamic Light Scattering (DLS)

Particle size distribution was plotted using the results obtained from DLS (Devi *et al*., 2012).

The Figure 48 shows the particle size as measured using the Malvern mastersizer of the AgMGsS sample. After analyzing the data, it was found that AgMGsS size in the range of 3-110 nm. However in AgMGsS, beyond 100 nm range the percentage of NPs present is very less. Figure 49 and 50 show the graphical representation of average particle size distribution of AgMGsT and AgMGsL in the range of 3-229 nm and 6-477 nm respectively. The highest fraction of AgMGsS, AgMGsT and AgMGsL present in the solution were of 34nm, 61nm and 71nm. From the plot it was evident that the solution consists of NPs having various size which are indeed in agreement with the results obtained by SEM analysis.

The ability of NPs to alter the biodistribution and pharmacokinetics of drugs, have important in *in vivo* therapeutic applications. In this respect, the size and surface characteristics of NPs are of prime importance. NPs of fewer diameters with hydrophilic surface have longer circulation in blood. Such systems prolong the duration of drug activity and also increase the targeting efficiencies to specific sites (Tripathi *et al*., 2010). The *particle size distribution* of AgMGsS, AgMGsT and AgMGsL were found to be 3-110 nm, 3-229 nm and 6-477 nm. These smaller diameter may increase the targeting efficiencies to specific sites to prolong the duration of the drug activity.

Figure 48

Particle size distribution histogram of AgMGsS

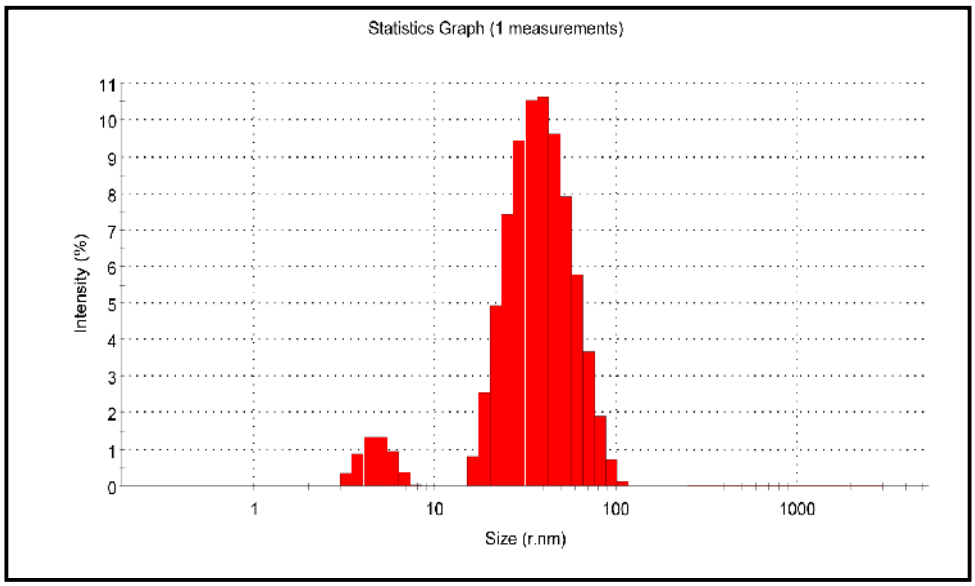

Figure 49

Particle size distribution histogram of AgMGsT

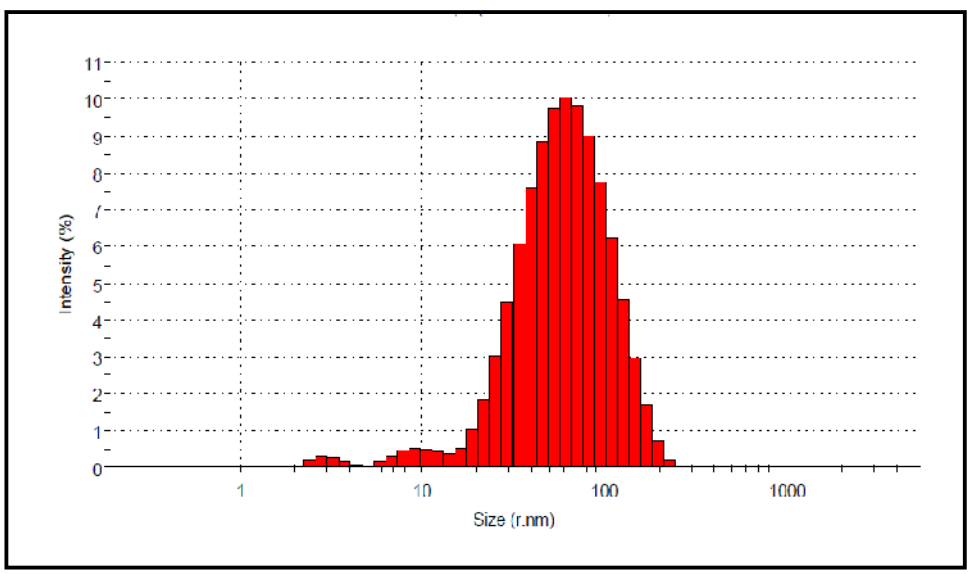

Figure 50

Particle size distribution histogram of AgMGsL

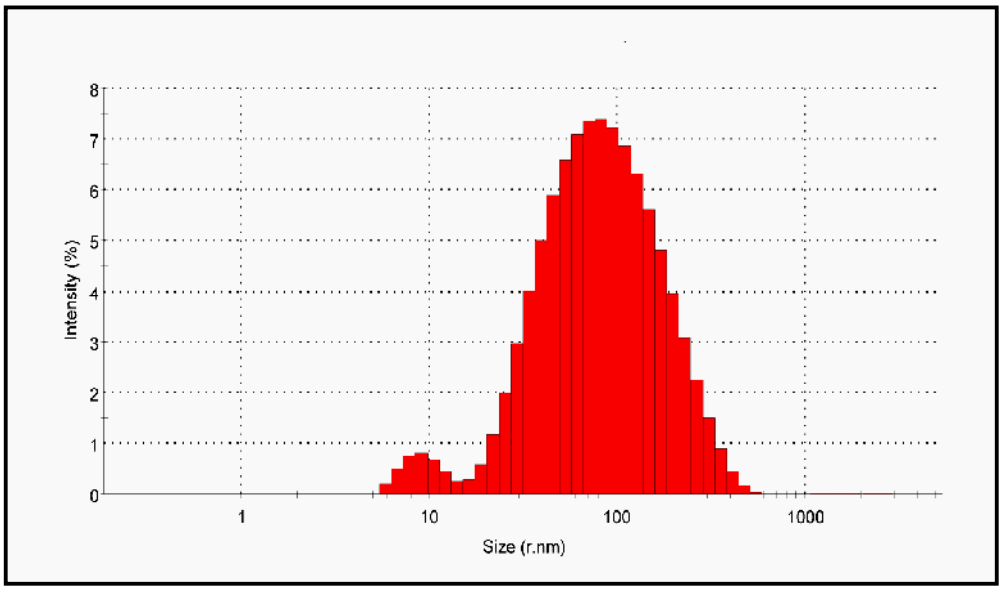

Ostad *et al*., 2010 showed the particle-size histogram of AgNPs of dextrose ranging from 1 nm to 28 nm. The mean diameter of ethanolic extract of *Polygala senega* Poly (d,l-lactide-co-glycolic acid) encapsulated AgNPs was found to be 147.7 nm (Paul *et al*., 2011). Phytolacca decandra AgNPs had 91nm particle size, with polydispersity index of 0.119 (Bhattacharya *et al*., 2012). Ethyl acetate of *Justicia genderussa* reduced AgNPs were distributed from 11-20 nm with average size of 16 nm (Chinna and Prabha, 2012). DLS data showed *Dioscorea oppositifolia* of rhizome extracts with the size of about 14 nm (Maheswari *et al*., 2012). DLS of AgNPs of leaf extract of *Vinca Roseus* represented the average particle size distribution of 45nm (Prakash and Paul 2012). Average size of spherical AgNPs of sodium citrate was about 30 nm (Zhou and Wang 2012).

4.1.2.6 Zeta-potential

Zeta-potential measurements were performed for direct comparison to conventional studies of NPs stability (Kumar and Yadav 2011; Hanaor *et al*., 2012). Zeta-potential analysis demonstrated that the AgMGsS, AgMGsT and AgMGsL had negative charges of −57.0mV, −47.3mV and −27.0mV respectively (Figures 51, 52 and 53). AgMGsS and AgMGsT were found to be more sufficiently

charged to maintain stable dispersion at room temperature in solution over several months of time than that of AgMGsL.

Zeta-potential of the NPs was measured in 0.1 mM NaCl using Malvern Zetasizer. The zeta potential is a measure of the charge of the particles, as such the larger the absolute value of the zeta potential the larger the amount of charge of the surface. In a sense, the zeta potential represents an index for particle stability. For the charged particles, as the zeta potential increases, the repulsive interactions will be larger leading to the formation of more stable particles with a more uniform size distribution (Kittler *et al*., 2010).

Figure 51

Zeta potential of AgMGsS

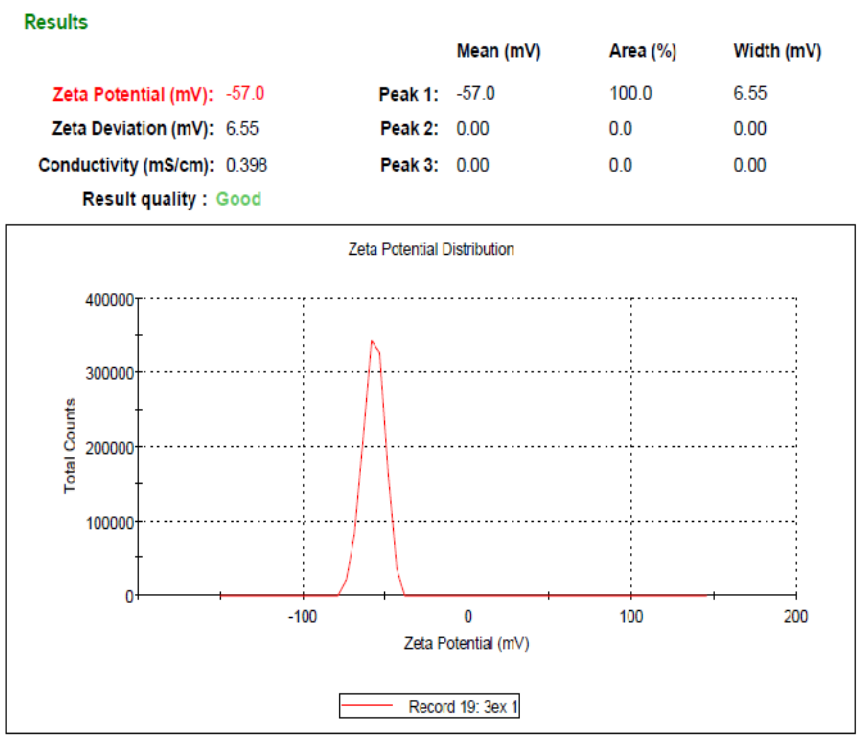

Figure 52

Zeta potential of AgMGsT

Results

		Mean (mV)	Area (%)	Width (mV)
Zeta Potential (mV): -47.3	Peak 1:	-47.3	100.0	6.89
Zeta Deviation (mV): 6.89	Peak 2:	0.00	0.0	0.00
Conductivity (mS/cm): 0.301	Peak 3:	0.00	0.0	0.00
Result quality : Good				

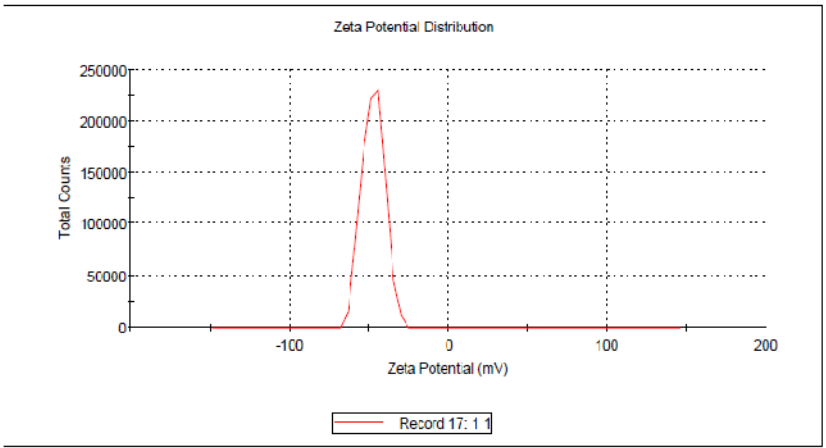

Figure 53

Zeta potential of AgMGsL

Results

		Mean (mV)	Area (%)	Width (mV)
Zeta Potential (mV): -27.0	Peak 1:	-27.0	100.0	7.25
Zeta Deviation (mV): 7.25	Peak 2:	0.00	0.0	0.00
Conductivity (mS/cm): 0.472	Peak 3:	0.00	0.0	0.00
Result quality : Good				

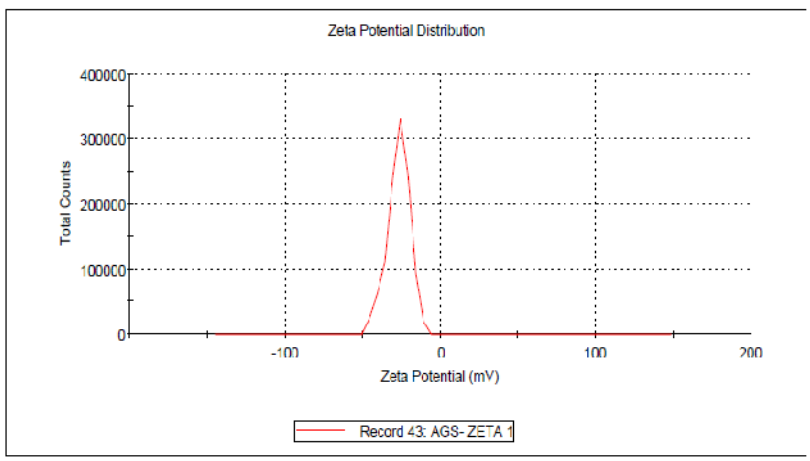

A similar surface charge analysis of 5-fluorouracil loaded albumin NPs was found to be -30.3 mV (Ambika *et al*., 2012). The zeta potential of ethanolic extract of *Ziziphus mauritiana* leaf NPs was found to be 30mV (Bhatia *et al*., 2011). Zeta potential measurements of AgNPs of *Sargassum tenerrimum* are highly stable with a value of –27 mV (Kumar *et al*., 2012). Zeta potential of AgNPs of *Rhododendron dauricum* flower aqueous extract solution was found to be -18 mV (Mittal *et al*., 2012). Garlic extract and citrate-stabilized NPs had negative charges of −31mV and −30mV (VonWhite *et al*., 2012). Zeta potential of AgMGsSTL synthesized using MGsSTL showed the good stability of AgMGsS, moderate stability of AgMGsT and incipient instability of AgMGsL.

4.1.2.7 X-RAY Diffraction (XRD) analysis

According to Mie scattering theory, a decrease in *Full Width Half Maximum* (FWHM) suggested an increase in AgNPs core-diameter. The morphology and the nanocrystalline size of AgNPs were determined from characteristic peaks obtained from the XRD image (Vijayaraj *et al*., 2012). Figures 54, 55 and 56 show the XRD pattern of AgMGsS, AgMGsT and AgMGsL. The data obtained was matched with the database of Joint Committee on Powder Diffraction Standards (JCPDS) file No. 04-0783. The presence of peaks at 2θ values at 38.15°, 46.28°, 77.34° for AgMGsS showed the number of strong Bragg reflections which correspond to (111), (200), (311) planes of silver and 2θ values at 38.60°, 46.32, 64.48°, 77.34° for AgMGsT showed the number of strong Bragg reflections which correspond to (111), (200), (220), (311) planes of silver. Where as 2θ value at 38.30° showed the number of strong Bragg reflections which correspond to (111) plane of silver for AgMGsL (Table 6). Thus, the XRD spectrum confirmed the crystalline structure of AgNPs. All the peaks in XRD pattern can be readily indexed to a face-centered cubic structure of silver.

The average particle size of AgNps was calculated by the use of full width at half maximum (FWHM) of *face-centered cubic* (111) using the Debye–Scherrer equation, $k\lambda / \beta \cos\Theta$, where K is the Scherrer constant with value from 0.9 to 1, λ is the wavelength of the X-ray, β is the full width at half maximum and θ is the Bragg angle in radians.

Table 6

X-RAY Diffraction pattern of AgMGsSTL

		2θ values			
AgMGsS	32.10°	38.15°	46.28°		77.34°
AgMGsT		38.60°	46.32°	64.48	77.34°
AgMGsL		38.30°			
Hkl(Diffraction peaks)		(111)	(200)	(220)	(311)

Debye-Scherrer's equation

$D = K\lambda / \beta . \cos\theta$

Where,

$\beta = \pi / 180 * FWHM$

(FWHM= Full Width Half Maximum)

K= 0.94

λ= 1.540598 Ao

Kλ= 0.94 * 1.540598 Ao

= 1.4482

Table 7

Measurement of the crystalline size of AgMGsS using Debye-Scherrer's equation

S.No	2θ	β= π / 180 * FWHM	Cosθ	D = Kλ / β.Cosθ
1.	32.10°	0.03	0.96	5.17nm
2.	38.15°	0.05	0.95	3.05nm
3.	46.28°	0.03	0.92	5.17nm
4.	77.34°	0.06	0.78	3.08nm

Table 8

Measurement of the crystalline size of AgMGsT using Debye-Scherrer's equation

S.No	2θ	β= π / 180 * FWHM	Cosθ	D = Kλ / β.Cosθ
1.	38.60°	0.03	0.94	4.83nm
2.	64.48°	0.04	0.85	4.26nm
3.	77.34°	0.04	0.78	4.67nm

Table 9

Measurement of the crystalline size of AgMGsL using Debye-Scherrer's equation

S.No	2θ	β= π / 180 * FWHM	Cosθ	D = Kλ / β.Cosθ
1.	38.30°	0.04	0.81	6.03nm

From the Scherrer equation the average crystalline size of AgMGsS was found to be about 5.17 nm, 3.05nm, 5.17nm and 3.08 nm as shown in Table 7. The average crystalline size of AgMGsT was found to be about 4.83 nm, 4.26nm and 4.67 nm (Table 8). And the average crystalline size of AgMGsL was found to be about 6.03 nm (Table 9).

The typical XRD pattern revealed the cubic structure of AgNPs. The observed peak broadening and noise were probably related to the effect of nanosized particles and the presence of various crystalline biological macromolecules in the plant extracts. The obtained results illustrated the silver ions had indeed been reduced to Agº by plant extract under reaction conditions. A number of Bragg reflections corresponding to the (111), (200), (220) and (311) sets of lattice planes are observed which may be indexed based on the face centered cubic (fcc) structures of silver and peaks were also observed suggesting that the crystallization of bio-organic phase occurs on the surface of the AgNPs (Krishnaraj *et al*., 2010).

Figure 54

XRD of AgMGsS

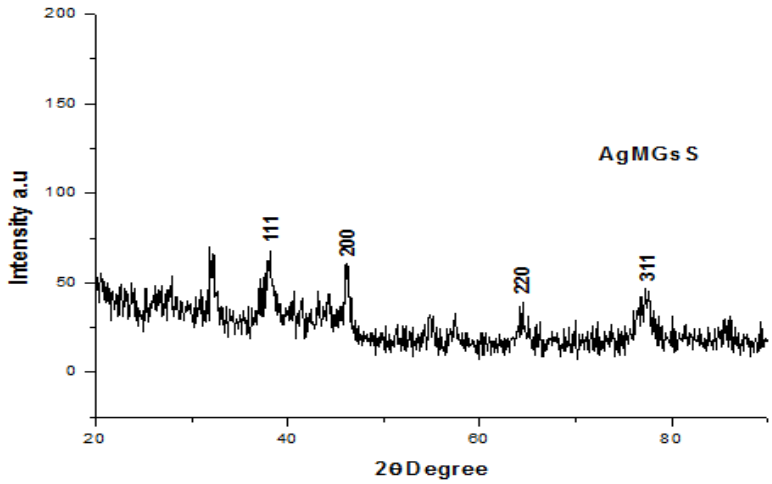

Figure 55

XRD of AgMGsT

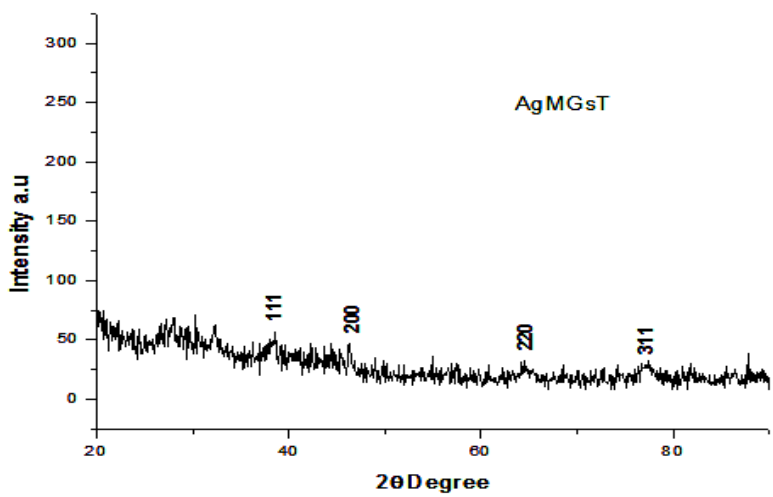

Figure 56

XRD of AgMGsL

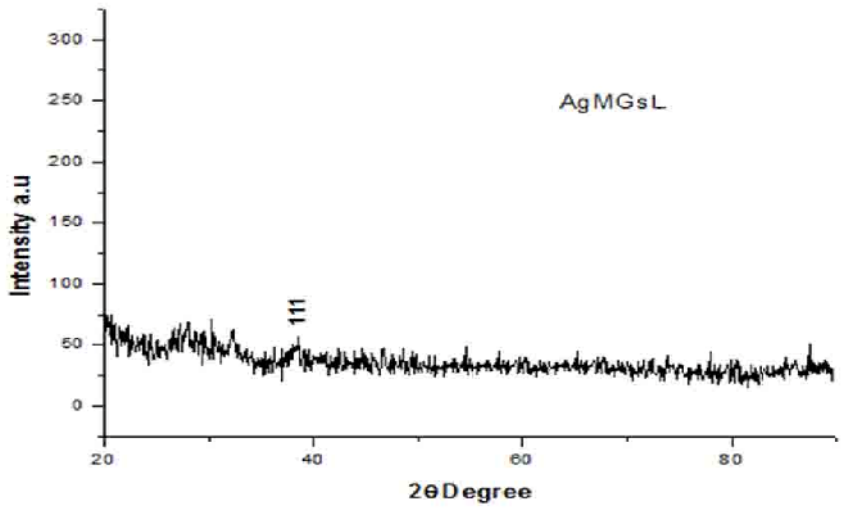

The XRD pattern of AgNPs of *Cissus quadrangularis* revealed a crystalline silver centered cubic structure with a particle size of the sample 41.0 nm derived from the FWHM of peak corresponding to (1 1 1) plane (Alagumuthu and Kirubha 2012). XRD pattern of the four diffraction peaks at 38.2°, 44.1°, 64.3° and 78° are indexed as (111), (200), (220) and (311) planes of face centered cubic silver indicated that the nanocrystals are present in the AgNPs of methanol extract from *Solanum xanthocarpum* berry (Amin *et al*., 2012). Bragg reflections corresponding to the (111), (200), (220) and (311) sets of lattice planes are observed which may be indexed based on the face centered cubic (fcc) structures of silver peaks suggesting that the crystallization of bioorganic phase occurs on the surface of the AgNPs of *Mollugo nudicaulis* (Anarkali *et al*., 2012). AgNPs synthesized from aqueous extracellular *Elettaria cardamomum* seed extract showed three intense peaks at 38^{o}, 47^{o}, and 77^{o} corresponding to 111, 200 and 311 planes in the whole spectrum of 2*θ* proposes the crystalline nature (Jobitha *et al*., 2012). XRD analysis of AgNPs synthesized by *Aristolochia bracteata* revealed ten peaks at degree (2θ) 10.00, 11.70, 12.60, 18.37, 21.29, 25.37, 27.80, 32.21, 38.40 and 46.07 and the average particle size to be 7.2nm (Raj *et al*., 2012). AgNPs synthesized using sphaernathus amaranthoides ethanol extract showed characteristic peaks (at 2θ =

30.8◦), marked with (111) sets of lattice planes which may be indexed based on the face-centered cubic and tubular structure of silver are crystalline in nature (Swarnalatha *et al*., 2012). *S*ilver NPs synthesized by *Sargassum* polycystum extract showed the presence of intense peaks of NPs (111), (200) and (211) which are indexed as crystalline silver centered cubic *phase* (Thangaraju *et al*., 2012). AgNPs of Euphorbia prostrata in the form of nanocrystals, as evidenced by the peaks at 2θ values of 23.22°, 27.85°, 30.91°, 31.80°, 32.00°, 34.62°, 35.34°, 38.26°, 44.45° ,45.38° ,64.58° and 77.49°. The pure silver lattice constant has been estimated to be Alpha=4.081(Zahir *et al*., 2012).

The XRD study showed the face-centered cubic lattice of AgNPs. It was concluded, that the typical XRD pattern confirm the crystalline structure of AgNPs of AgMGsSTL.

Reduction of silver ions present in the aqueous solution of silver complex during the reaction with the ingredients present in the MGsSTL observed at 360nm to 440nm in UV-Visiblespectroscopy revealed the presence of AgNPs. The XRD shows the crystalline size and SEM analysis showed the particle size between 30-70nm as well as the spherical structure of the NPs. FTIR analysis confirmed the bioreduction of Ag+ ions to AgNPs due to the reduction by capping material of plant extract. Morphology evaluation via TEM showed spherical NPs and a band width by DLS. No clusters were observed, which confirmed the high negative values for the zeta potential which ensures sufficient particle repulsion and a stabile colloidal solution.

Plant extract can be efficiently used in the synthesis of AgNPs as a greener route. Control over the shape and size of NPs seems to be very easy with the use of plants. Such NPs produced using plants have been used in various applications for human benefit. The reduction of the metal ions led to the formation of AgNPs of fairly well-defined dimensions using the MGsSTL. Further, the above AgNPs revealed an anticancer property against DLA. The AgNPs synthesized via green route are highly toxic to DLA cancer cells hence has a great potential in biomedical applications. In conclusion, we have explored a very cost effective green route for

the synthesis of biocompatible AgNPs with very effective antitumor properties. This green chemistry approach has many advantages such as eco-friendly, cost effective and easily scaled up to large scale synthesis.

Phase II

In Phase II, *in vitro* antioxidative and antitumorigenic potential of the MGsSTL and AgMGsSTL were evaluated by assessing their free radical scavenging efficacy, cytotoxic and apoptotic effect to Dalton's lymphoma ascites (DLA) tumor cells.

4.2 *In vitro* antioxidant and antitumorigenic potential of MGsSTL and AgMGsSTL

In vitro antioxidative role of MGsSTL and AgMGsSTL was evaluated by their ability to scavenge the radicals (DPPH, hydroxyl and superoxide) and non radicals (hydrogen peroxide and nitric oxide) against the standard Vitamin C. *In vitro* antitumorigenic effect to DLA tumor cells were evaluated by their cytotoxic effect (MTT assay and trypan blue exclusion assay) and the apoptotic effect (flow cytometry) to DLA tumor cells.

4.2.1 *In vitro* antioxidant potential of MGsSTL and AgMGsSTL

The *in vitro* antioxidant activity of MGsSTL and AgMGsSTL was assessed by studying their ability to scavenge radicals such as DPPH, hydroxyl and superoxide and non radicals such as hydrogen peroxide and nitric oxide compared with the standard Vitamin C.

4.2.1.1 Scavenging of DPPH radical (DPPH)

In living systems, free radicals are constantly generated and they can cause extensive damage to tissues and biomolecules leading to various disease conditions, especially degenerative diseases, and extensive lysis. An alternative solution to the problem is to consume natural antioxidants from food supplements and traditional medicine. Recently, many natural antioxidants have been isolated from different plant materials. An antioxidant works in stopping the oxidation by

neutralizing the free radicals produced. In order to neutralize the free radicals, the antioxidant itself undergoes oxidation.

Figure 57

Percentage DPPH radical scavenging activity of MGsSTL, AgMGsSTL and Vitamin C

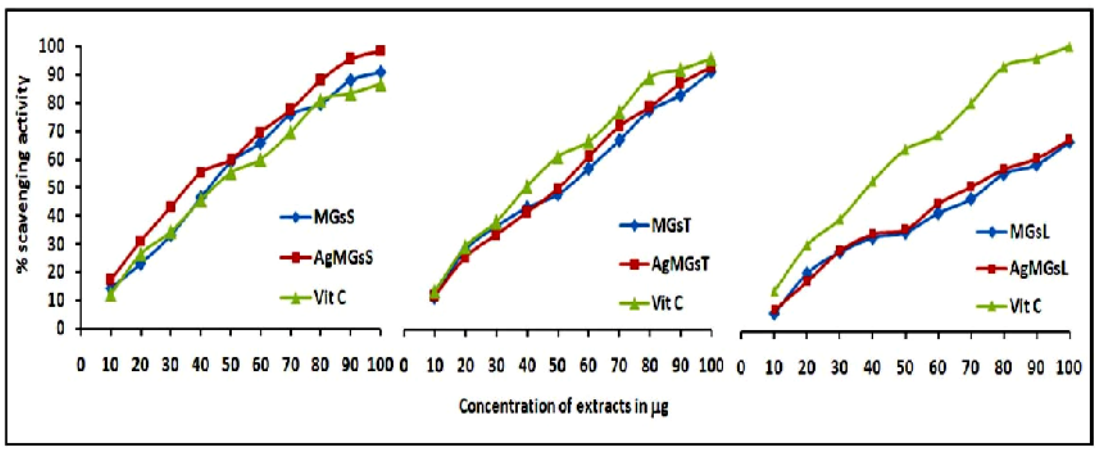

The DPPH is the commonly used reagent to evaluate free radical scavenging activity of antioxidants. DPPH is a stable free radical and accepts an electron or hydrogen radical to become a stable diamagnetic molecule. The reduction capability of DPPH radical is determined by the decrease in absorbance at 517 nm induced by antioxidants (Lagnika *et al*., 2011). Figure 57 shows the dose dependent DPPH radical scavenging activity and the IC_{50} values of MGsSTL (37µg, 53 µg and 80 µg), AgMGsSTL (30 µg, 50 µg and 74 µg) respectively and standard Vitamin C (40 µg).

The reducing ability of MGsSTL and AgMGsSTL depends on the presence of reductants, which have been shown to exert antioxidant action by breaking the free radical chain reactions by donating a hydrogen atom. This increased scavenging capacity of MGsSTL and AgMGsSTL elicited may be due to the presence of high levels of phytochemical constituents. Similar dose dependent DPPH scavenging effect was also observed by both *Syzygium cumini* seed extract and silver nanoparticle of *Syzygium cumini* seed extract when compared with

ascorbic acid (Banerjee and Narendhirakannan 2011); Methanol extracts of *Conocarpus erectus* leaves, stems, fruits and flowers) showed high free radical scavenging activity toward DPPH radical (Abdel-Hameed *et al*., 2012)*;* methanolic extracts of the bark of *Ficus glomerata* (Ahmed and Tariq 2012); silver NPs from *Piper nigrum* fruit extract when compared with ascorbic acid (Mani *et al*., 2012); NPs derived from *Salvia officinalis* L. leaf extract, *Ricinus communis* leaf and fruit extracts (Salem *et al*., 2012); Diethyl ether phytochemical fraction of gold NPs of *Justicia gendarussa* leaf (Fazaludeena *et al*., 2012) and silver NPs using *Alternanthera sessilis* (Niraimathi *et al*., 2013).

4.2.1.2 Scavenging of Hydroxyl radical ($OH^{\cdot}$)

Hydroxyl radical, was produced from either metal catalyzed Haber–Weiss reaction or Fenton reaction. These radicals are the major acitive oxygen species responsible for lipid peroxidation resulting various deleterious biological effects to induce carcinogenesism and mutagenesis. In this process, the ferric ion is reduced by superoxide, with subsequent oxidation of ferrous ion by H_2O_2 forming hydroxyl radical thereby initiating the series of oxidative reactions (Manian *et al*., 2008 and Ramkumar *et al*., 2009).

Figure 58

Percentage hydroxyl radical scavenging activity of MGsSTL, AgMGsSTL and Vitamin C

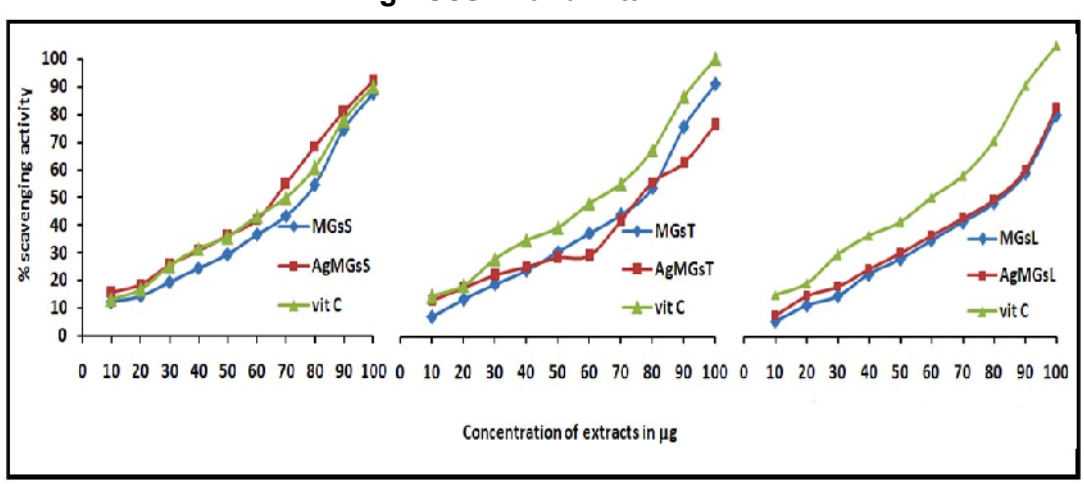

The hydroxyl radical scavenging activity of MGsSTL, AgMGsSTL and standard Vitamin C was found to be dose dependent as shown in Figure 58 and their IC_{50} values were found to be as (71 μg, 76 μg and 84 μg), (61 μg, 74 μg and 82 μg) and (63 μg) respectively.

Similar dose dependent inhibition of $OH^{\cdot}$ generation was observed by free radical scavenging activity of fruit extract of Cucumis trigonus (Balakrishnan and Kokilavani 2011), Avicennia marina (Forssk) Vierh pneumatophore (Lincy *et al*., 2012), Dioscorea oppositifolia tuber extract (Paulpriya and Mohan 2012), ethanolic extract of Nymphaea pubescens (Rushender *et al*., 2012) and AgNPs of Shorea roxburghii (Subramanian *et al*., 2013).

4.2.1.3 Scavenging of Superoxide radical ($^{\cdot}O_2^-$)

Superoxide anion is an oxygen-centered radical with selective reactivity. This species is produced by a number of enzyme systems in auto-oxidation reactions and by nonenzymatic electron transfers that univalently reduce molecular oxygen. Overproduction of superoxide anion radical, contributes to redox imbalance and are associated with harmful physiological consequences. Superoxide is biologically important since it can be decomposed to form stronger oxidative species such as singlet oxygen and hydroxyl radicals, which are very harmful to the cellular components in a biological system (Sivanandam *et al*., 2012).

Figure 59

Percentage superoxide radical scavenging activity of MGsSTL, AgMGsSTL and Vitamin C

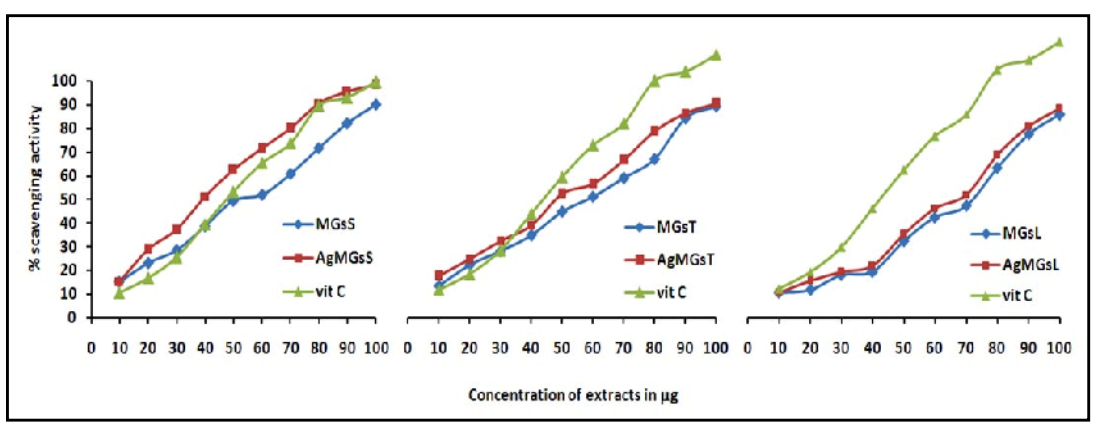

The MGsSTL (45 µg, 61 µg and 72 µg), AgMGsSTL (33 µg, 52 µg and 69 µg) and standard Vitamin C (42 µg) showed dose dependent scavening activity of superoxide radical as shown in Figure 59. Thus, MGsSTL and AgMGsSTL could maintain redox homeostasis in body by inhibiting superoxide anion production.

Similar dose dependent inhibition of $^{\cdot}O_2^-$ generation was observed by free radical scavenging activity of methanolic extract of *Vitis vinifera, Oroxylum indicum and* Policosanol isolated from *Saccharum officinarium* (D'Mello *et al*., 2012); isolated tannins from the alcoholic extract of *Phyllanthus amrus* against standard antioxidants such as Curcumin and ascorbic acid (Ujwala *et al*., 2012) and AgNPs of *Cassia tora* leaf (Velavan *et al*., 2012). Gold and silver NPs serve as strong hydroxyl, superoxide, nitric oxide and DPPH radical scavengers in contrast to their corresponding metal oxides (Ramamurthy *et al*., 2013).

4.2.1.4 Scavenging of Hydrogen peroxide (H_2O_2)

Hydrogen peroxide, although not a radical species play a role to contribute oxidative stress. The generation of even low levels of H_2O_2 in biological systems may be important. Naturally-occurring iron complexes inside the cell believed to react with H_2O_2 *in vivo* to generate highly reactive hydroxyl radicals and this may be the origin of many of its toxic effects (Ashwini *et al*., 2010).

Figure 60

Percentage hydrogen peroxide scavenging activity of MGsSTL, AgMGsSTL and Vitamin C

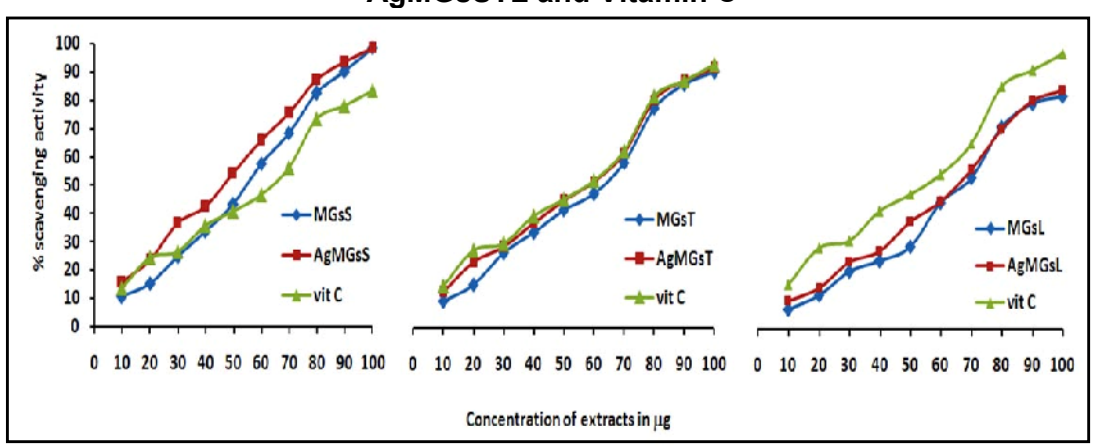

The MGsSTL (50 μg, 62 μg and 68 μg), AgMGsSTL (41 μg, 58 μg and 66 μg) and standard Vitamin C (58 μg) and showed a dose dependent hydrogen peroxide scavenging activity (Figure 60). Scavenging of H_2O_2 by phytochemicals present in MGsSTL and AgMGsSTL which can donate electrons to H_2O_2 and thus neutralizing it in to water.

Similar dose dependent H_2O_2 scavenging effect was also observed by the organic fractions of *Garcinia kola* and *Njavara rice bran* (Okoko *et al*., 2009); leaf extracts of Ziziphus mucronata (Kwape and Chaturvedi 2012); methanolic extract of dried pulp of *Garcinia pedunculata* (Mudoi *et al*., 2012) and Mature pod wall of *Cicer arietinum* Linn (Vadnere *et al*., 2012).

4.2.1.5 Scavenging of Nitric Oxide (NO)

Nitric oxide radicals are produced by macrophages at the time of the inflammatory response. Because of its mutagenic nature it interferes in the DNA processes thereby it has been associated with various carcinomas and nflammatory conditions. NO reacts with superoxide radical and forms high reactive metabolite peroxynitrite (ONOO–) anion (Shajeela *et al*., 2012).

The MGsSTL (61 μg, 72 μg and 83 μg), AgMGsSTL (58 μg, 70 μg and 80 μg) and standard Vitamin C (60 μg) showed increased scavening activity of nitric oxide as shown in Figure 61 with minimum IC_{50} concentration.

Figure 61

Percentage nitric oxide scavenging activity of MGsSTL, AgMGsSTL and Vitamin C

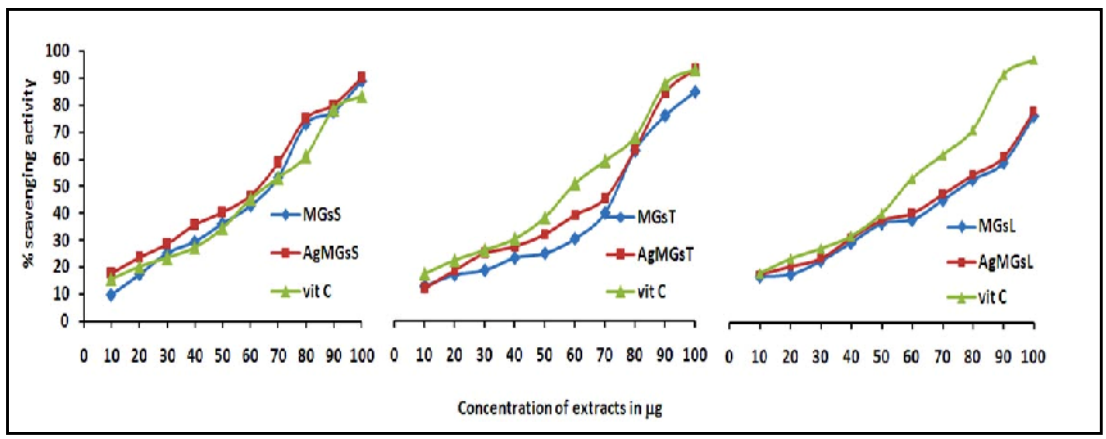

Suppression of released NO may be partially attributed to direct NO scavenging, as the extracts of MGsSTL and AgMGsSTL decreased the amount of nitrite generated from the decomposition of Sodium nitroprusside *in vitro.* Similar dose dependent inhibition of NO generation was observed by the *Lantana camara* leaves extract (Grace-Lynn *et al*., 2012); methanolic extract of *Pisonia grandis* (MEPG), ethylacetate fraction of *Pisonia grandis* and ethanolic fraction of *Pisomia grandis* and Ascorbic acid standard (Jayakumari *et al*., 2012); mangrove plant *Excoecaria agallocha* Linn leaves extract (Poorna *et al*., 2012) and also methanol extract of *A. malaccensis* (Sahoo *et al*., 2012).

The DPPH radical scavenging efficacy of AgMGsS (30 μg) which was followed by MGsS (37 μg) > standard Vitamin C (40 μg)> AgMGsT (50 μg) > MGsT (53 μg) > AgMGsL (74 μg) > MGsL (80 μg). $OH^{\cdot}$ radical scavenging efficacy of AgMGsS (61 μg) which was followed by standard Vitamin C (63 μg) > MGsS (71 μg) > AgMGsT (74 μg) > MGsT (76 μg) > AgMGsL (82 μg) > MGsL (84 μg). $^{\cdot}O_2^-$ radical scavenging efficacy of AgMGsS (33 μg) which was followed by standard Vitamin C (42 μg) > MGsS (45 μg) > AgMGsT (52 μg) > MGsT (61 μg) > AgMGsL (69 μg) > MGsL (72 μg). H_2O_2 scavenging efficacy of AgMGsS (41 μg) which was followed by MGsS (50 μg) > standard Vitamin C (58μg) > AgMGsT (58 μg) > MGsT (62 μg) > AgMGsL (66 μg) > MGsL (68 μg). NO scavenging efficacy of AgMGsS (58 μg) which was followed by standard Vitamin C (60 μg) > MGsS (61μg) > AgMGsT (70 μg) > MGsT (72 μg) > AgMGsL (80 μg) > MGsL (83 μg).

Scavening of DPPH and H_2O_2 by MGsS was found to be more effective than that of standard Vitamin C. Scavening of selective radicals and non radicals was found to be effective by AgMGsS than that of standard Vitamin C. These free radical scavenging activities of MGsSTL, AgMGsSTL were found to be comparable to the standard Vitamin C and indicated their *in vitro* antioxidant potential.

The DPPH is the commonly used reagent to evaluate free radical scavenging activity of antioxidants. DPPH is a stable free radical and accepts an electron or hydrogen radical to become a stable diamagnetic molecule. The reduction capability of DPPH radical is determined by the decrease in absorbance at 517 nm induced by antioxidants (Kala *et al*., 2012). The MGsSTL and AgMGsSTL showed a significant dose dependent reduction in the DPPH radicals it may be due to the presence of active compounds like flavonoids, alkaloids and their derivatives.

Hydroxyl radical is the most reactive free radical in the biological system and it has been regarded as the highly damaging to almost every molecule found in the biological system. It can conjugate with nucleotides in DNA and cause strand breakage which leads to ultimately mutagenesis, carcinogenesis and cytotoxicity (Pan and Mei, 2010). Hydroxyl radical, was produced from either Metal catalyzed Haber–Weiss reaction or Fenton reaction. These radicals are the major acitive oxygen species responsible for lipid peroxidation resulting various deleterious biological effects. Naturally-occurring iron complexes inside the cell believed to react with H_2O_2 *in vivo* to generate highly reactive hydroxyl radicals and this may be the origin of many of its toxic effects (Thirunavukkarasu *et al*., 2011). Results from our study revealed the significant antioxidant activity of MGsSTL and AgMGsSTL and their Phytochemial components are probably involved in their antiradical activity.

One of the main sources of superoxide radical is the enzyme xanthine oxidase (XO). Superoxide radical is known to be very harmful to cellular components as a precursor of more reactive species. Drugs possessing superoxide scavenging activity decreases the reduction of NBT, which is a measure of $^{\cdot}O_2^-$ scavenging activity. One risk of the superoxide generation is related to its interaction with nitric oxide to form Peroxynitrite which is a potent antioxidant that causes nitrosative stress in the organ systems (Valko *et al*., 2007). The superoxide scavenging activity of MGsSTL, AgMGsSTL and ascorbic acid were increased markedly with the increase concentrations.

Scavenging activity of H_2O_2 by the MGsSTL and AgMGsSTL may be attributed to their secondary metabolites and their derivatives, which can donate electrons to H_2O_2 thereby neutralizing it into water (Mathew and Abraham, 2006). Hydrogen peroxide, although not a radical species play a role to contribute oxidative stress. The generation of even low levels of H_2O_2 in biological systems may be important. Hydrogen peroxide is a weak oxidizing agent and can inactivate a few enzymes directly, usually by oxidation of essential thiol (-SH) groups. It rapidly transverses cell membrane and once inside the cell interior, H_2O_2 can probably react with Fe^{2+} and possibly Cu^{2+} ions to form hydroxyl radical and this may be the origin of many of its toxic effects (Chanda and Dave, 2009). Thus, the removal of H_2O_2 is very important for antioxidant defence in cell or food systems.

The role of NO in various disease states has attracted the attention of scientists worldwide. NO radicals are produced by macrophages at the time of the inflammatory response. Because of its mutagenic nature it interferes in the DNA processes thereby it has been associated with various carcinomas and inflammatory conditions (Pour *et al*., 2011). The nitric oxide does not interact with bioorganic macromolecules such as DNA or proteins directly. Under aerobic conditions, the nitric oxide molecule is very unstable and reacts with the oxygen to produce intermediates such as NO2·, N2O4· and N3O4· and stable products like nitrate and nitrite. NO reacts with superoxide radical and forms high reactive metabolite peroxynitrite anion ($ONOO^-$) which is highly toxic to humans (Sasidharan *et al*., 2007; Okoko 2009). The current study showed that the MGsSTL and AgMGsSTL may have the property to counteract the effect of nitric oxide formation and in turn may be of considerable interest in preventing the ill effects of excessive nitric oxide generation. The reduction in the radicals on treatment with the extract shows the potent free radical scavenging activity of the MGsSTL and AgMGsSTL.

Figure 62

IC_{50} values of MGsSTL and Vitamin C

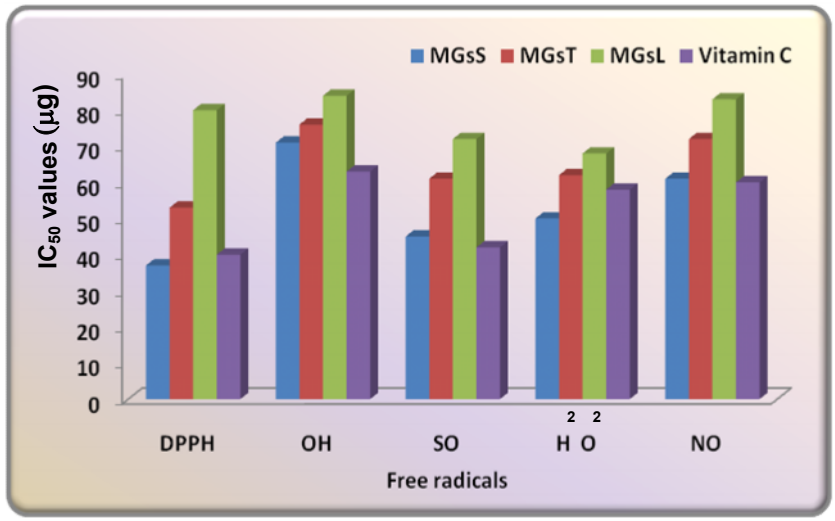

The free radical scavenging efficacy of MGsS was found to be high with minimum concentration of the extract {DPPH (37 µg) > $^{\cdot}O_2^-$ (45 µg) > H_2O_2 (50 µg) > NO (61 µg) > $OH^{\cdot}$ (71 µg)} as shown in Figure 62 which was followed by MGsT {DPPH (53 µg) > $^{\cdot}O_2^-$ (61 µg) > H_2O_2 (62 µg) > NO (72 µg) > $OH^{\cdot}$ (76µg)} MGsL {H_2O_2 (68 µg) > $^{\cdot}O_2^-$ (72 µg) > DPPH (80 µg) > NO (83 µg) > $OH^{\cdot}$ (84 µg)} when compared to standard Vitamin C {DPPH (40 µg) > $^{\cdot}O_2^-$ (42 µg) > H_2O_2 (58 µg) > NO (60 µg) > $OH^{\cdot}$ (63 µg)} indicated its *in vitro* antioxidant potential.

The free radical scavenging efficacy of AgMGsS was found to be high with minimum concentration of the extract {DPPH (30 µg)> $^{\cdot}O_2^-$ (33 µg) > H_2O_2 (41 µg) > NO (58 µg) > $OH^{\cdot}$ (61 µg)} as shown in Figure 62 which was followed by AgMGsT {DPPH (50 µg) > $^{\cdot}O_2^-$ (52 µg) > H_2O_2 (58 µg) > NO (70 µg) > $OH^{\cdot}$ (74 µg)} > AgMGsL {H_2O_2 (66µg) > $^{\cdot}O_2^-$ (69 µg) > DPPH (74 µg) > NO (80 µg) > $OH^{\cdot}$ (82 µg)} compared to standard Vitamin C {DPPH (40 µg) > $^{\cdot}O_2^-$ (42 µg) > H_2O_2 (58 µg) > NO (60 µg) > $OH^{\cdot}$ (63 µg)}. The free radical scavenging efficacy of AgMGsS was found to be higher than that of AgMGsT and AgMGsL. All the extracts showed free radical scavenging activities and indicated their *in vitro* antioxidant potential.

Figure 63

IC_{50} values of AgMGsSTL and Vitamin C

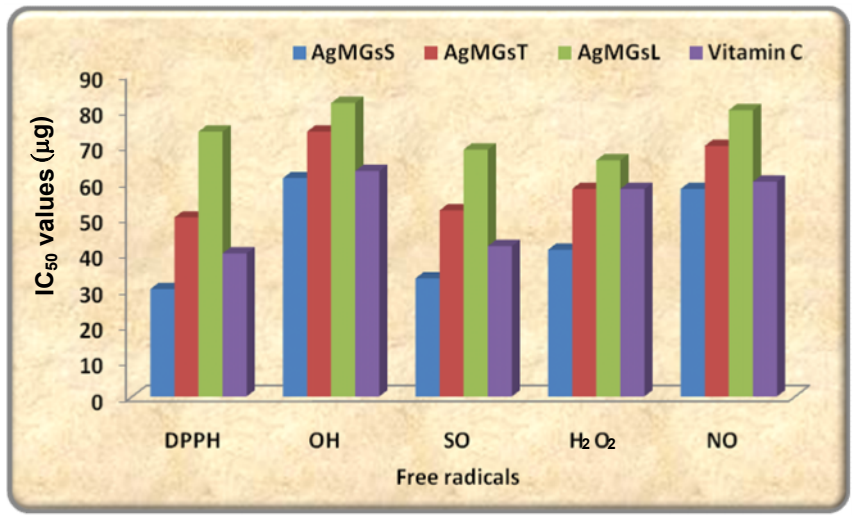

From the above results it was clear that the AgMGsS> AgMGsT> AgMGsL have higher free radical scavenging activity than that of MGsS> MGsT> MGsL. Moreover, the free radical scavenging efficacy of AgMGsS was found to be higher than that of all other extracts (MGsSTL and AgMGsTL) as shown in the Figure 62 and 63. These free radical scavenging activities of above extracts indicated their *in vitro* antioxidant potential. The reducing ability of a compound depends on the presence of reductants which have been shown to exert antioxidant action by breaking the free radical chain by donating a hydrogen atom. The biosynthesized AgNPs (AgMGsSTL) are found to have very potent reducing ability. It can be stated that medicinal value of this traditional plant have been supported by the results which show positive quenching activity against the free radicals.

Since free radicals are important contributors to various degenerative diseases, the observed antioxidant properties of the MGsSTL and AgMGsSTL might be useful for the development of newer and more potent antioxidants. The biosynthesized AgNPs can be used as potential free radical scavengers and can be used against the various damages caused by free radicals.

4.2.2 *In vitro* antitumorigenic potential of MGsSTL and AgMGsSTL to DLA tumor cells

The control of cell proliferation is crucial in maintaining cellular homeostasis and loss of this mechanism is a principle hallmark of cancer cells. Thus the inhibition of tumor cell growth without side effects is recognized as an important target for cancer therapy (Wahab *et al*., 2009). Antitumor agents, that can induce apoptosis, may be able to affect the steady state of cell proliferation that are helpful in the cancer management and therapy. Since it has been suggested that apoptosis plays a critical role in tissue homeostasis, apoptosis modulation has become an interesting target for both therapeutic and preventive approaches to cancer treatment (Lee *et al*., 2003).

In vitro antitumorigenic effect of MGsSTL and AgMGsSTL was evaluated against DLA tumor cells by MTT cell proliferation assay and trypan blue exclusion method and also apoptotic effect to DLA cells by flow cytometry.

4.2.2.1 MTT cell proliferation assay

Measurement of cell viability and proliferation forms the basis for numerous *in vitro* assays of a cell population's response to external factors. The reduction of tetrazolium salts is now widely accepted as a reliable way to examine cell proliferation.

To evaluate the effect of MGsSTL and AgMGsSTL on DLA cancer cell proliferation, the cells were exposed to increasing doses of MGsSTL and AgMGsSTL for 24 hours in the presence of MTT. As shown in Figure 64 cell viability were markedly decreased after exposure to MGsSTL and AgMGsSTL in a dose-dependent manner. The extracts MGsSTL and AgMGsSTL killed 50 percent of DLA tumor cells at a concentration (ED_{50} values) of 29 µg, 39 µg and 80 µg for MGsS, MGsT, MGsL respectively and of 21 µg, 24 µg and 77 µg for AgMGsS, AgMGsT, AgMGsL respectively as shown in Figure 65 was used in *in vivo* studies. These results demonstrated that MGsSTL and AgMGsSTL mediated a concentration and time dependent increase in toxicity towards DLA cells. AgMGsS

showed more cytotoxic effect to DLA tumor cells than that of MGsSTL and AgMGsTL.

Figure 64

***In vitro* cytotoxic effect of MGsSTL and AgMGsSTL to DLA tumor cells by MTT cell proliferation assay**

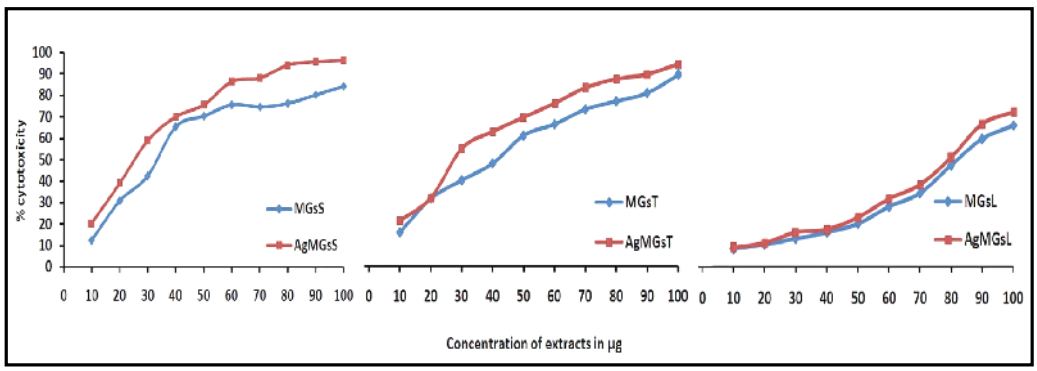

Figure 65

ED $_{50}$ values of MGsSTL and AgMGsSTL to DLA tumor cells by MTT cell proliferation assay

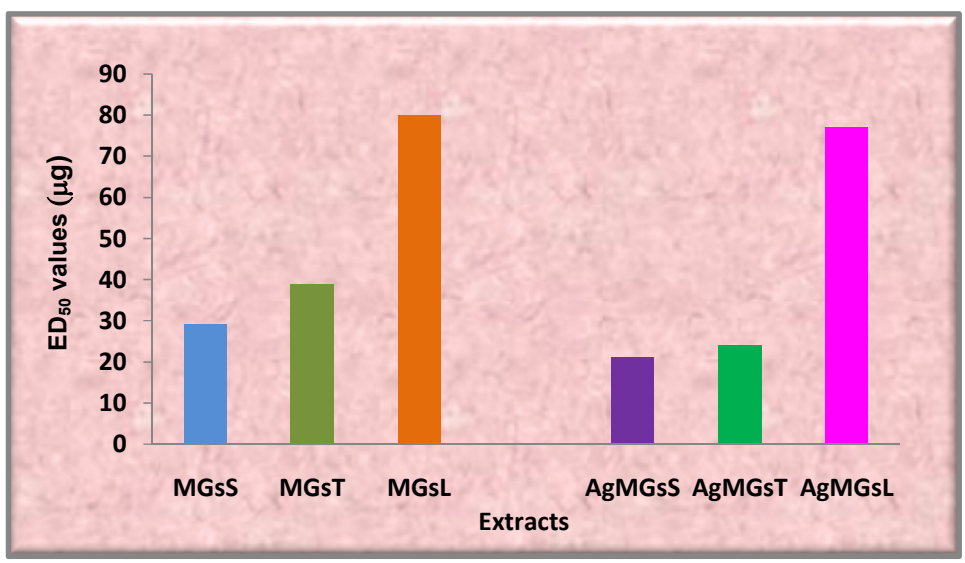

The cytotoxic effect of MGsSTL and AgMGsSTL on cell viability has a major role in antitumor activity, thereby reducing cell proliferation. The cytotoxic effects of AgMGsSTL are the result of the encapsulation of AgNPs by the active

physiochemicals which in turn interact with the functional groups of intracellular proteins (Martins *et al*., 2010).

These results corroborated with earlier reports of Safaepour *et al*., (2009) who also investigated a similar cytotoxic effect by the significant inhibition of the growth of Fibrosarcoma-Wehi 164 cell line by AgNPs of *Pelargonium graveolens* and *Azadirachta indica*. Amentoflavone extracted from the plant of *Selaginella tamariscina* was found to be effective in inhibiting the proliferation of HL-60, MCF-7, HeLa, BEL-7402, PANC-1 and HL-60 (Jing *et al*., 2010). Methanolic extract of bark of *Careya arborea* Roxb was found to be cytotoxic to DLA and EAC cell lines in a dose dependent manner (Subhadradevi *et al*., 2010). Antitumor potency of AgNPs employing table sugar as a capping and a reducing agent was seen against HT144 (malignant skin melanoma) and H157 (squamous cell lung carcinoma) as compared to the clinically used reference compounds vincristine and methotrexate (Nazir *et al*, 2011). Satyavani *et al*., (2011) reported, the cytotoxic effect of AgNPs synthesized from calli extract of *Citrullus colocynthis* on Human epidermoid larynx carcinoma (HEp -2) cell line, Biochemically synthesized Au and AgNPs of *Azardirecta indica, Cephalandra indica, Calotropis procera and Syzygium jambolanum* showed toxicity towards HEpG-2 cells (D'Britto *et al*., 2012). Ethyl acetate extract of the *Solanum anguivi* showed antiproliferative activity against HEpG-2 and MCF-7 cell lines (Gandhiappan and Rengasamy 2012), Exponential increase was noticed in the growth inhibition of HeLa cell line by the administration of hydroalcoholic extract of *Bougainvillea glabra* (Joshny *et al*., 2012). *Nyctanthes arbor-tristis* showed potent anticancer activity towards MDA-MB 231 Breast Cancer Cell Lines and also DPPH scavenging activity (Kumari *et al*., 2012). Satyavani *et al*., (2012) also investigated a similar significant cytotoxic effect of AgNPs of *Suaeda monoica* on Human Epidermoid Larynx Carcinoma cell line. AgNPs of aqueous extract of *Coleus amboinicus lour* showed the antioxidant activity and cytotoxicity against the Ehrlich's ascite carcinoma (EAC) cell line (Subramanian and Suja 2012). *Tecomastans ethanolic* leaf extract showed a significant antiproliferative activity against MCF- 7 cancer cell ine (Thirumal *et al*., 2012).

4.2.2.2 Trypan blue exclusion assay

Trypan blue is a vital stain used to selectively colour the dead tissues. It is a diazo dye. Live cells or tissues with intact cell membranes are not coloured as trypan blue is not absorbed; however, it traverses the membrane in a dead cell and are shown as a distinctive blue colour under a microscope. Since live cells are excluded from staining, this staining method is also described as a dye exclusion method. Staining facilitates the visualization of cell morphology (Fayed 2009). Trypan Blue is a blue acid dye that has two azo chromophore groups. Trypan Blue is an essential dye, used in estimating the number of viable/ dead cells present in a population (Vinayak *et al*., 2011).

The *in vitro* cell viability assay by trypan blue exclusion method was carried out to evaluate the antitumor potential of MGSSTL and AgMGsSTL against DLA tumor cells. The effect of MGsSTL and AgMGsSTL to DLA tumor cells is recorded in Figure 66 and 67 and also in plate V. Incubation of DLA tumor cells with MGsSTL and AgMGsSTL produced a concentration dependent cytotoxic effect which was indicated by the increase in number of dead cells with increasing concentrations of MGsSTL and AgMGsSTL. The 10µg concentration of MGsS, MGsT and MGsL showed 24.32%, 19.69% and 9.68% of dead cells. where as in higher concentration of 100µg MGsS, MGsT and MGsL showed 90.20%, 69.61% and 42.03% of dead cells. The 10µg concentration of AgMGsS, AgMGsT and AgMGsL showed 36.23%, 27.35% and 11.76% of dead cells, where as in higher concentration of 100µg AgMGsS, AgMGsT and AgMGsL showed 97.22%, 74.18% and 43.80% of death cells as shown in Figure 66.

The results showed that DLA tumor cell proliferation was significantly inhibited by MGsS, AgMGsS, MGsT, AgMGsT, MGsL and AgMGsL with an ED_{50} value i.e 50% of tumor cell death at 40µg, 30 µg, 53 µg, 37 µg, 88 µg and 82 µg respectively and were shown in Figure 67. Thus, synthesized AgMGsSTL were found to be the potential cytotoxic agent to DLA tumor cells compared with MGsSTL.

Figure 66

***In vitro* cytotoxic effect of MGsSTL and AgMGsSTL to DLA tumor cells by trypan blue exclusion assay**

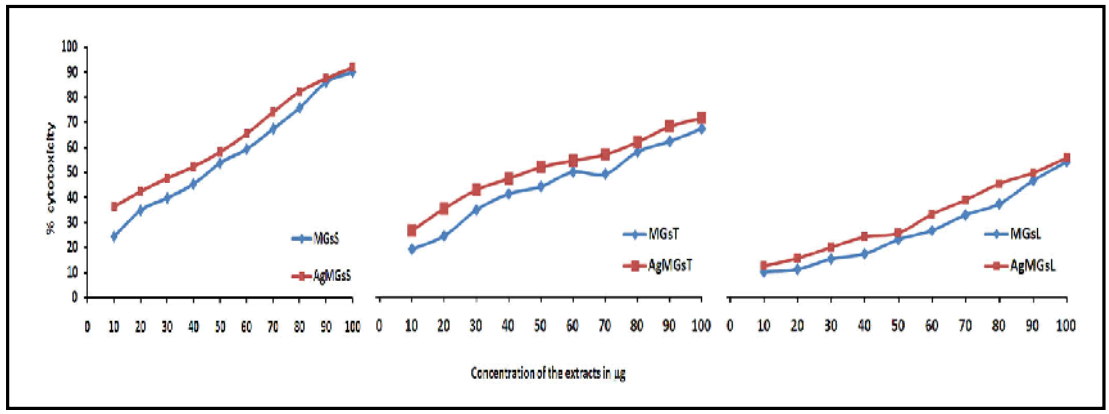

Figure 67

ED $_{50}$ values of MGsSTL and AgMGsSTL to DLA tumor cells by trypan blue exclusion assay

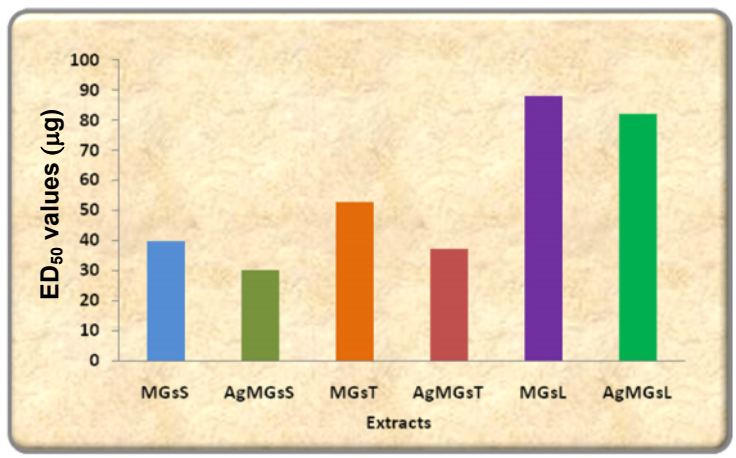

Adhvaryu *et al*. (2010) also showed maximum cell cytotoxicity effect of four ayurvedic herbs such as *Curcuma longa L., Ocimum sanctum L., Tinospora cordifolia (wild), and Zizyphus mauritiana* to DLA tumor cells. Ethanolic and water extracts of some Sweet basil (*Ocimum basilicum*) possessed high cytotoxic and antioxidant activities against EAC Cells (Taie *et al*., 2010).Patel *et al*., (2011) also reported the better cytotoxic activity of the *Temoxifen citrate* NP to MCF-7 cancer cell line. Sivabalan *et al*., (2011) study also revealed the cidal activity of chitosan and Eudragit NPs of 5- fluorouracil to DLA cells in trypan blue assay. Ethanolic

extracts of Egyptian flora possessed high cytotoxic and antioxidant activities against EAC Cells (Enein *et al*., 2012). Tin (IV) oxide NPs/graphene (SnO2/GR) nanocomposites provide viable option for enhancing the thermal deposition and specificity of hyperthermia treatments for elimination of human prostate cancer (Cheng *et al*., 2012). Methanolic leaf extract of Orthosiphon thymiflorus have significant antitumor activity against DLA tumor cell (Sini *et al*., 2012). Dichloromethane and methanol extracts of *Scrophularia oxysepala* extracts significantly inhibited cell growth and viability in a dose and time dependent manner in MCF-7 cells as well as Human umbilical vein endothelial cells (Valiyari *et al*., 2012).

Plate V

DLA cells before and after treatment with extracts in trypan blue exclusion method

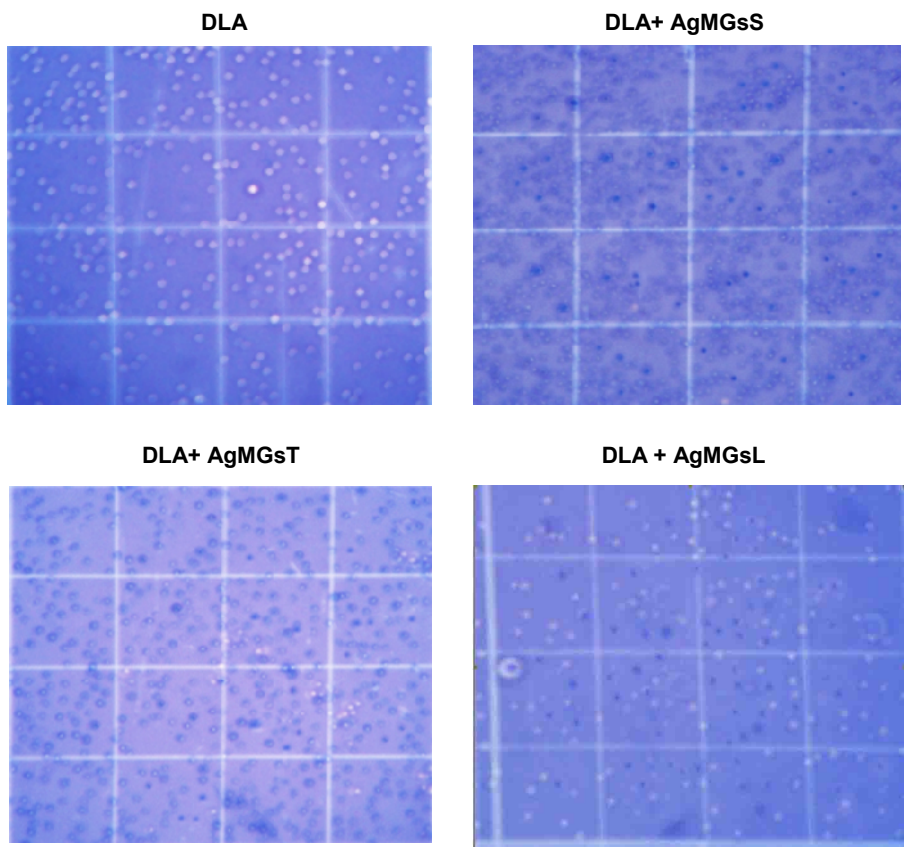

The DLA tumor cell proliferation was significantly inhibited by MGsSTL with an ED_{50} value of (40µg, 53 µg, 88 µg) and AgMGsSTL with the ED_{50} values of (30 µg, 37 µg and 82 µg) respectively (Figure 67). Thus, the synthesized AgMGsS was found to be the more potential cytotoxic agent to DLA tumor cells than that of all other extracts (MGsSTL and AgMGsTL).

Thus the inhibition of tumor cell growth without side effects is recognized as an important target for cancer therapy. In this study MGsSTL and AgMGsSTL inhibited the growth of DLA tumor cells in a dose dependent manner. The cytotoxic potency of the extracts was confirmed by the *in vitro* cytotoxic assay methods to DLA tumor cells.

4.2.2.3 Apoptotic effect of AgMGsSTL to DLA tumor cells by flow cytometry

Apoptosis or programmed cell death has been characterized as a fundamental cellular activity, occurring under a wide varity of physiological and pathological conditions. It has been established that the onset of tumor is attributable to the loss of equilibrium between cellular apoptosis and proliferation (Khan, 2012). Initiation of apoptosis, is an important issue in cancer treatment as cancer cells frequently have acquired to block apoptosis and thus are more resistant to chemotherapeutic drugs (Keum *et al*., 2000).

Tumor cells fail to undergo apoptosis, as they acquire malignant potential and are resistant to chemotherapeutic drugs. Apoptosis has quickly surfaced as a potential target for cancer prevention/ treatment at various stages of carcinogenesis. Therefore, induction of apoptosis by dietary bioactive compounds can be an excellent approach to inhibit the promotion and progression of carcinogenesis and to remove genetically damaged, preinitiated, or neoplastic cells from the body (Encalada *et al*., 2011).

Flow cytometry analysis using Annexin V-Biotin and propidium iodide staining proved the apoptotic effect of AgMGsSTL to DLA cells by. Flow cytometry provides a rapid and reliable method to quantify viable cells in a cell suspension. Determination of cell viability is critical when evaluating the response to cytotoxic

drugs. One method to assess cell viability is through the use of dye exclusion. Live cells have intact membranes that exclude the dye that easily penetrate the damaged, permeable membranes of non-viable cells. Propidium iodide (PI) is a membrane impermeant dye that is generally excluded by the viable cells. It binds to double stranded DNA by intercalating between the base pairs. The Propidium Iodide (PI) staining solution may be used to assess plasma membrane integrity in Annexin V apoptosis assay (Mei *et al*., 2012). Apoptosis is a physiological process of cell elimination and the ability to induce apoptosis is an important property of the anticancer agents.

Apoptosis or programmed cell death is an essential physiological process that plays a critical role in development and tissue homeostasis. In the present study MGsSTL and AgMGsSTL were able to inhibit the *in vitro* growth of DLA cells significantly. Flow cytometry data of PI – Annexin V dual staining confirmed that AgMGsSTL could be able to induce apoptosis on cancer cells. The cell cycle checkpoint maintains the order and fidelity of cell cycle events in eukaryotes (Nigg, 2001). DNA damage and mutations could be detected by it, and the damaged cells were arrested in specific checkpoint to repair. If the damaged DNA was repaired, the cells could enter into the next phase of cell cycle or apoptosis would happen (O'Neil 2006; Branzei 2008). It was suggested that DNA damage repair mechanism might be activated by MGsSTL and AgMGsSTL in DLA cells which resulted in normal distribution of cells in the different cell cycle phases. DLA cells were left untreated or treated for 12 hours with AgMGsSTL to induce apoptosis. Cells were incubated with Annexin V-Biotin, followed by incubation with buffer in Propidium Iodide (PI) staining solution. Cells were then analyzed by flow cytometry. Untreated cells were primarily Annexin V-Biotin and PI negative, indicating that they were viable and not undergoing apoptosis. After a treatment with AgMGsSTL three populations of cells were identified: Cells that had already died or were in late stage of apoptosis (Annexin V-Biotin and PI positive), cells undergoing apoptosis (Annexin V-Biotin positive and PI negative), and cells that were viable and not undergoing apoptosis (Annexin V-Biotin and PI negative).

Flow cytometry analysis was followed using propidium iodide (PI) and Annexin V staining to confirme apoptosis of DLA cells. DLA cells were untreated (DLA tumor cell) and treated for 12 hrs with ED_{50} values (DLA + 25 µg of AgMGsS, DLA + 30 µg of AgMGsT and DLA + 79 µg AgMGsL). Results are representative of three independent experiments, with DLA tumor cells.

Figure 68

Apoptotic effect of AgMGsS to DLA cells by fluorescent-activated cell sorting analysis

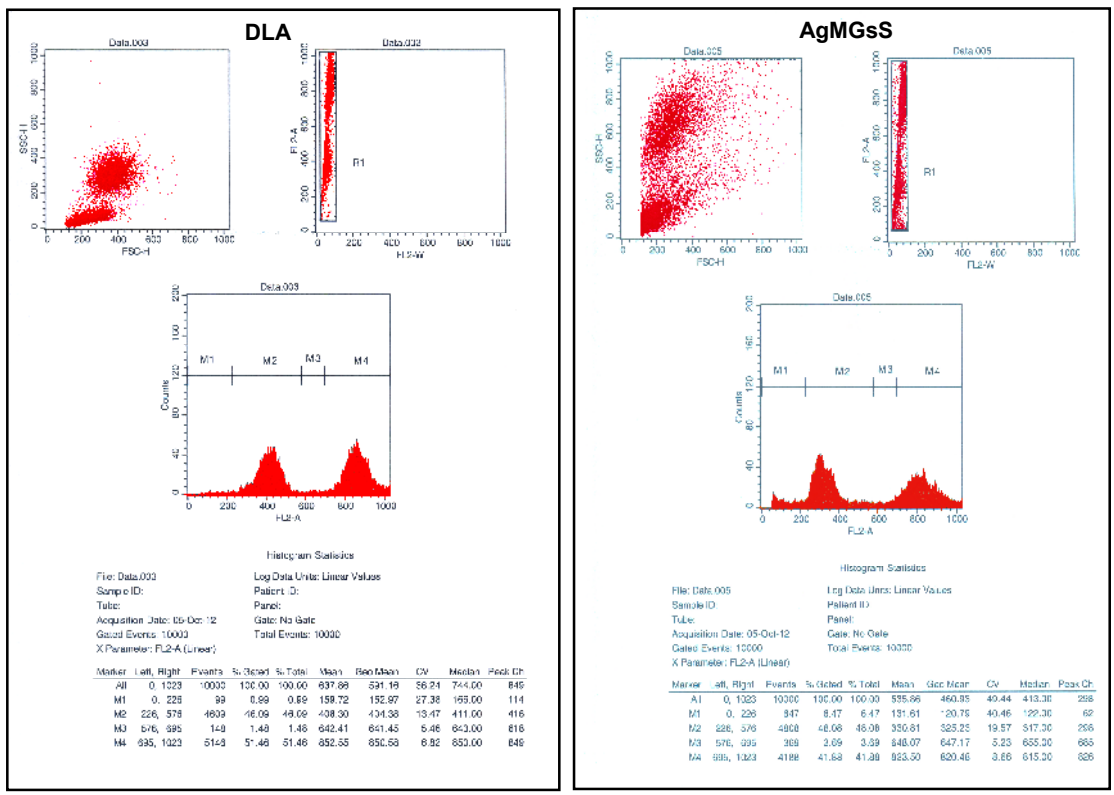

Annexin V-Biotin and PI positive cells were detected in AgMGsSTL treated DLA cells. AgMGsS showed 6.47%; AgMGsT showed 4.26% and AgMGsL showed 2.50%. Annexin V-Biotin and PI positive cells when compared with 0.99%, of Annexin V-Biotin and PI negative cells detected in untreated cells (Figures 68 and 69). Results were analyzed using the CELL Quest software program. Results were statistically significant when compared with (Annexin V-Biotin and PI positive cells detected in treated tumor cells versus annexin V-Biotin and PI negative cells detected in untreated cells), each other. These results showed that AgMGsS,

AgMGsT and AgMGsL treatment have apoptosis inducing effect to DLA tumor cells.

Figure 69

Apoptotic effect of AgMGsT and AgMGsL to DLA cells by fluorescent-activated cell sorting analysis

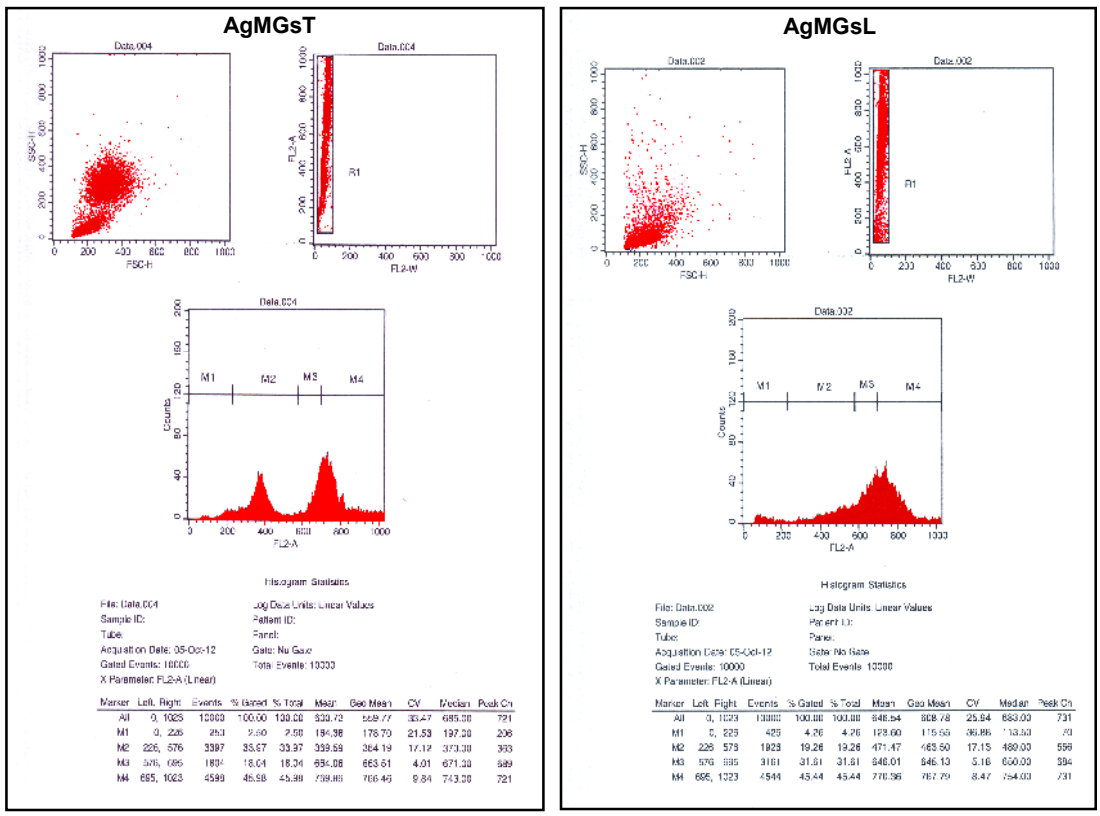

During the last decade, a number of plants have been reported for their antiproliferative and apoptotic properties. Awang *et al*., (2010) noticed the cytotoxic and apoptotic properties of 1'-(*S*)-1'-Acetoxychavicol acetate isolated from the *Alpinia conchigera* to five human tumor cell lines by flow cytometric analysis in annexin-V and PI dual staining and demonstrated that cell death occurred via apoptosis. *Goniothalamin* root extract showed a promising cytotoxicity and apoptosis effect against cervical cancer (HeLa) cells (Alabsi *et al*., 2012). Annexin- V staining showed the apoptosis inducing effect of polysaccharides PST001 isolated from seed kernel of *Tamarindus indica* to murine cancer cells DLA and EAC (Aravind *et al*., 2012).

Growth inhibitory effect and induction of apoptosis as casticin (flavonoid compound) was associated with cell cycle arrest at G2/M phase (Ding *et al*., 2012). Oskoueian *et al*., (2012) also reported the the apoptosis induction of *Jatropha curcas* to MCF-7 and HeLa cell lines in a dose-dependent manner. Apoptotic effect to human promylocytic leukemia HL60 cells was induced by isatin, extracted from flower of a folklore medicinal plant *Couroupita guianensis* and was confirmed by flow cytometry (Premanathan *et al*., 2012). *Polygonum avicular* induced apoptosis in MCF-7 cells and confirmed its anticancer property (Roudkenar *et al*., 2012). Withaferin A inhibited the growth of ovarian carcinoma cell lines CaOV3 and SKOV3 by inducing apoptosis and cell cycle arrest (Zhang *et al*., 2012). Yusup *et al*., (2012) also showed the involvement of *Savda Munziq* ethanol extract in antiproliferation, induction of apoptosis, cell cycle arrest, and regulation of apoptosis-related gene expression Bcl-2 and Bax activity pathway in colon cancer cells. *Melissa officinalis* also showed cytotoxicity against breast cancer cell lines (MCF-7, MDA-MB-468 and MDA-MB-231) by inducing Annexin-positive cells (Saraydin *et al*., 2012).

Apoptotic assay, confirmed the apoptotic inducing effects of AgMGsSTL to DLA cancer cells. The knowledge and understanding on how AgMGsSTL potentiates apoptosis as shown in this study is of great importance in further understanding the mechanisms underlying tumorigenesis. This knowledge will provide the basis for newly targeted therapies, hence giving cancer researchers a better insight for future chemotherapeutic approaches.

The *in vitro* anticancer study reported that the formulated MGsSTL and AgMGsSTL were found to have cidal activity to DLA cancer cells in a sustained manner. This study revealed the potency of AgMGsSTL to bring about apoptotic inducing effect to DLA tumor cells. Results of the present study suggested that MGsSTL and AgMGsSTL could induce tumor cell death by physiological and pathological means.

Based on the above reported results, it can be stated that AgMGsSTL have more potential antitumor activity than that of MGsSTL. Thus implicating its use in

prevention and cure of cancer. The free radical hypothesis supported the fact that the antioxidants effectively inhibited the tumor. The observed properties may be attributed to the antioxidant and antitumor principles present in the MGsSTL and AgMGsSTL.

Though the *in vitro* study may provide an effective antioxidant and antitumorigenic potential of MGsSTL and AgMGsSTL, a long term *in vivo* study is required to confirm the above results in DLA induced Swiss albino mice.

Phase III

4.3 *In vivo* antioxidative and antitumorigenic effect of MGsSTL and AgMGsSTL in DLA tumor induced mice

In Phase II, *in vivo* antioxidative potential of MGsSTL and AgMGsSTL in Swiss albino mice was evaluated by assessing the activities of enzymic antioxidants, levels of non enzymic antioxidants, levels of lipid peroxides in comparison with the standard antioxidant Silymarin for 20 days and 60 days treatment periods. The *in vivo* antitumorigenic effect of MGsSTL and AgMGsSTL was assessed by evaluating the activities of enzymic antioxidants, the levels of nonenzymic antioxidants, levels of lipid peroxides and increase in life span of DLA tumor induced Swiss albino mice in the presence and absence of MGsSTL and AgMGsSTL for 20 days and 60 days treatment periods. The histological status of the experimental mice was also evaluated.

4.3.1 Effect of MGsSTL and AgMGsSTL on the activities of enzymic antioxidants

Liver damage leads to the accumulation of fat and necrosis in the centrilobular region of the liver. As a consequence, the microsomal enzyme activities are found to decrease. Due to lipid peroxidation, the water soluble enzymes leak into plasma from the liver. It is shown by the significant decrease in triglycerides and protein enzymes in the liver of the tumor inoculated animals (Badami *et al*., 2003).

Table 10

Activities of hepatic enzymic antioxidants in controls and experimental Swiss albino mice

Groups	Catalase (U / mg protein)[a]		Superoxide dismutase (U / mg protein)[b]		Glutathione S transferase (U/mg protein)[c]		Glutathione peroxidase (U / mg protein)[d]		Glutathione reductase (U / mg protein)[e]	
	20 days	60 days	20 days	60 days	20 days	60 days	20 days	60 days	20 days	60 days
PBS	23.92	24.52	2.41	2.55	4.89	5.20	15.93	16.35	8.00	8.25
DMSO	23.99	24.05	2.32	2.40	5.14	5.81	15.66	16.12	7.10	7.12
Paraffin oil	26.72	27.22	2.91	3.13	5.45	6.31	16.96	17.70	7.90	8.85
Silymarin	37.05	42.12	5.95	11.76	9.90	11.63	18.70	22.57	11.19	16.03
MGsS	40.10	55.26	6.00	13.16	10.12	13.54	18.88	25.86	14.25	18.62
AgMGsS	45.27	66.89	6.50	18.10	12.15	14.09	19.93	33.27	15.20	20.11
MGsT	36.10	39.47	4.83	5.55	7.18	8.38	16.59	18.75	11.20	16.06
AgMGsT	38.01	43.19	5.88	6.80	8.26	10.20	17.91	20.12	11.36	16.64
MGsL	30.53	36.76	2.89	3.25	6.81	7.16	16.50	18.59	7.25	8.78
AgMGsL	35.77	37.71	3.22	3.86	6.92	7.43	17.80	18.85	7.31	8.93
DLA+MGsS	30.01	50.41	3.10	12.17	3.29	6.55	12.27	20.17	10.10	16.48
DLA+AgMGsS	36.20	56.86	6.25	17.54	3.51	6.96	13.16	21.96	12.85	18.94
DLA+MGsT	31.35	35.86	2.79	3.76	2.92	6.28	11.21	16.35	6.02	9.46
DLA+AgMGsT	34.00	39.47	4.88	5.86	3.06	6.88	11.92	17.88	6.26	9.93
DLA+MGsL	25.68	30.30	1.81	2.72	1.98	5.72	8.93	16.16	4.84	8.18
DLA+AgMGsL	30.14	38.30	1.93	2.95	2.02	6.21	9.00	16.25	4.88	8.29
DLA	18.88		1.40		1.77		5.76		3.88	
One way ANOVA with DLA (p<0.05)	**1.335**		**0.262**		**0.290**		**0.535**		**0.184**	
One way ANOVA without DLA (p<0.05)	**0.095**	**1.203**	**0.398**	**0.444**	**0.298**	**0.362**	**0.543**	**0.714**	**0.185**	**0.188**
Two way ANOVA without DLA (p<0.05)	**1.010**		**0.238**		**0.350**		**0.325**		**0.194**	

The values are mean ± SD of six animals

U[a]- Amount of enzyme required to decrease the absorbance by 0.05 units at 240nm.

U[b]- Amount of enzyme that gives 50% inhibition of the extent of NBT reduction/min.

U[c]- Micro moles of CDNB conjugated / min.

U[d]- Nanomoles of GSH oxidized / min.

U[e]- Millimoles of NADPH oxidized / min.

Antioxidant enzymes are considered to be a primary defense that prevents biological macromolecules from oxidative damage. Many plant secondary metabolites have been shown to act as potent antioxidants (Rao et al., 2005). Antioxidants protect cellular components by acting as radical scavenger, hydrogen donors, electron donors, peroxide decomposer, singlet oxygen quencher and metal-chelating agents (Fang *et al*., 2002). The effects of ROS on living organism depend on the intensity of oxidative stress, efficacy of antioxidant systems and many other factors. The adaptive response is usually realized via synthesis of new molecules of antioxidant enzyme which takes place simultaneously with inactivation of the enzyme by ROS (Vijayabaskaran et al., 2010).

The activities of enzymic antioxidants CAT, SOD, GST, GPx and GR in the liver of vehicle controls – (PBS, DMSO and Paraffin oil), tumor control – (DLA), standard- silymarin and experimental groups {MGsS, AgMGsS, MGsT, AgMGsT, MGsL, AgMGsL, MGsS+ DLA, AgMGsS+ DLA, MGsT+ DLA, AgMGsT+DLA, MGsL+DLA, AgMGsL+ DLA} of mice were evaluated and are shown in Table 10.

4.3.1.1 Effect on Catalase activity (CAT)

CAT activity was found to be significantly increased in mice administered with MGsSTL and AgMGsSTL when compared to control groups on 20 days and 60 days of treatment periods. Compared to paraffin oil the standard antioxidant silymarin showed significant increase in the activity of CAT in all treatment periods. The CAT activity was found to be more significant in AgMGsS treated mice which was followed by MGsS> AgMGsT> MGsT than that of silymarin treated mice. DLA tumor induced mice showed a significant decrease in CAT activity on 20 days of treatment period. CAT activity was found to be significantly increased in MGsST and AgMGsST administration individually and to DLA tumor induced mice on all treatment periods except MGsL and AgMGsL in 20 days treatment period (Figure 70 and Table 10).

Figure 70

Effect of MGsSTL and AgMGsSTL on the activities of CAT in normal and DLA induced Swiss albino mice

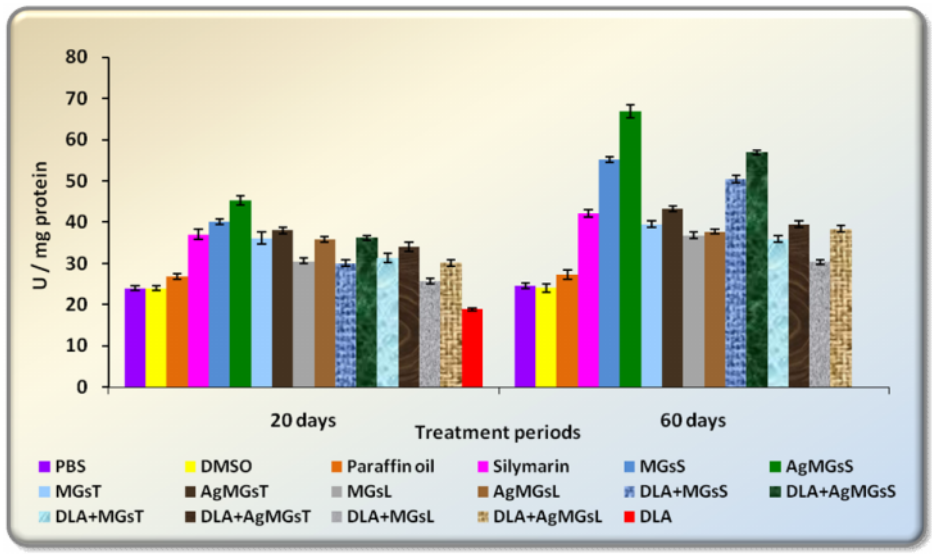

The significant elevation of SOD and CAT by the MGSSTL and AgMGsSTL treatment may be due to the potent antioxidant activity of their phytochemical constituents.

Administration of MGsSTL and AgMGsSTL increased the CAT activity, which may be indicating the antioxidant and free radical scavenging property of MGsSTL and AgMGsSTL. The antitumor activity of MGsSTL and AgMGsSTL was accompanied with the increase of antioxidant status. The free radical hypothesis supported that the antioxidant effectively inhibited tumor and observed investigations may be attributed to the antitumor and antioxidant principles present in the extract.

4.3.1.2 Effect on Superoxide dismutase activity (SOD)

A decrease in SOD and CAT activity in DLA bearing mice may be due to loss of Mn-SOD activity in DLA cells and a loss of mitochondria. The administration of MGsSTL and AgMGsSTL for 20 days and 60 days significantly increased the activities of SOD and CAT.

Figure 71

Effect of MGsSTL and AgMGsSTL on the activities of SOD in normal and DLA induced Swiss albino mice

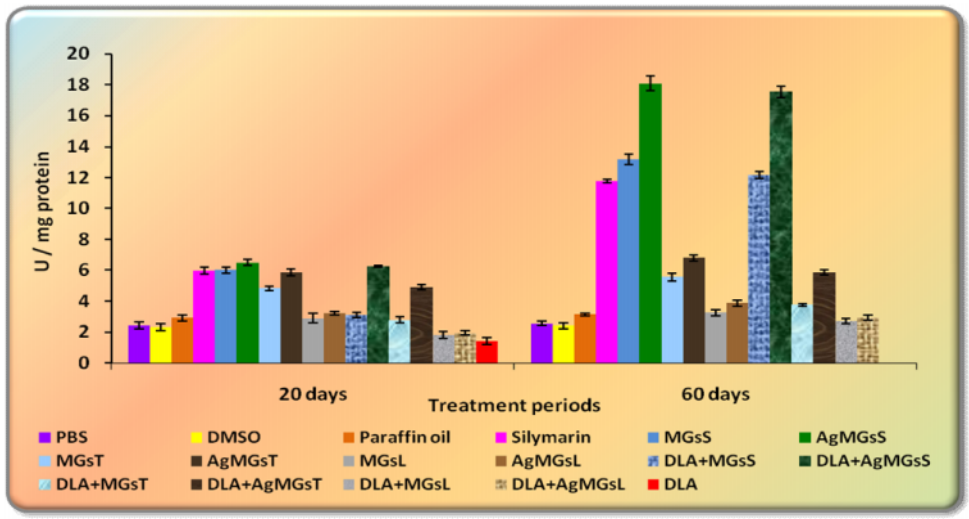

The SOD activity was found to be significantly increased in the mice administered with MGsSTL and AgMGsSTL when compared to control mice in 20 days and 60 days treatment periods. The silymarin administered mice showed a significant increase in SOD activity when compared to paraffin oil control in all the treatment periods. The DLA tumor induced mice showed significant low level of SOD activity when compared to all the other controls and experimental groups. Compared to the standard antioxidant silymarin group, AgMGsS showed more SOD activity which was followed by MGsS in both the experimental periods. In DLA tumor induced mice MGsST and AgMGsST showed significant enhanced activity of SOD in 60 days treatment period when compared to 20 days treatment period (Figure 71 and Table 10).

4.3.1.3 Effect on Glutathione S- transferase activity (GST)

The GST activity was found to be significantly increased in the mice administered with MGsSTL and AgMGsSTL when compared to control mice on 20 days and 60 days treatment periods. The silymarin administered mice showed a significant increase in GST activity when compared to paraffin oil control in all the treatment periods.

Figure 72

Effect of MGsSTL and AgMGsSTL on the activities of GST in normal and DLA induced Swiss albino mice

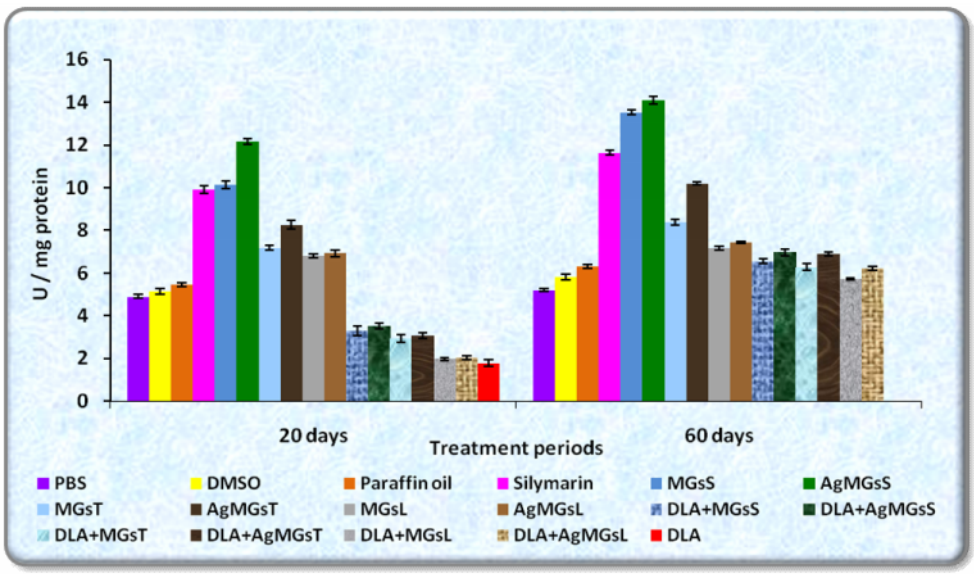

The GST activity was found to be more significant in AgMGsS treated mice which was followed by MGsS than that of silymarin treated mice. The DLA tumor induced mice showed significant low level of GST activity when compared to all the other controls and experimental groups in 20 days. In DLA tumor induced mice MGsST and AgMGsST showed significant enhanced activity in 20 days treatment period (Table 10 and Figure 72).

4.3.1.4 Effect on Glutathione Peroxidase activity (GPx)

In our present study, the activity of GPx was found to be increased significantly by MGsSTL and AgMGsSTL in 20 days and 60 days treatment periods when compared to control groups (Table 10 and Figure 73).

Compared to paraffin oil control mice, the activity of GPx was found to be increased in silymarin treated mice in all treatment periods. Compared to the standard antioxidant silymarin group AgMGsS alone showed more GPx activity on 20 days and AgMGsS > MGsS showed more GPx activity on 60 days treatment periods.

Figure 73

Effect of MGsSTL and AgMGsSTL on the activity of GPx in normal and DLA induced Swiss albino mice

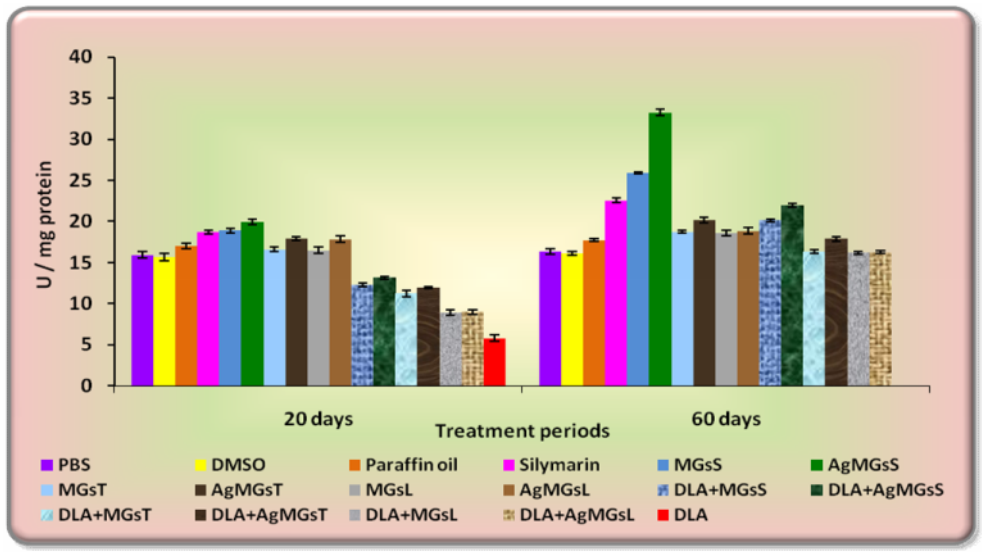

The activity of GPx in DLA tumor induced mice administered with MGsSTL and AgMGsSTL was found to be significantly increased in 20 days treatment period. DLA tumor induced mice showed a reduction in the activity of GPx in the liver on 20 days of treatment period due to the oxidative stress increased by DLA tumor induced intoxication and that has been reverted by the co-administration of MGsSTL and AgMGsSTL to the DLA transplanted mice. This effect may represent an important mechanism of protection by the fractions, since by having increased the ability to remove peroxides, cells may be less susceptible to oxidative stress induced damage. GPx is an antioxidant enzyme that is highly expressed and removes peroxides and peroxynitrite.Low activities of GPx is one of the early consequences of a disturbance of the pro-oxidant/ antioxidant balance.

4.3.1.5 Effect on Glutathione Reductase activity (GR)

In the present research, increase in the activity of GR was observed in the liver of MGsSTL and AgMGsSTL administered mice in comparison with the control groups on 20 days and 60 days treatment periods.

Figure 74

Effect of MGsSTL and AgMGsSTL on the levels of GR in normal and DLA induced Swiss albino mice

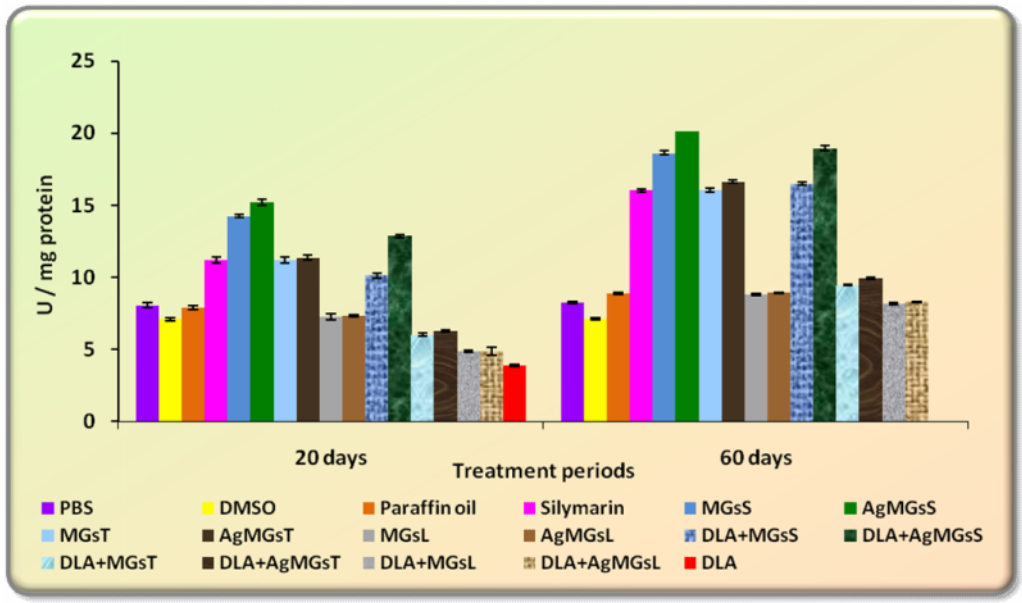

The silymarin administered mice showed a significant increase in GR activity when compared to paraffin oil control in all the treatment periods. The GR activity was found to be more significant in AgMGsS treated mice which was followed by MGsS> AgMGsT than that of silymarin treated mice. Also, liver GR activity was significantly depressed in DLA tumor bearing mice compared to that of control groups and experimental groups. However, this significant decrease in GR activity was reversed upon the administration of MGsSTL and AgMGsSTL to DLA induced mice (Table 10 and Figure 74).

4.3.2. Effect of MGsSTL and AgMGsSTL on the levels of non enzymic antioxidants

The levels of non enzymic antioxidants Vitamin A, Vitamin E, Vitamin C and Reduced Glutathione (GSH) in the liver of control and experimental groups of mice on two different treatment periods (20 days and 60 days) are shown in the Table 11 and figure 75 –78.

4.3.2.1 Effect on the levels of Vitamin A

The effect of MGsSTL and AgMGsSTL on the levels of Vitamin A in the liver of experimental mice is shown in Table 11 and Figure 75. The administration of MGsSTL and AgMGsSTL to normal mice afforded a significant increase in hepatic Vitamin A content in comparison with vehicle control groups on all the treatment periods. Silymarin treated group showed significant increased level of Vitamin A in 20 days and 60 days of treatment periods when compared to paraffin oil treated group. Compared to the standard antioxidant silymarin group, AgMGsS which was followed by MGsS> AgMGsT>MGsT showed more significant hepatic Vitamin A levels. The DLA tumor induced mice showed a decreased level of Vitamin A in 20 days of treatment period. All the extract treated groups showed more significant raise in the Vitamin A content in the liver when compared to that of DLA tumor induced mice.

4.3.2.2 Effect on the levels of Vitamin E

Significantly increased level of Vitamin E was found in MGsSTL and AgMGsSTL administered mice when compared to control mice in 20 days and 60 days of treatment periods (Table 11 and Figure 76). Compared to paraffin oil control the silymarin treated mice showed significant increase in the level of Vitamin E in all the treatment periods. On 20 days and 60 days treatment periods the level of Vitamin E was increased significantly in AgMGsS which was followed by MGsS> AgMGsT> MGsT administered mice when compared to the silymarin treated group. The level of Vitamin E was found to be significantly decreased in DLA tumor induced mice in 20 days of treatment period. But the coadministration of MGsSTL and AgMGsSTL to DLA induced animals showed significantly increased Vitamin E levels.

Table 11

Levels of hepatic non enzymic antioxidants in controls and experimental Swiss albino mice

Groups	Vitamin A (μg/g tissue)		Vitamin E (μg/g tissue)		Vitamin C (mg / g tissue)		Reduced glutathione (nmoles /g tissue)	
	20 days	60 days	20 days	60 days	20 days	60 days	20 days	60 days
PBS	3.95	4.21	3.01	4.02	0.83	0.99	1.65	1.75
DMSO	3.52	3.66	3.02	3.21	0.80	0.82	1.37	1.48
Paraffin oil	4.23	4.65	3.20	4.49	1.01	1.12	1.90	2.17
Silymarin	4.81	6.54	6.28	8.41	3.12	4.49	3.38	4.47
MGsS	6.42	9.77	9.92	12.29	3.33	6.06	4.72	7.32
AgMGsS	7.71	12.20	10.01	16.03	5.11	9.40	5.01	8.85
MGsT	4.98	6.84	7.25	9.59	2.74	3.06	3.99	4.70
AgMGsT	6.12	8.26	8.36	11.15	4.00	4.71	4.25	5.04
MGsL	3.74	4.08	5.35	6.69	1.71	1.98	2.60	2.98
AgMGsL	4.20	4.86	6.21	7.19	2.09	2.48	2.76	3.04
DLA+MGsS	4.35	7.67	7.58	10.84	2.98	4.69	3.86	5.55
DLA+AgMGsS	6.82	8.23	8.37	11.73	3.01	4.95	3.94	5.96
DLA+MGsT	2.80	5.29	4.93	5.53	1.49	1.86	2.92	3.27
DLA+AgMGsT	3.05	5.67	5.26	6.60	1.53	1.92	2.99	3.45
DLA+MGsL	2.55	4.99	3.17	5.16	1.06	1.39	2.02	2.45
DLA+AgMGsL	2.64	5.01	3.95	5.35	1.21	1.50	2.04	2.50
DLA	2.15		1.12		0.36		1.01	
One way ANOVA with DLA ($p<0.05$)	**0.075**		**0.568**		**0.157**		**0.092**	
One way ANOVA without DLA ($p<0.05$)	**0.076**	**0.176**	**0.162**	**0.125**	**0.104**	**0.139**	**0.092**	**0.151**
Two way ANOVA without DLA ($p<0.05$)	**0.027**		**0.111**		**0.102**		**0.099**	

Figure 75

Effect of MGsSTL and AgMGsSTL on the levels of Vitamin A in normal and DLA induced Swiss albino mice

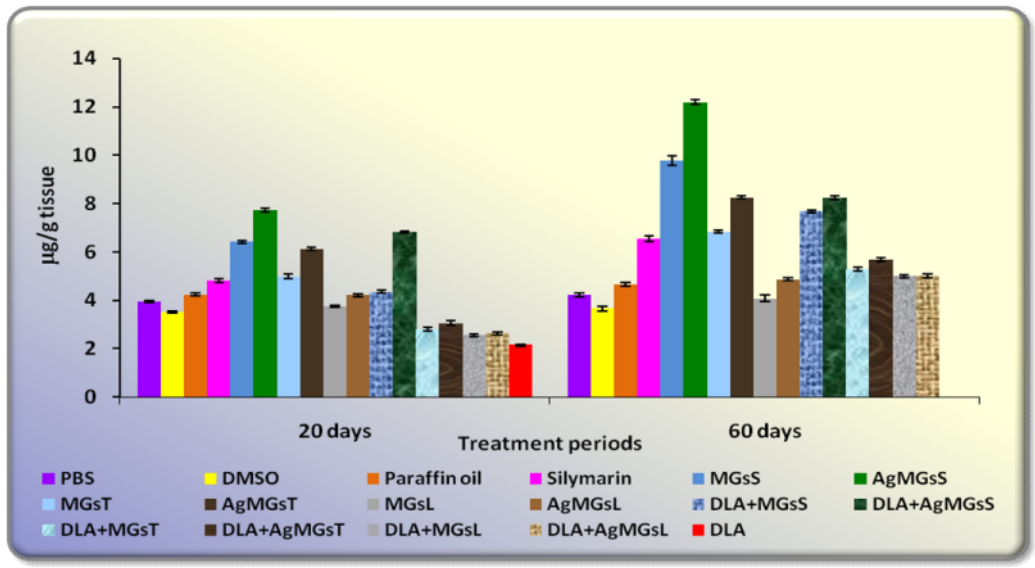

Figure 76

Effect of MGsSTL and AgMGsSTL on the levels of Vitamin E in normal and DLA induced Swiss albino mice

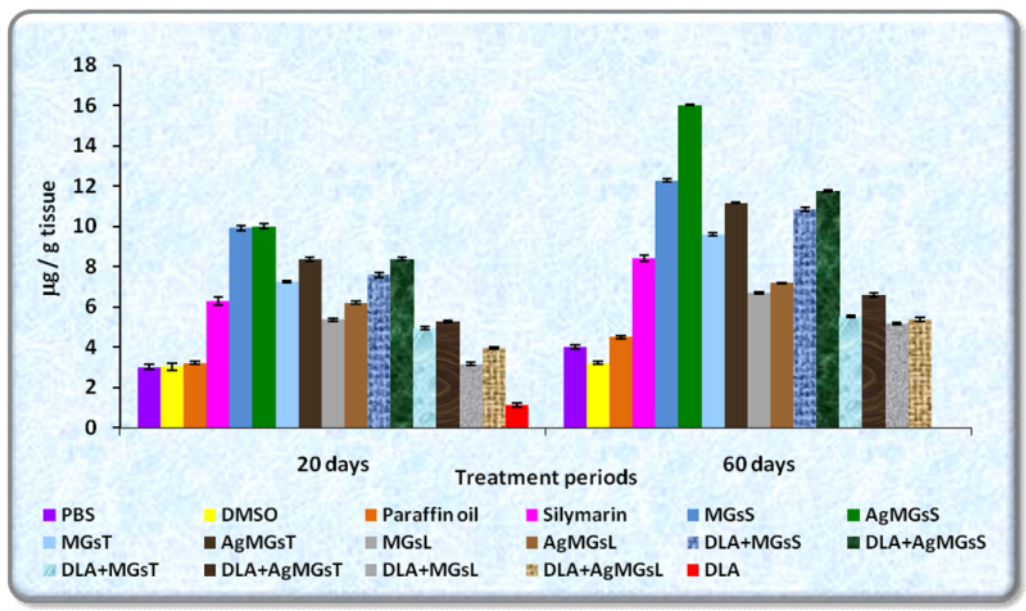

4.3.2.3 Effect on the levels of Vitamin C

The levels of Vitamin C in the MGsSTL and AgMGsSTL treated groups were significantly increased in comparison with the control groups (PBS, DMSO and Paraffin oil) in 20 days and 60 days of treatment periods. Compared to paraffin oil control the silymarin treated mice showed significant increase in the level of Vitamin C in all the treatment periods. The Vitamin C activity was found to be more significant in AgMGsS treated mice which was followed by MGsS> AgMGsT than that of silymarin treated mice as shown in Table 11 and Figure 77. Inoculation of DLA tumor cells significantly reduced the Vitamin C content in 20 days of treatment period. But the DLA induced mice treated with MGsSTL and AgMGsSTL showed significant increase in the levels of Vitamin C when compared to DLA control group in 20 days treatment period and also in 60 days treatment period.

Figure 77

Effect of MGsSTL and AgMGsSTL on the levels of Vitamin C in normal and DLA induced Swiss albino mice

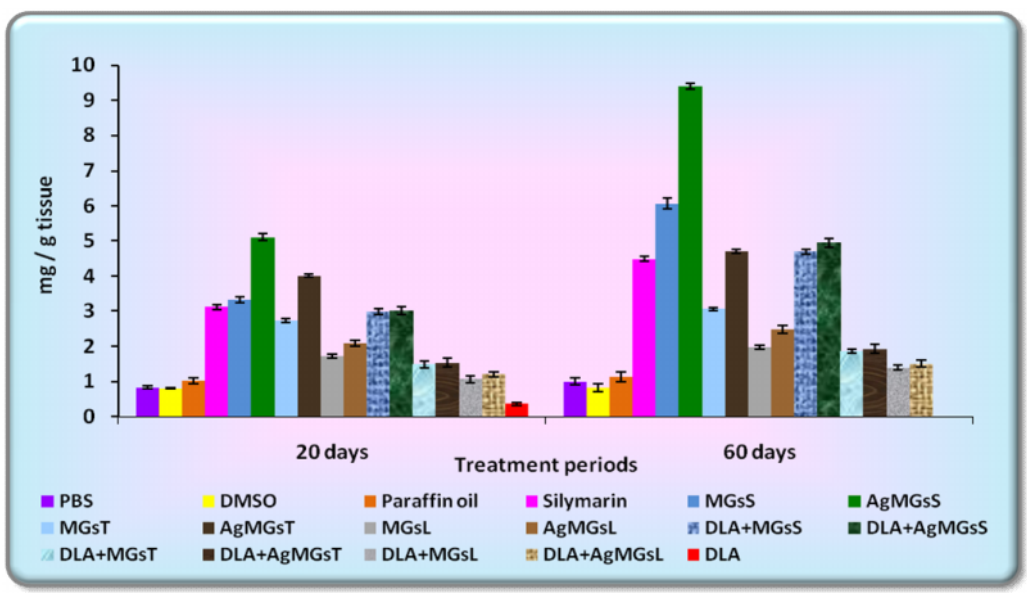

4.3.2.4 Effect on the levels of Reduced glutathione (GSH)

In this study, the GSH content in liver of mice were significantly elevated by the intraperitoneal administration of MGsSTL and AgMGsSTL when

compared to that of the vehicle control groups. The GSH level was found to be increased in silymarin treated mice in 20 days and 60 days of treatment period when compared to the vehicle control paraffin oil treated mice. AgMGsS treated mice showed more significant GSH level than that of the standard antioxidant silymarin treated group in both the treatment periods. The hepatic GSH content in liver of DLA tumor bearing mice was significantly reduced in comparison with normal control and all the experimental groups. The coadministration of MGsSTL and AgMGsSTL to DLA induced animals showed significantly increased GSH levels as shown in Table 11 and Figure 78.

Figure 78

Effect of MGsSTL and AgMGsSTL on the levels of GSH in normal and DLA induced Swiss albino mice

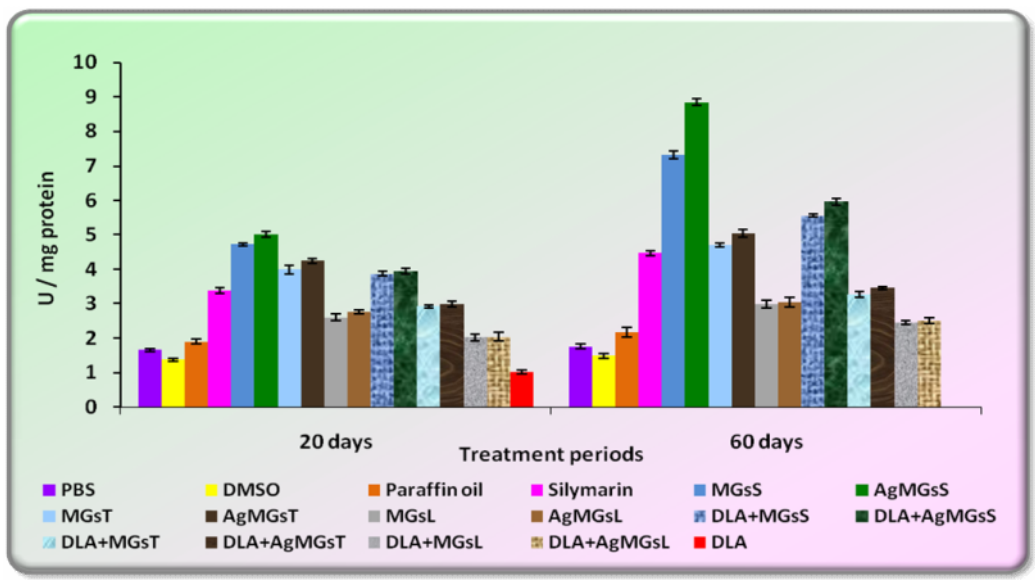

4.3.3. Effect of MGsSTL and AgMGsSTL on the rate of lipid peroxidation (LPO)

Increased LPO would cause degeneration of tissues. Lipid peroxide formed in the primary site would be transferred through circulation and provoke damage by propagating the process of LPO. Malonaldehyde bis (dimethyl acetal) (MDA), the end product of LPO was higher in carcinomatous tissue than in non diseased organs, and their levels were correlated with advanced clinical

stages and the impairment is related to tumor progression (Manoharan *et al*., 2008). Moreover, it has been claimed that MDA acts as a tumor promoter and cocarcinogenic agent because of its high cytotoxicity and inhibitory action on protective enzymes. Vitamin E prevents the process of LPO and as reducing agents that prevent oxidative reactions, often by scavenging ROS before they can damage cells (Ristow and Zarse 2010).

Table 12

Levels of hepatic MDA in controls and experimental Swiss albino mice

Groups	Lipid peroxides (nmoles of MDA/mg protein)	
	20 days	60 days
PBS	3.62	3.57
DMSO	3.90	3.60
Paraffin oil	3.61	3.45
Silymarin	3.15	1.68
MGsS	3.02	1.45
AgMGsS	2.99	1.22
MGsT	3.10	1.48
AgMGsT	2.80	1.32
MGsL	3.52	1.85
AgMGsL	3.25	1.78
DLA+MGsS	3.31	1.86
DLA+AgMGsS	3.12	1.48
DLA+MGsT	4.42	2.27
DLA+AgMGsT	4.03	2.01
DLA+MGsL	5.31	3.79
DLA+AgMGsL	5.02	3.73
DLA	7.53	
One way ANOVA with DLA (p<0.05)	0.461	
One way ANOVA without DLA (p<0.05)	0.108	0.098
Two way ANOVA without DLA (p<0.05)	0.0986	

Figure 79

Effect of MGsSTL and AgMGsSTL on the levels of MDA in normal and DLA induced Swiss albino mice

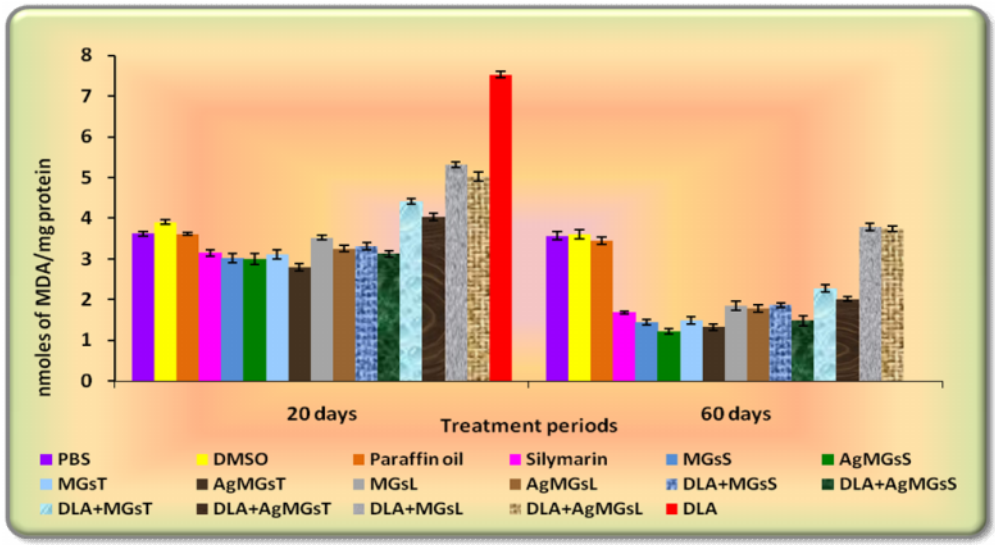

Table 12 and Figure 79 show the levels of lipid peroxide (MDA) in the liver of control and experimental groups of mice. Administration of MGsSTL, AgMGsSTL and silymarin showed a significant decrease in MDA levels when compared to that of normal control groups in both the treatment periods. The level of MDA was found to be significantly decreased in AgMGsS treated mice which was followed by MGsS> AgMGsT than that of silymarin treated mice. A significant increase in the levels of MDA was observed in DLA tumor bearing mice when compared to all the other control and experimental animals. But, the coadministration of MGsSTL and AgMGsSTL to DLA tumor induced mice showed significant decrease in the levels of MDA when compared to DLA control mice in 20 days treatment period. Coadministration of MGsSTL and AgMGsSTL to DLA tumor induced mice showed significant decrease in the levels of MDA in 60 days treatment period when compared to 20 days treatment period. The decrease in the rate of LPO in 60 days treatment period was found to be ranged from 1.5 to 2.5 times when compared to 20 days treatment period by MGsSTL and AgMGsSTL

Oxidative stress that occurs in the cells, due to the imbalance between the prooxidant/antioxidant systems, cause injury to biomolecules such as nucleic acids, proteins, structural carbohydrates, and lipids. Among these targets, lipids are basically damaged because of the formation of LPO products which initiate and propagate free radical reactions (Nordberg and Arner 2001). *Euphorbia neriifolia* extract significantly restored the activity of endogenous enzymic antioxidants (SOD and CAT) and decreased the MDA level in the liver and exhibited significant protective effect against N-Nitrosodiethylamine induced liver toxicity in mice (Pracheta *et al*., 2011). Ethanolic extract of *Salvia leucantha* Cav possesses potent antitumor activity against EAC cells by decreasing the levels of MDA and increasing the activity of enzymatic antioxidants GSH, SOD and CAT (Sridharan *et al*., 2012).

These observations are consistent with earlier studies which showed that tumor cells generate and release peroxides into circulation which can subsequently oxidize GSH. Tumor cells also sequester antioxidants from circulation to promote tumor growth. This may be one of the reasons for the declined antioxidant status with enhanced LPO in the DLA treated rats (Jasmine *et al*., 2008). MGsSTL and AgMGsSTL supplement to DLA exposed mice significantly enhanced the antioxidants and decreased the rate of LPO, and protected the cells from DLA induced neoplastic transformation.

Our findings are also supported by Singh *et al*., (2009) who showed decrease in LPO in the liver of CCl_4-treated rats by the coadministration of Embelin (from Embelia ribes). Hydroalcoholic extract of *Sansevieria roxburghiana* rhizome treatment significantly decreased LPO and recovered GSH, SOD and CAT towards normal as compared to EAC control animals (Haldar *et al*., 2010). *Aegle marmelos* leaf extract in DLA bearing mice decreased the levels of hepatic MDA and increased the levels of hepatic antioxidants and nonenzymic antioxidants (Chockalingam *et al*., 2012). Reddy *et al*., (2012) reported that quercetin administeration increased the antioxidant enzymes of CAT, GPx and SOD and decreased the lipid peroxide level in

Dimethyl Benzanthracene induced breast cancer in female Wistar rats. Saroja *et al*., (2012) also showed that the administration of flavonoid fraction of *Terminalia Catappa* significantly enhanced the antioxidant levels and reduced the lipid peroxide levels in ELA tumor induced mice.

The administration of MGsSTL and AgMGsSTL individually and to DLA tumor induced mice increased the activity of enzymic antioxidants (CAT, SOD, GST, GPx and GR), level of non ezymic antioxidants (Vitamin A, Vitamin C, Vitamin E and GSH), decreased the MDA levels and showed the antioxidant activity which inturn is responsible for their antitumor potential against DLA tumor.

In vitro and *in vivo* antitumorigenic effect of AgMGsSTL was found to be more significant than that of MGsSTL. Among AgMGsSTL, AgMGsS showed maximum antitumorigenic activity.

Catalase and peroxidases are important enzymes present in the intracellular spaces, where they can regulate the level of H_2O_2. Catalase is a haem protein with an extremely high turnover rate. Catalase present in the peroxisomes of nearly all aerobic cells, serves to protect the cell from the toxic effects of H_2O_2 by catalyzing its decomposition into molecular oxygen and water (Koksal *et al*., 2011). The SOD is a metalloprotein, that converts two superoxide radicals into H_2O_2 and O_2. To eliminate H_2O_2, before the Fenton reaction which can create highly reactive hydroxyl radicals, organisms use CAT - a homotetrameric ferri heme containing enzyme and/or GPX- a selenium dependent enzyme (Lenzen 2008)**.** SOD represent the first line of protection against superoxide anions because it catalyzes dismutation of superoxide anions into H_2O_2 and molecular oxygen (Ramnath *et al*., 2002). Balamurugan and Muralidharan (2010) who showed oxidative stress reducing effect of methanol extract of *Indigofera tinctoria* leaves on β-amyloid peptide induced Alzheimer's disease in mice with significant increase in CAT and SOD activities and the levels of GSH.

In the presence of xenobiotics, GST, GPx generally help in the detoxification by conjugating GSH with toxic electrophiles conferring a selective inhibition of the growth of DLA and EAC tumor cells (Sathiyanarayanan *et al*., 2006).

Tumor cells produce more peroxides when they proliferate actively after inoculation of tumor. This rise in peroxides indicated the intensification of oxygen free radical production (Monajemi *et al*., 2005). Cells which are equipped with enzymatic antioxidant mechanisms play an important role in the elimination of free radicals. High levels (up to 0.05 µmol/h per 104 cells) of H_2O_2 are constitutively released from a wide variety of human tumors. SOD and CAT are involved in the clearance of superoxide and H_2O_2. Decrease in SOD and CAT activities described in tumors is regarded as markers of malignant transformation. Lowered activities of SOD and CAT were reported in several cancers (Kavitha and Manoharan 2006). Dongre *et al*., (2008) showed a significant increase in CAT and SOD activities when treated with methanol extract of *Hypericum hookerianum* against the DLA cells bearing mice. A decrease in SOD and CAT activity in DLA bearing mice may be due to loss of Mn-SOD activity in DLA cells and a loss of mitochondria. Paclitaxel loaded NPs showed greater tumor growth inhibition effect *in vivo* on transplantable tumor, compared with Taxol in male NMRI mice (Danhier *et al*., 2009). Elevated activities of SOD and CAT was noticed in methanol leaf extracts of *Hymenocardia acida* Tul. (Hymenocardiaceae) treated rats (Ogbunugafor *et al*., 2010). Natesan *et al*., (2007) also reported significant increase in SOD activity based on ethanomedical use of *Careya arborea* Roxb bark in the treatment of DLA tumor.

Our results by the administration of MGsSTL and AgMGsSTL for 20 days and 60 days have shown significantly increased activities of SOD and CAT which are consistent with those of previous studies as shown above may be indicating their antioxidant and free radical scavenging property. The antitumor activity of MGsSTL and AgMGsSTL was accompanied with the increase of antioxidant status. The free radical hypothesis supported that the antioxidants

effectively inhibited tumor and the observed investigations may be attributed to the antitumor and antioxidant principles present in the extract. The significant elevation of SOD and CAT by the MGSSTL and AgMGsSTL treatment may be due to the potent antioxidant activity of their phytochemical constituents.

The GST, one of the major phase II detoxification enzymes are involved in the metabolism of xenobiotics and play an important role in cellular protection against oxidative stress. The GSTs are a family of enzymes that catalyse the formation of thioester conjugates between the endogenous tripeptide glutathione and xenibiotic compounds (Rajkapoor *et al*., 2004). GSTs can catalyse a larger number of reactions including nucleophilic aromatic substitutions, Michael additions, isomerisation and reduction of hydroperoxides, conjugation of many hydrophobic and electrophilic compounds with GSH. GSTs play a major role in detoxification of epoxides derived form polycyclic aromatic compounds (PAHS) and α-β-unsaturated ketones. Moreover, a number of endogenous compounds, such as prostaglandins and steroids are metabolized via glutathione conjugation. The major biological function of GST appears to be defense mechanism against reaction and toxic electrophiles such as ROS that arise through normal metabolic processes (Dauod *et al*., 2004).

The GST is the enzyme that adds glutathione primarily to lipophilic or electrophilic substances and thus mediates the reaction forming thioether (R-S-G) of glutathione. It is therefore known to be the enzyme involved in the detoxification by transferring or excreting toxic materials and peroxidized materials in the body. In addition, the free radical-mediated oxidation of lipid in cell membrane is proceeded by chain reactions, and antioxidants such as spices react as a chain breaking antioxidants, and thus delay the chain propagation (Semiz and Sen 2007). The increase in the GST activity in general, used as indication for the antitumor activity of the tested materials in tumor transplanted animals. Therefore, this enzyme has been used as the antitumor factor. In the tumor cells, the increase of cellular enzymes that regulate the cell oxidative stress such as SOD and GST and antioxidants such as GSH induce cancer regression and stimulate large number of tumor necrosis factor-alpha

(Gupta *et al*., 2004). Cytotoxic effect of methanol extract of *Indigofera linnaei* against EAC, DLA and human cancer cell lines showed the increase in enzymatic antioxidants such as SOD, CAT, GPx and GST (Kumar *et al*., 2011). Treatment of DLA- bearing Swiss albino mice with methanol extract of *Dillenia pentagyna* showed increase in GSH level and GR activity (Rosangkima and Prasad 2007). Egyptian flora also showed increase in enzymic antioxidants like SOD, GPx and GST against EAC bearing mice (Amr *et al*., 2009). Dibirdik *et al*., (2010) also reported the potent in vivo activity of PEGylated liposomal NP formulation of quinazoline derivative 4-(4'-hydroxyphenyl)-amino-6,7-dimethoxy quinazoline against breast cancer cells in the MMTV/*Neu* transgenic mouse model. Citrus essential oil treatments increased the activities of GST, increased the cellular GSH level and inhibited LPO and thus exhibited significant antitumor and antioxidant effects to Ehrlich ascites Carcinoma Cells (Mohamed *et al*., 2010). Ethyl acetate fraction of unripe *Carica papaya* fruits caused significant increase in the activities of GR, GPx, GST, CAT in Albino mice liver of both sexes (Oloyede *et al*., 2011). Ethanol extract of *Polygala rosmarinifolia* in DLA induced Swiss albino mice showed significant increase in the GST activity (Alagammal *et al*., 2012). The significant reduced activity of GST observed in our study in DLA induced mice may be partly due to lack of its substrate GSH, which also occurs due to the reduced activity of GR.

The GPx and CAT participate in the removal of H_2O_2, GPx being the main controller of H_2O_2 metabolism. Glutathione peroxidase may be responsible for H+, OH- and hydrogen scavenging in both the enzymatic and nonenzymatic test in addition to secondary metabolites present in the plant. Cells are also equipped with enzymatic antioxidant mechanisms that play an important role in the elimination of free radicals. SOD, CAT, and GPx are involved in the clearance of superoxide and H_2O_2. SOD catalyses the diminution of superoxide into H_2O_2, which has to be eliminated by GPx and/ or CAT. These enzymes have been induced by the administration of plant extracts (Meng *et al*., 2010). Similar findings were observed in the present investigation with DLA bearing mice. The administration of MGsSTL and AgMGsSTL significantly increased the

SOD, GPx and CAT activities. Ethanolic extract of *Hypericum hookerianum* significantly increased SOD, CAT, GPx and GSH in restraint stress induced Swiss albino mice (Subakanmani and Umadevi 2012). After treatment with *Pleurotus cornucopiae* SS-02 exopolysaccharide showed significant increase in the activities of SOD, GPx and CAT in mice (Zhang *et al*., 2012). Our finding was supported by Verma and Chakraborty (2008) who showed the significant increase in the activities of enzymatic antioxidants (SOD, CAT, GPX, GRX and GST) in mice by the administration of *Emblica officinalis* aqueous extract. Colloidal silver had cytotoxic effects to MCF-7 breast cancer cells and elevated the antioxidant activities of SOD, GPx and CAT (Franco-Molina *et al*., 2010). Kathirvel and Ravi (2011) also showed an increase in SOD, CAT and GPx activities in mice administered with the ethanol extract of *Ocimum basilicum.* SOD, CAT, GSH and GPx activities were found to be increased significantly along with a reduced MDA content in ethanol extract of *Clitoria ternatea* treated albino male rats induced with Acetaminophen (Sarumathy *et al*., 2011). Methanolic extract of *Castanopsis indica* leaves showed direct cytotoxicity to EAC cells by significantly inducing the hepatic antioxidant GPx (Dolai *et al*., 2012). Catalpol an effective component of *Rehmannia glutinosa* Libosch decreased the MDA level and increased the activities of CAT, GPx and SOD in doxorubicin treated H9C2 cells (Wu and Mao 2012). Gynandropsis gynandra extracts exerted its chemopreventive efficacy by preventing the rate of LPO and influenced the enzymatic antioxidants (CAT, SOD and GPx) in aflatoxin B_1 induced male albino rats (Sivanesan and Begum 2007).

Increase in the activity of GR will further increase the concentration of ascorbic acid. Increase in GSH and GPx will decrease the concentration of H_2O_2 signaling by further decreasing the oxidative stress. Increase in GST activity will decrease the concentration of active oxygen species (Singh *et al*., 2009). The increased levels of ROS in cancer due to their increased production and/ or decreased destruction of free radical scavenger enzymes function has been linked to altered activity of enzymatic antioxidants such as GR, CAT, GPx and SOD. The decreased activities of GPx and GR in liver resulted in the

involvement of deleterious oxidative changes, insufficient availability of GSH and also number of deleterious effects due to the accumulation of toxic products. Glutathione, a potent inhibitor of neoplastic process, plays an important role as an endogenous antioxidant system that is found particularly in high concentration in liver and is known to have key function in the protective process (Dubey *et al*., 2010). Glutathione reductase (GR) is another major antioxidant enzyme that catalyzes the NADPH-dependent reduction of GSSG to GSH, thus maintaining GSH levels in the cell (Rajesh and Latha 2004). Significant elevation of the activity of GR following MGsSTL and AgMGsSTL treatment was evident, thereby helping the cell to maintain the basal level of GSH, which is important for many other GSH dependent detoxification reactions. GSH participates in spontaneous scavenging of electrophiles or free radicals and in reactions catalyzed by enzymes like GPX and GST (Bharali *et al*., 2003). GR also plays an essential role in the cellular defence against oxidative stress and a controlled decrease in the level of GR in human fibroblasts resulted in lowering the cell viability. When GR activity is impaired, the ability of the cell to reduce GSSG to GSH may be devastated, leading to GSSG accumulation within the cytosol (Chavkova *et al*., 2001). Decrease in GSH level as observed in DLA induced mice may be due to alteration in the GSH:GSSG ratio. The increase in thiol enzymes (GR, GPx and GST) activities after MGsSTL and AgMGsSTL treatment could be one of the other possible steps involved in the increase of GSH level by the reduction of GSSG or by the elimination of oxidation of GSSG from the cell. Thus, stimulating cellular antioxidant machinery, and resulting in antitumor activity.

Methanolic extract of *Cleome chelidonii* against 7,12-Dimethylbenz(a) anthracene (DMBA)-induced skin papillomagenesis in mice model increased the activities of enzymic antioxidant SOD, CAT, GPx, GR and GST and the level of nonenzymic antioxidant like GSH (Parimalakrishnan *et al*., 2009). Cytotoxicity of ZnONPs against three types of cancer cells such as human hepatocellular carcinoma HepG2, human lung adenocarcinoma A549, and human bronchial epithelial BEAS-2B showed decrease in the rate of LPO and increase in GSH,

SOD, CAT, GPx, and GR (Akhtar *et al*., 2012). Hepatic antioxidant GR activity increased significantly with coadministration of *Cnidoscolus chayamansa* to EAC and DLA induced Swiss albino mice (Pillai *et al*., 2012). Ramachandraiahgari *et al*., (2012) also reported increased activities of SOD, CAT, GPx and GR in hepatic and renal tissue of ethanolic extract of *Aloe vera* treated diabetic rats. *Abrus precatorius* L. (Leguminosae) in HepG2 cells and *N*-nitrosodiethylamine induced hepatocellular carcinoma Swiss albino rats increased the activities of GPx, GST, SOD, CAT and increased the levels of GSH and decreased the levels of TBARS (Kartika *et al*., 2010). The above observation was supported by Kameshwaran *et al*., (2012) in *Tecoma stans* to EAC model, showed anticancer activity by increasing the activities of GSH, SOD, CAT and decrease in MDA levels.

In the present study MGsSTL and AgMGsSTL administration resulted in the significant increase of CAT, SOD GST, GPx and GR indicating the induction of these antioxidants help in exerting a possible antitumorigenic effect in DLA treated mice.

Mammalian cells possess elaborate enzymatic SOD, CAT and GPx and nonenzymatic GSH, Vitamin A and C antioxidant defense mechanisms to detoxify radicals. GPx detoxifies H_2O_2 using GSH and Vitamin A as co-substrate. GSH and Vitamin A, the most important intracellular antioxidant protect cells against damage by ROS (Circu, *et al*., 2009). Vitamin A is a fat-soluble Vitamin, which is essential for growth maintenance and differentiation of epithelial cells. Vitamin A breaks the chain of LPO in the cell membrane and prevents the formation of lipid peroxide. Vitamin A acts as a powerful, free radical scavenger (Singlet oxygen) and chain breaking antioxidant. The function of Vitamin A as radical scavenging antioxidants, can protect the cells from oxidative damage (Kumar *et al*., 2005). Raghavan and Kumari (2006) reported that the ethanolic extract of *Terminalia arjuna* in alloxan induced diabetic rats showed significant increase in SOD, CAT, GPx, GST, GR, GSH, Vitamin A, Vitamin C and Vitamin E. Gurunagarajan and Pemaiah, (2010) also reported the significant increase in Vitamin A level when mice treated with ethanolic extract

of *Lenotic naptaefol* against EAC cell lines. Administration of berberine, an isoquinoline alkaloid to 7,12-dimethylbenz[a]anthracene induced skin carcinogenesis, significantly increased the activities of enzymatic antioxidants and nonenzymatic antioxidants such as SOD, CAT, GPx , GSH, and Vitamin A (Manoharan *et al*., 2010). *Ammannia baccifera* significantly decreased the rate of LPO and increased the activities of SOD, CAT, GSH, Vitamin A and D in DLA bearing Swiss albino mice (Loganayaki and Manian 2012). Significant decrease in Vitamin C, E and GSH in DLA induced mice could be due to their increased utilization to sacvenge the free radicals generated and the products of lipid peroxidation due to tumor burden.

Vitamin E protects the body from oxidation, a normal aging process by which oxygen breaks down the body's tissues. It works to neutralize free radicals, which are naturally occurring unstable molecules that can damage our body's healthy molecules by taking electrons to balance themselves. When enough Vitamin E is present in the body, unstable free radicals get their electrons from the Vitamin E molecules and leave the healthy molecules alone, thus causing less damage to the tissues (Traber 2007). The decreased level of Vitamin E and Vitamin C found in the liver of DLA induced mice as compared with control mice could be due to the increased oxidative stress, which accompanies the decrease in the level of antioxidants and may be related to the casuation of tumor growth. Low level of Vitamin E observed in DLA induced mice compared to normal controls suggested decreased regeneration of Vitamin E from its radical. During the oxidative stress, the ascorbic acid was found to be in oxidized form. The change in ascorbic acid level is in good agreement with the early decrease in Vitamin E. Regeneration of Vitamin E requires ascorbic acid, an aqueous phase antioixdant, which in turn requires GSH (Annamalai *et al*., 2003). Since Vitamin C and E are synergistic antioxidants administration of MGsSTL and AgMGsSTL significantly improved the Vitamin E level in the liver of DLA induced mice. The results obtained were found to be similar with Santhi *et al*., (2010) who reported that the levels of nonenzymic antioxidants

(Vitamin A and E) were significantly enhanced in ELA transplanted Swiss albino mice when treated with protein fraction of *Cynodon dactylon* leaf. Fungal taxol were found to be effective against 7, 12 dimethyl benz (a) anthracene induced mammary tumors in Sprague Dawley rats by significantly increasing the SOD, CAT, GPx, Vitamin C, Vitamin E and GSH (Vennilaetal., 2010). NAMI-A[imidazolium*trans*-tetrachloro(dimethylsulfoxide)imidazoleruthenium(III)] loaded NPs exhibited superior antitumor effect by delaying metastatic tumor growth in T739 mice both *in vitro* and *in vivo* (Yong-guang *et al*., 2011). *Momordica charantia* against cyclophosphamide induced liver damage in Winstar rats showed increase in enzymic antioxidants SOD, CAT, GPx, GST and GR and also levels of nonezymic antioxidants glutathione, Vitamin C and Vitamin E (Senthilkumar *et al*., 2012).

Vitamin C maintains first natural antioxidant defense and acts as a powerful inhibitor of LPO. Vitamin C is an electron donor and therefore a reducing agent. It is called as an antioxidant because, by donating its electrons, it prevents other compounds from being oxidized (Wei *et al*., 2009). Vitamin C is an excellent hydrophilic antioxidant, and it readily scavenges ROS and peroxyl radical (Packer 1997). Also act as a coantioxidant by regenerating the Vitamin A, E and GSH from radicals. We have observed a decreased level of Vitamin C in liver of DLA bearing mice. This decrease level could be due to the increased utilization of Vitamin C in deactivation of the increased level of ROS or to decrease in the GSH level (Chatterjee and Nandi, 1991). Administration of MGsSTL and AgMGsSTL improved the level of Vitamin C in the liver of DLA tumor induced mice, may be expected to enhance the GSH level or stimulation of the system to recycle the dehydro ascorbic acid back to ascorbic acid. Chakraborty and Verma (2010) also reported the significant enhanced effect of *Ochratoxin* with the aqueous extract of *Emblica officinalis* on the non enzymic antioxidants (Vitamin A and C) in mouse. Ethanolic extract of *Tinospora cordifolia* in Aflatoxin B1 induced mice hepatic tissues elevated the enzymatic (SOD, CAT, GPx, GR and GST) and levels of nonenzymatic (GSH, Vitamin C) antioxidants (Guptaa *et al*., 2011).

The AgNPs of alpha Lipoic acid administration aided the significant tumor growth delay in DLA tumor bearing mice (Ramachandran and Nair 2011). *Enicostemma littorale* leaf extract in alloxan-induced experimental diabetes rats significantly increased the levels of Vitamin C, Vitamin E and GSH (Kumar *et al*., 2012; Subramanian *et al*., 2012). Treatment of *Gracilaria edulis* in EAc bearing Swiss albino mice increased the activity of hepatic enzymic antioxidants SOD and CAT and the levels of nonenzymic antioxidants GSH and Vitamin C and E (Sundaram *et al*., 2012).

Our findings are supported by Kathiriya *et al*., (2010) who reported significant decrease in liver MDA levels and increase in CAT and GSH levels in ethanolic extract of *Oxalis corniculata* Linn treated EAC induced Swiss albino mice. The effect of methanolic extract of *Tabebuia rosea* leaves against DLA induced Swiss albino mice also decreased the levels of lipid peroxides and increased the levels of GSH, SOD and CAT (Hemamalini *et al*., 2012). The liver tissue GSH levels were significantly elevated in the methanolic extract of *Leucas plukenetii (Roth) Spreng* (Nandy *et al*., 2012). Administration of methanolic extract of *Nymphaea nouchali* flowers showed increase in antioxidant activity (CAT, SOD and GSH) in EAC induced Swiss albino mice (Alam *et al*., 2012).

The increase in enzymic and nonenzymic antioxidant and decrease in the ratio of LPO levels by the coadministration of MGsSTL and AgMGsSTL to DLA tumor induced mice may be responsible for antitumor activity.

It can be stated that the probable mechanism by which MGsSTL and AgMGsSTL exert their protective action against DLA induced hepatocellular metabolic alterations could be by the stimulation of hepatic regeneration through an improved enzymic antioxidant, nonenzymic antioxidant status and LPO levels, cytotoxic effect to block the bioactivation of DLA or due to the apoptotic effect accelerate the detoxification of DLA cells and ILS of DLA tumor induced mice. So, MGsSTL and AgMGsSTL can be ranked as the natural antioxidants,

potent antitumor agents and the complementary and alternative medicine recommended for cancer treatment.

4.3.4. Effect of MGsSTL and AgMGsSTL on the mortality rate of DLA tumor induced mice

The *in vivo* cytotoxic studies were carried out to follow the antitumor activity in terms of increase in life span (ILS) of DLA tumor bearing mice treated with MGsSTL and AgMGsSTL. The effect of MGsSTL and AgMGsSTL on the average life span of DLA tumor bearing Swiss albino mice is shown in Table 13.

Table 13

The average life span of DLA tumor induced mice treated with MGsSTL and AgMGsSTL

Groups	ED_{50} in µg / 100 µl/g.b.wt / 1 x 10^6 cells	Average number of mice survived after transplantation of DLA tumor cells (days)					Average life span
		15	30	45	60	75	
DLA	-	6/6	0/6	0/6	0/6	0/6	20
DLA+MGsS	33	6/6	6/6	6/6	6/6	6/6	75
DLA+AgMGsS	25	6/6	6/6	6/6	6/6	6/6	75
DLA+MGsT	38	6/6	6/6	6/6	6/6	5/6	72
DLA+AgMGsT	30	6/6	6/6	6/6	6/6	5/6	74
DLA+MGsL	82	6/6	6/6	6/6	6/6	2/6	58
DLA+AgMGsL	79	6/6	6/6	6/6	6/6	2/6	60

Values are mean of six mice per group

The DLA tumor bearing mice life span was found to be 15-25 days with the average life span of 20 days. Coadministration of MGsS, MGsT, MGsL, AgMGsS, AgMGsT and AgMGsL inhibited the growth of DLA tumor cells and increased the life span to 75 days, 72 days, 58 days, 75 days, 74 days and 60 days respectively and indicated their antitumorigenic effect.

Treatment with MGsSTL and AgMGsSTL reduced the intraperitoneal tumor burden, by detoxifying the tumor cells and increased the life span of the tumor induced mice. The steadfast criteria for judging the potency of any anticancer drug is the prolongation of life span of tumor induced animals (Gorelik *et al*., 2008). It can therefore be inferred that MGsSTL and AgMGsSTL increased the life span of DLA bearing mice. In the present study, it was accomplished that MGsSTL and AgMGsSTL have antioxidant activity which in turn raised the life span of DLA induced mice and confirmed their antitumorigenic effect.

This hypothesis is strongly supported by the previous study of Liu *et al*., (2010) who reported that N-trimethyl chitosan encapsulated Camptothecin (CPT-TMC) treated group increased the survival of mice to 42 days by efficiently inhibiting the B16-F10 cell proliferation. Ethanolic extract of *Butea monosperma (Lam) Taub* increased the life span of EAC treated mice to 30 days (Rekha and Jayakar 2011). Mean survival time increased to 74% in the DLA tumor bearing Swiss albino mice treated with methanolic and aqueous extract of *Ulva fasciata* (Abirami and Kowsalya 2012).

Ethanol extract of *Impatiens balsamina* showed significant increase in life span of DLA tumor bearing mice to 78% (Baskar *et al*., 2012). Jayaseelan *et al*., (2012) also reported the increase in life span of DLA and EAC tumor bearing mice treated with methanolic extract of roots of *Desmodium triangulare* to 64 days and 50 days respectively. Antitumor effect of the *Alangium salviifolium* wang flowers against EAC showed increase in life span to 40 days (Nahar *et al*., 2012). Methanolic extract of the leaves of *Leea indica* (*L. indica*) enhanced the survival time against EAC in Swiss albino mice to 69.33% (Raihan *et al*., 2012).

It may be concluded that MGsSTL and AgMGsSTL increased the life span of DLA bearing mice and proved their antitumorigenic effect by arresting the tumor growth.

4.3.5 Effect of MGsSTL and AgMGsSTL on the Histological appearance of hepatocytes of normal and DLA induced Swiss albino mice

The histopathological observation of liver section under light microscope was done to observe the effect of MGsSTL and AgMGsSTL in DLA tumor induced mice on the structural integrity of liver cells as shown in Plate VI and VII. Control groups (PBS, DMSO, Paraffin oil) showed normal lobular architecture with intact central vein and sinusoids, normal portal triad and preserved hepatocytes. Liver sections of Swiss albino mice treated with the MGsSTL and AgMGsSTL as showed normal lobular pattern, contain a large spherical nucleus as compared to the normal control group. DLA induced animals showed severe necrosis, surrounding fibrosis, perivenular inflammation and vacuole formation. However, mice treated with MGsSTL, AgMGsSTL and silymarin showed reduced vacuole formation and inflammation and almost normal hepatocellular architecture was observed. Histopathological examination showed a protective effect of MGsSTL and AgMGsSTL on hepatotoxicity. The prevention of necrosis formation due to the treatment of MGsSTL and AgMGsSTL may be due to diminution of oxidative stress and free radicals.

Histological view of the hepatocytes of MGsSTL and AgMGsSTL in normal and DLA induced Swiss albino mice

Plate VI a (PBS) Hepatocytes of PBS showed the Liver parenchyma with congestion of blood vessels

Plate VI b (DMSO) The hepatocytes of DMSO group showed the liver parenchyma with cetral vein congestion and congestion of blood vessels.

Plate VI c (Paraffin oil) The hepatocytes with nuclei of paraffin oil group were found to be normal with congestion of central veins.

Plate VI d (silymarin) The hepatocytes of silymarin treated mice found to be normal with marked sinusoidal and central vein congestion.

Plate VI e (MGsS) The hepatic cells of MGsS treated mice were found to be normal with congestion of central veins.

Plate VI f (AgMGsS) The hepatocytes of AgMGsS induced mice showed the normal portal triad, parenchyma with nuclei and marked sinusoidal/ central vein congestion.

Plate VI g (MGsT) The hepatic cells of MGsT induced mice showed the normal congestion of sinusoidal and central veins. There is a mixed inflammatory infiltration in between the hepatocytes within hepatic lobules.

Plate VI h (AgMGsT) The AgMGsT treated mice showed normal appearance of hepatic cells with congestion of sinusoidal and central veins.

Plate VI i, j (MGsL and AgMGsL) The MGsL and AgMGsL treated mice showed mild degeneration of hepatic cells and congestion of sinusoidal and central veins. There is mixed inflammatory infiltrate in between the hepatocytes.

Plate VII k (DLA) The DLA treated mice showed increased size of hepatocytes, enlarged hyper chromatic nuclei, dilated sinusoidal and central vein congestion including severe necrosis.

Plate VII m, n and p (MGsS, AgMGsS and AgMGsT) The MGsS, AgMGsS and AgMGsT in DLA induced mice showed normal hepatocytes with conjestion of sinusoidal and central veins.

Plate VII o (MGsT) The hepatocytes of MGsT in DLA induced mice showed the normal hepatocytes with conjestion of sinusoidal and central veins. There is a mild chronic inflammatory infiltration in between hepatocytes.

Plate VII q (MGsL) The hepatocytes of MGsL in DLA induced mice showed the normal parenchyma and congestion of blood vessels.

Plate VII r (AgMGsL) The hepatocytes of AgMGsL in DLA induced mice showed the liver parenchyma with increased size of hepatocytes and enlarged hyper chromatic nuclei. There is marked sinusoidal and central vein congestion.

PlateVI

Histological view of the hepatocytes of controls, MGsSTL and AgMGsSTL treated Swiss albino mice

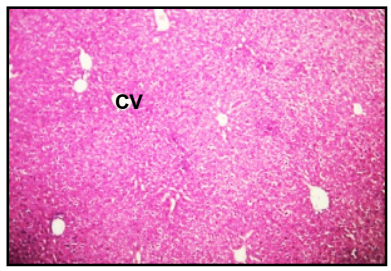

a. PBS

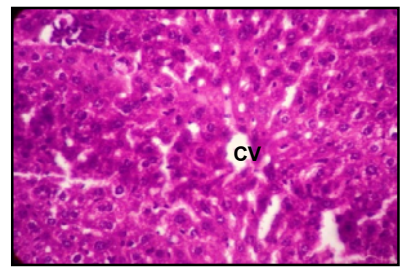

b. DMSO

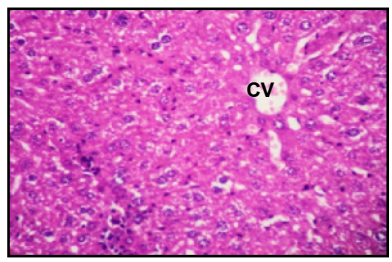

c. Paraffin Oil

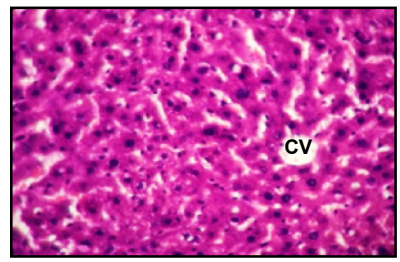

d. Silymarin

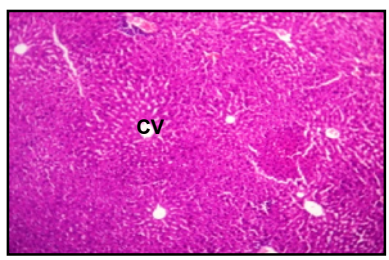

e. MGsS

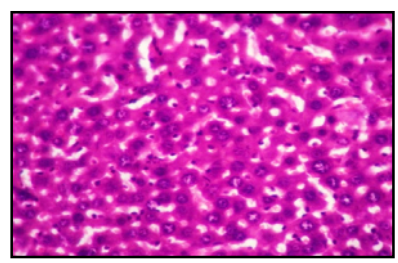

f. AgMGsS

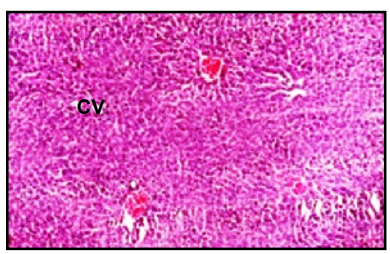

g. MGsT

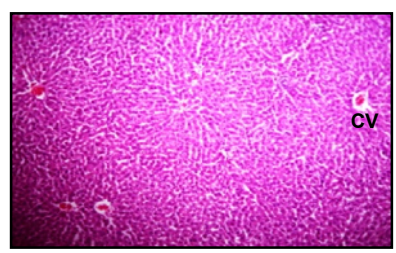

h. AgMGsT

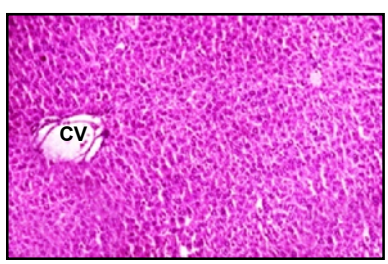

i. MGsL

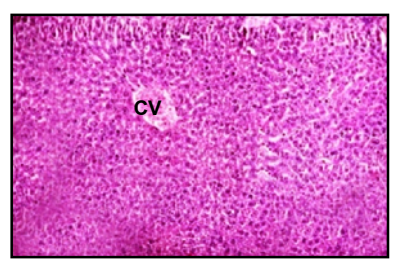

j. AgMGsL

Plate VII

Histological view of the hepatocytes of controls, MGsSTL and AgMGsSTL in DLA induced Swiss albino mice

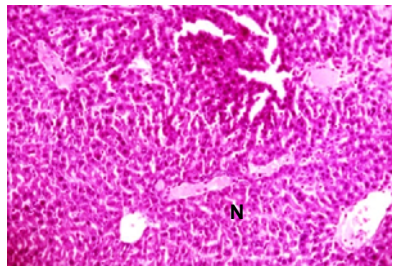

k. DLA

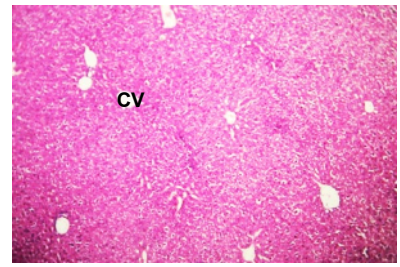

l. PBS

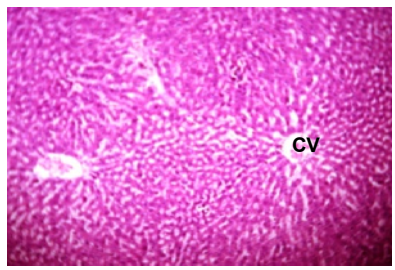

m. DLA + MGsS

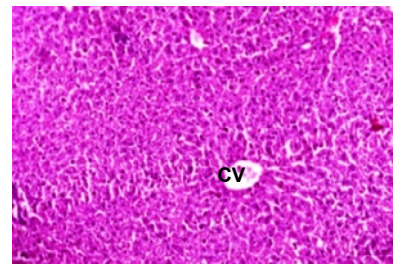

n. DLA + AgMGsS

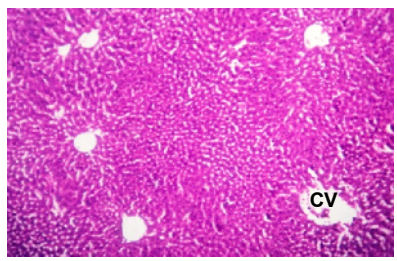

o. DLA + MGsT

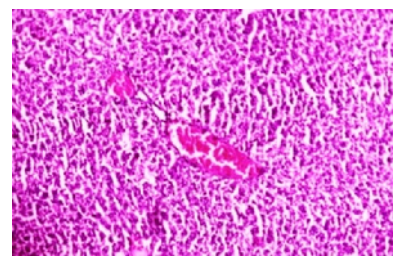

p. DLA + AgMGsT

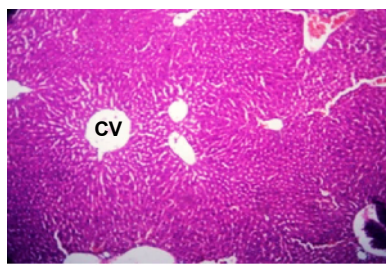

q. DLA + MGsL

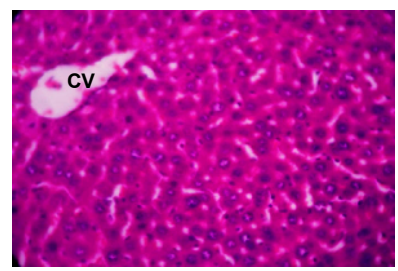

r. DLA + AgMGsL

N – Necrosis **CV – Cental Vein**

These marked changes in the hepatic architecture could be explained on the basis that DLA treatment manifested its toxic effect through the generation of ROS. The resulting effect was the production of elevated amounts of malondialdehyde and conjugated dienes, which caused deleterious effects on the membranous components of hepatocytes (D'Archivio *et al*., 2008).

These result corroborated with earlier report of Lee *et al*., (2006) who reported that the histological examination of heart tissue revealed myocardial morphological changes of tissues that could be clearly related to treatment with Gelatin-doxorubicin (GD) and PEGylated gelatin-doxorubicin (PGD) NPs both remarkably suppressed pulmonary metastasis. AgNPs treated smears showed very few pleomorphic cells with hyperchromatic nuclei and significant reduction in malignant cell clumps against DLA cells (Sriram *et al*., 2010).Tumor suppression activity of sol-gel Pt(NH3)4Cl2/SiO2 NPs in C6 tumor cells was reported by Pez *et al*., 2011. Heparin–folic acid–retinoic acid NPs treated animals showed their liver architectures as conserved and no apparent tissue or cellular damages suggesting cytoxicity against KB (Korean Culture Line Bank) cancer cell line (Oh *et al*., 2012). Hamed *et al*., (2012) also showed the anticancer activity of plant extracts of cabbage, cauliflower, carrot and cinnamon against HepG2 cancer cell line. Mice treated with *Acacia nilotica* extract against DAL induced solid and ascitic tumors showed reduced vacuole formation and inflammation and almost normal hepatocellular architecture (Sakthivel *et al*., 2012).

In the present study, the histological examination of the liver of DLA inoculated Swiss albino mice showed marked changes indicating the toxic effects of this tumor. The normal effects observed due to the treatment with AgMGsSTL compared to MGsSTL supported their potent hepatoprotective antioxidant and antitumor effect.

In conclusion, AgMGsSTL were effective in inhibiting the tumor growth in DLA tumor models when compared to MGsSTL. Both the *in vitro* and *in vivo* biochemical parameters, life span and histological studies supported their antioxidant and antitumorigenic properties.